Chapter 1

Introduction

The development of communication systems over the past decade has had a significant impact on the modern life of people in today's society. Demand for faster and easier ways to communicate and transfer information worldwide with real time processing is a basic requirement for current communication systems. This demand is driving communication technology towards a higher data rate, higher mobility, and higher carrier frequencies to enable reliable transmission over mobile or broadband wireless communication systems.

However, at high transmission rates, wireless communication links become unreliable and have fundamentally low capacity due to path loss, shadowing and interference. In the near future, we will be surrounded by several alternatives in the setting up of an un-wired connection over the radio interface. Several types of communications are available, from the satellites that provide low data rates but global coverage; cellular systems with continental coverage to high data rates; local area networks; and personal area networks with a maximum range of a few hundred meters.

In reality, we would obtain a crowded frequency spectrum since there are many different communications that share limited frequency resources. To use a signalling strategy that is spectrally efficient is thus of the utmost importance. This requirement poses real challenges to the designers of future wireless systems. In order to satisfy these requirements, a key development in the current state of wireless technology is necessary. A popular technique to efficiently utilize the available resources is a multiple access technique, which allows multiple users to share the resources at the same time. A Code Division Multiple Access (CDMA) technique is one of available multiple access schemes. However, it introduces various impediments in the system. One of the most serious problems is caused by the unavoidable interference amongst concurrent users. This interference becomes significant and disastrous when the number of active users increases or the power of certain users is dramatically higher than that of others.

1.1 Motivation

Space utilization is one of the most promising techniques for the enhancement of future wireless system performance without additional use of limited resources, such as power, frequency bandwidth and time. This brings us to the concept of using multiple antenna elements for the transmission and/or reception of signals. Smart antennas and adaptive antennas, employing multiple antenna elements, were introduced for wireless communication systems with the advent of analog and digital signal processing and high speed analog to digital converters.

Using multiple antennas when transmitting over a wireless link has some benefits, which need to be discussed. Due to the use of multiple antennas, the antenna gain or array gain can be increased leading to an increased range and coverage. It is useful in remote areas with low populations. Therefore, the number of base stations in large areas can be reduced. Moreover, the transmit power of mobile units can be reduced due to the increased gain of the receiver base station antenna arrays.

Multiple antennas can also be used to counteract the negative effect of channel fading. Sufficiently spaced multiple antennas transmit copies of the same signal through the channel with different fading. The probability that all signal copies are in a deep fade simultaneously is low. Thus, spatial diversity increases the robustness of the wireless link and its performance. Moreover, the antennas, which are sufficiently spaced, can transmit different signals that carry independent information data at the same time. Since these signals undergo independent fading through the wireless channel, they obtain an intrinsic signature from the channel itself, allowing separation of transmitted data at the receiver. Therefore it provides higher spectral efficiency.

However, the use of multiple antennas to transmit information data independently and simultaneously in the same channel introduces interference. In practice, if we simultaneously transmit information signals using multiple transmit antenna elements, the signal from one transmit antenna will interfere with the signals from other antennas. Such interference is called co-channel interference (CCI).

Spatial diversity from the spatial dimension provided by multiple antennas and spatial multiplexing (SM), which increase the transmission rates by transmitting information data independently and simultaneously with multiple antennas, are the main concepts of this thesis. Unfortunately, the need for multiple access techniques and the improvements promised by the use of multiple antenna topologies contrasts with the uncertainty of the wireless media. Spatial diversity and SM techniques perform remarkably well if the wireless channel is fairly static or there is a slow change in the characteristics. In high mobility environments, the wireless channel becomes very changeable and causes the transmitted signal waves to unpredictably hit various objects and be reflected and diffracted in multipath replicas with different directions and times of arrival at the receiver. This phenomenon is common in wireless communications and it reduces the quality of the received signal, with the risk of breaking the communication link. As a consequence, multiple antenna techniques generally suffer from this channel distortion to the extent of introducing a form of self-interference, caused by the superposition of delayed replicas of the same multi-antenna signal. In such scenarios, where interference among users, transmit antennas and channel impairments are added together, very robust, reliable and efficient detection techniques are required.

It has been shown recently that space-time coding techniques significantly improve the transmission quality across fading wireless channels, by exploiting transmit and receive diversity. Space-Time Trellis Codes (STTCs), in particular have been extensively studied in order to combat the effect of fading, and various code design criteria have been developed in order to achieve the highest possible antenna diversity and coding gain [1] [2]. However, the presence of multiple antennas at the transmitter, along with multiplath and multiple users inevitably introduces not only inter-symbol interference (ISI) and multiple access interference (MAI), but also the co-channel interference (CCI), caused by the interference from other antennas in the system. The simplest approach for CDMA systems is a single user matched filter (MF) [3] or the conventional MF detector. This conventional MF detector is an optimal for single user. However, in the multiuser systems, the conventional MF of a desired user will suffer from the multiple access interference (MAI). Thus, the conventional MF detector, which neglects the presence of the MAI and CCI, is not sufficient to deal with interference in such a scenario and an enhanced detector, which takes into account the structure of MAI, the CCI and the ISI, is required.

Many advanced signal processing techniques proposed to mitigate interference and multipath channel distortion fall largely into multiuser detection and space-time processing. The optimum linear multiuser minimum mean square error (MMSE) detector was first introduced by Verdu [4] and was shown to be near-far resistant in the sense that a very good performance level can be guaranteed regardless of the transmitted users' energies. Multiuser detection has been successfully analyzed for synchronous and asynchronous CDMA over Gaussian channels, where the decorrelating detector and the MMSE detector employ a linear filter to eliminate the MAI and to minimize the mean square value of the MAI-plus-noise [3, 5, 6]. The problem of multipath distortion has been addressed for a single input multiple output (SIMO) CDMA system by combining a space-time matched filter and MMSE equalization with the turbo principle in an iterative fashion [7-9]. This solution exploits the receive and multipath diversity and enhances the signal-to-noise ratio (SNR) and the reliability of the detected signal at the receiver. Unfortunately, the increased performance of the iterative multiuser MMSE detection comes at the expense of an enormous and often prohibitive computational complexity. This justifies the search for alternative suboptimal detectors, which are capable of achieving an acceptable performance at a much lower complexity. Iterative and multistage receivers employing successive interference cancellers (SIC) and parallel interference cancellers (PIC) have been widely studied in the literature of CDMA systems [7-11]. Their ability to remove the MAI from the received signal with relatively low hardware and computational complexity is one of the attractive features of these receivers. However, although SIC based receivers generally show better performance than PIC based detectors, their serial nature introduces high processing delays. These low complexity iterative receivers perform incredibly well for SIMO CDMA systems, where only MAI and ISI are present. When employing multiple antennas at the transmitter, the resulting level of interference at each receiving antenna is increased due to additional CCI, unless coherent reception can be guaranteed. Furthermore, in a frequency selective channel the multipath distortion damages the orthogonality of the spreading codes and this effect is exacerbated when the signals coming from the different antennas are not symbol synchronous at the receiver, i.e., if the signals transmitted from different antennas undergo different delay profiles. This problem has been addressed by H. Yang et al.,[12], where an iterative multiuser MMSE detector for the multipath CDMA system has been applied in the system with multiple antennas. The resulting detector suppresses and cancels the ISI and CCI in the received signal at the chip level. It also benefits from the output of the decoders in the previous iteration, in terms of a posteriori probabilities of the transmitted signal, regenerating and canceling the MAI at the current iteration. However, H. Yang et al., [12], only considered the MAI in the regeneration-cancellation process and not the CCI. Moreover, the signals transmitted from different antennas are assumed to have no relative delays at the receiver. Furthermore, the computational complexity of this detector is extremely high, since a multiuser MMSE equalizer, operating at the chip level, is employed at each iteration.

The computational complexity is an important issue that impacts on receiver design. Generally, in all publications cited in this section, the knowledge of the wireless channel state information (CSI) is assumed to be available only at the receiver. Another assumption is that detectors are dependent on perfect knowledge of the CSI. This implies that the computational complexity is relatively high due to the matrix inversion operation for the channel matrix required for determining CSI. However, imperfect knowledge of

CSI will significantly degrade the system performance. Therefore such a high receiver computational complexity makes this detector type impractical in real systems. This motivated the research for this thesis to focus on investigating sub-optimal multiuser detection algorithms with good performance and complexity trade-offs.

Recently, M. Honig et al.[13, 14], has proposed an adaptive iterative multiuser receiver based on the MMSE decision feedback algorithm for single input and single output systems. J. Li et. al. [15]., have proposed an adaptive co-channel interference cancellation scheme for an STC system. However, the adaptive receiver design is based on the linear detection. The performance of the adaptive receiver will be degraded in the rich interference environment. J. Choi et al., [16] has proposed the adaptive receiver for MIMO channels. However, the adaptation is based on the recursive mean square (RLS) algorithm. Although, this receiver can effectively remove the interference but it comes with a cost of the computational complexity. J. Jiang [17] has proposed an adaptive receiver for V-Blast systems, however this receiver based on partial channel state information (CSI), which comes with some complexity expense..

The goal of the thesis is to consider mitigating the problem of imperfect CSI and a reduction of the system computational complexity in space-time (ST) coding and DS-CDMA multiple input multiple output systems for application in cellular wireless communications. Several new low computational complexity receivers, which can provide a satisfactory system performance in space-time (ST) codes and DS-CDMA MIMO system, are proposed.

More specifically, the focus of the thesis is on the computational complexity and system performance of adaptive iterative receivers based on the least mean square (LMS) algorithm. The time domain and frequency domain adaptive iterative receivers are investigated. The adaptive iterative receivers have a low computational complexity compared to non-adaptive ones. Moreover, in this thesis, the computational complexity consideration is restricted to the detector computational complexity only, since we use the same decoder structures in all proposed receiver types.

An adaptive iterative receiver based on joint adaptive iterative detection and decoding that adaptively suppresses and cancels co-channel interference is proposed. The LMS algorithm [18] and Maximum A Posteriori (MAP) [19] algorithm are utilized in the receiver structure [20]. Since the adaptive LMS algorithm has a slow convergence speed, a partially filtered gradient LMS (PFGLMS) [21] algorithm is also applied to improve the convergence speed and tracking ability of the adaptive detector with a slight increase in complexity. The computational complexity of the LMS and PFGLMS adaptive iterative receivers is significantly lower than that of the non-adaptive iterative MMSE receiver.

To further reduce the computational complexity, the frequency domain adaptation has been investigated. It is well known that the linear convolution process can be carried out in either the time domain or the frequency domain, however, the frequency domain approach has been shown to have a much lower computation complexity [22-28].

Therefore, performing the convolution in the frequency domain rather than performing it in the time domain can further reduce the computational complexity as shown in Chapters 4 and 6 for space-time coding systems and DS-CDMA systems, respectively.

1.2 Thesis outline

The thesis consists of seven chapters. The fundamentals of wireless MIMO systems and the MIMO system model are described in Chapter 2. This description is extended to include specific transmitter topologies, such as space-time coding and SM, which are the basis of the two most common MIMO transmission architectures [2, 29]. These architectures are described in detail with emphasis on the problem of CCI, as well as unavoidable ISI, in the context of MIMO channels. A maximum a posteriori probability (MAP) and a turbo coding principle are described for the example of convolutional and turbo codes. Then, multiuser systems and multiple access techniques are briefly discussed with the focus on CDMA techniques and their intrinsic problem of MAI. Finally, a description of common detection techniques is provided, with particular interest on the use of iterative processing methods to enhance the performance of the detector without noticeably increasing the receiver complexity.

In Chapter 3, a non-adaptive receiver, based on the MMSE algorithm, and a time domain adaptive iterative receiver, based on LMS and PFGLMS algorithms, for layered space-time coding [20] is described. The main purpose is to investigate and compare the performance and complexity of the non-adaptive and adaptive iterative receivers. The simulation results show that the performance of the proposed adaptive iterative receiver based on the PFGLMS and LMS algorithms approaches the performance of the non-adaptive MMSE receiver, with a significant reduction in the computational complexity.

The proposed frequency domain adaptive iterative receiver is described in Chapter 4. An adaptive iterative receiver, based on the conventional LMS and PFGLMS algorithms, operating in the frequency domain is investigated. Simulation results show that the performance of the time and frequency domain PFGLMS detectors is very similar in slow fading channels. Similarly, the time and frequency domain LMS detectors have the same performance. However, the computational complexity in the frequency domain receivers is significantly reduced compared to the time domain approaches both for the LMS and PDFLMS based receivers.

The multiuser CDMA receiver operating in the time domain for MIMO channels is presented in Chapter 5. A layered space-time coded CDMA (LSTC-CDMA) system is discussed. The system is based on an assumption that there is no knowledge of channel state information (CSI), spreading sequences and fading coefficients. A normalized least mean square (NLMS) feed-forward filter and a feedback iterative parallel interference canceller operating in the time domain are employed. The computational complexity of the system is calculated. The system performance is evaluated by using a semi-analytical approach that is compared to that of simulation results. The results show that there is an excellent agreement between the two approaches.

In Chapter 6, the simulation results and the computation complexity of the layered space-time coded CDMA (LSTC-CDMA) system operating in the frequency domain is presented. The performance comparison between the time and frequency domain adaptive iterative receiver is also depicted. Moreover, a comparison of the computational complexity of the time and frequency domain detectors is also provided.

Conclusions to the thesis are discussed in the last Chapter.

1.3 Contributions

In Chapter 3, due to a high computational complexity in the non-adaptive iterative MMSE receiver, we propose a low computational complexity adaptive iterative receiver, based on a joint adaptive iterative detection and decoding algorithm for layered space-time code systems. The proposed adaptive iterative receiver, utilizing the adaptive least mean square (LMS) and a partially filtered gradient LMS (PFGLMS) is considered. The system performance and complexity of the proposed receivers are compared to that of the non-adaptive iterative MMSE receiver. The results show that the proposed adaptive iterative receiver can suppress and remove the interference (CCI) from other antennas and the performance approaches the performance of the non-adaptive receiver with the number of iterations. The analysis of the computational complexity also shows that the receiver complexity, based on the adaptive LMS and PFGLMS iterative detector, is significantly reduced in comparison with the non-adaptive MMSE receiver.

Moreover, the system performance and complexity of the PFGLMS based receiver and the LMS based receiver is also considered. The results show that the proposed PFGLMS based receiver has a faster convergence speed and better tracking ability compared to the LMS based receiver in both rich scattering environments and fast fading channels with a slight increase in the complexity in terms of the number of multipliers and adders. Therefore the PFGLMS receiver needs a shorter training period than that of the LMS receiver. The adaptive LMS and PFGLMS iterative detections can save about 83% and 69% in computational complexity respectively compared to the non-adaptive iterative MMSE receiver as in the given example in Chapter 3. Some of these results have been published in [30, 31].

In Chapter 4 the main contribution is the proposed adaptive iterative receiver, based on the time domain adaptive iterative receiver in Chapter 3, operating in the frequency domain. The computational complexity and the performance of the time and frequency domain LMS and PFGLMS adaptive algorithms are investigated. The computational complexity of the frequency domain LMS is dramatically reduced by about 63% compared to the time domain LMS detector. Similarly, the frequency domain PFGLMS detector can save about 75% in computational complexity compared to the time domain PFGLMS approach. The system performance of the time and frequency domain approaches is identical for each type of adaptive receiver. Hence, the proposed frequency domain adaptive iterative receiver outperforms the time domain adaptive iterative receiver in terms of the computational complexity with the same performance.

The proposed adaptive iterative receiver for the MIMO-CDMA system using the time domain approach is the main contribution in Chapter 5. In MIMO-CDMA systems, the co-channel interference (CCI) from the adjacent transmit antennas and the multiple access interference (MAI) considerably degrade the system performance. An adaptive iterative receiver based on a joint an adaptive normalized LMS (NLMS) detector and maximum a posteriori (MAP) decoder, is proposed. The proposed adaptive receiver effectively suppresses and removes the CCI and MAI by using the interference suppression and cancellation techniques. Simulation results show that the performance of the proposed adaptive iterative receiver approaches the interference-free single user performance for high signal-to-noise ratio (SNR). Part of the results of this contribution were published in [32].

To further reduce the computational complexity of the time domain adaptive iterative receiver proposed in Chapter 5, a novel low frequency domain adaptive iterative receiver, based on the time domain adaptive iterative receiver structure, is proposed in Chapter 6. The difference between the proposed frequency domain receiver and the time domain receiver is that the frequency domain adaptive detector performs adaptation in the frequency domain but the time domain receiver performs adaptation in the time domain. The computational complexity of the frequency domain approach is considerably lower than that of the time domain approach. As shown in an example in Chapter 6, the performance of the frequency domain approach is about 75% lower in the computational complexity than that of the time domain approach with the same performance. The results of this contribution is published in [32].

Chapter 2

Wireless MIMO systems

The next generation (4G) broadband wireless communication systems are expected to provide users with wireless multimedia services such as high-speed Internet access, wireless television and mobile computing. The rapidly growing demand for these services is driving communication technology towards higher data rates, higher mobility, and higher carrier frequencies to enable reliable transmission over mobile radio channels. Multiple Input Multiple Output (MIMO) systems have recently emerged as one of the most significant technical advances in modern communications. This technology promises to solve the capacity bottleneck in wireless communication systems. The fundamental information theory results demonstrate that the asymptotic capacity of MIMO Rayleigh fading channels grow linearly with the minimum number of transmit and receive antennas. The key principle that will enable ultimate capacity utilization is the full use of diversity techniques. In particular, there is a trend towards diversity in multiple domains. For instance, space-time coding is a technique where space and time diversities are combined to achieve performance gains without bandwidth expansion. However, the presence of multiple transmitted streams, impairments of the propagation channel and multiple users transmitting at the same time, yield various forms of interfering scenarios at the receiver antennas of a wireless system. Therefore, to mitigate against interference across the symbols transmitted from different antennas, detection techniques are an essential part of a well design transceiver.

2.1 Introduction

In this chapter, a basic analysis of MIMO systems is provided for the case of point-to-point transmission, where one user utilizes all the available resources in the system. The concept of the MIMO channel is described, and it is shown that the presence of multiple transmit antennas is a potential source of interference, i.e., CCI. Two main techniques for realizing a MIMO system, i.e., space-time coding and spatial multiplexing (SM), are introduced. It is shown that space-time coding can be effectively used to increase the diversity order of a system by introducing spatial (or antenna) diversity at the transmitter in the form of coding over the space and the time dimension. As a result, the CCI is dealt with at the receiver by using appropriate detection schemes. On the other hand, SM techniques are inherently affected by the CCI, because they simultaneously transmit different and independent symbols from each antenna.

A brief survey of various multiple access techniques is given with particular emphasis on CDMA schemes, where the presence of multiple users introduces MAI at the receiver. The aggregation of CCI and MAI renders the MIMO multiuser system very complex in terms of implementation, particularly at the receiver where efficient detection techniques are required to tackle the overall interference. Optimal detection techniques can deliver very high performance, even in high interfering environments, but this comes at the expense of a very high and often prohibitive hardware and computation complexity. For this reason, the investigation of suboptimal receiver structures, with acceptable trade-off between performance and complexity, is one of the widest areas of research in wireless communications. This chapter is concluded by introducing some basic suboptimal detection schemes, some of which will be used in the remainder of this thesis. In particular, adaptive and iterative detection techniques are briefly described at the end of this chapter and they will be the focus of Chapter 3, where a more detailed analysis will be given.

2.2 MIMO System Model

Recently, a large amount of research has addressed MIMO wireless systems. This research is encouraged by the demand for higher system capacity. In principle, using multiple antenna arrays at both ends of the link can dramatically enhance the system capacity [33]. Let us consider a single point-to-point MIMO system with N transmit antennas at the transmitter and M receive antennas at the receiver. A MIMO system model can be depicted as in Figure. 2.1.

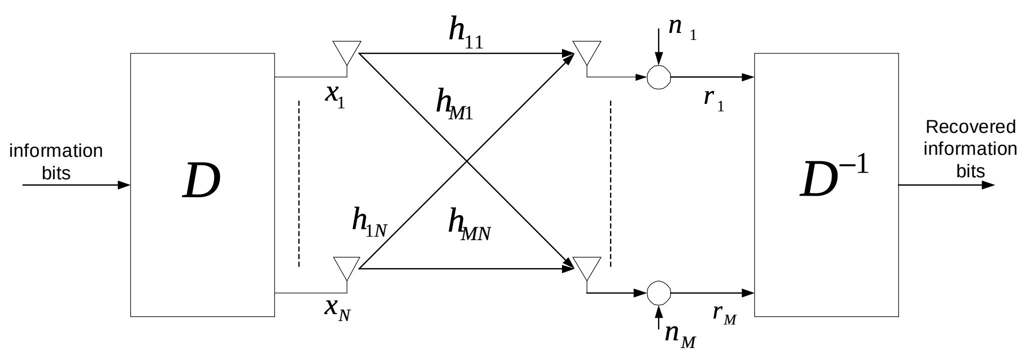

Figure. 2.1 MIMO system block diagram

The information bits are first transformed by a generic processor $\boldsymbol{D}$ to generate the transmitted signal, represented by an $N \times 1$ column vector $\mathbf{x} = [x_1, \mathbf{K}, x_N]^T$. The total transmitted power is constrained to P and elements of $\mathbf{x}$ are zero mean, independent and identically distributed (i.i.d) random variables with equal average power of $P_t = P / N$. The signal x_i transmitted from antenna i, where $i = 1, \mathbf{K}, N$, passes through the wireless channel and arrives at the receive antenna *j*, where $j = 1,\ldots,M$. The total received signal at the receive antenna *j* is expressed as

$$r_j = \sum_{i=1}^{N} h_{ji} x_i + n_j \tag{2.1}$$

where h_{ji} is a sample of complex random variable that describes the channel between transmit antenna *i* and receive antenna *j*. n_j is a zero mean i.i.d. additive white Gaussian noise (AWGN) complex sample at the receive antenna *j*. The total received signal vector, denoted by **r**, can be represented as

$$\mathbf{r} = \mathbf{H}\mathbf{x} + \mathbf{n} \tag{2.2}$$

where **r,** defined by $\mathbf{r} = [r_1,\ldots,r_M]^T$, is an $M\times 1$ column vector of the received signals across the *M* receive antennas, , **H** is an $M \times N$ complex channel matrix gain, given by

$$\mathbf{H} = \begin{bmatrix} h_{1,1} & \cdots & h_{1,N} \\ \vdots & \ddots & \vdots \\ h_{M,1} & \cdots & h_{M,N} \end{bmatrix} \tag{2.3}$$

x is an $N\times 1$ vector of the transmitted symbols across the *N* transmit antennas and **n** is an $M\times 1$ vector of the AWGN noise with zero mean and noise variance of σ^2 at the receiver. We denote the average power at the output of each receive antenna by P_r. The average *SNR* at each receiver branch is given by $\gamma = P_r / \sigma_n^2$ and is independent of *N*. Accounting for the channel attenuations h_{ji}, we can write the average SNR at the receive antenna *j* as

$$\gamma = \frac{P_r}{\sigma_n^2} = \frac{P_t \sum_{i=1}^{N} E\left[|h_{ji}|^2\right]}{\sigma_n^2} \tag{2.4}$$

However, for normalization purposes and without loss of generality, we assume that the received power at each of the M receive antennas is equal to the total transmitted power, i.e., $P = P_r$. Therefore we obtain the normalization constraint for the elements of $\mathbf{H}$ as

$$\sum_{i=1}^{N} E\left[\left|h_{ji}\right|^2\right] = N \ , \ j = 1,\ldots,M \tag{2.5}$$

Finally, the symbols transmitted by different antennas are received simultaneously at each receive antenna. Therefore, the signal transmitted from antenna i, for $i = 1,\ldots,N$, will be interfered with by the signals from the remaining antennas in the same channel.

The simplest MIMO receiver is a filter matched to the multi-channel impulse response (fading factor in the flat fading channel)

$$y = \mathbf{H}^H \mathbf{r} = \mathbf{H}^H \mathbf{H}\mathbf{x} + \mathbf{n}' \tag{2.6}$$

Defining the *correlation matrix* as

$$\mathbf{G} = \mathbf{H}^H \mathbf{H} = \begin{bmatrix} G_{1,1} & \cdots & G_{1,N} \\ \vdots & \ddots & \vdots \\ G_{N,1} & \cdots & G_{N,N} \end{bmatrix} \tag{2.7}$$

where $G_{j,i}$ $\left(j, i = 1,\ldots,N\right)$ is the correlation between the j-th and i-th transmit antennas. The interference due to the correlation is defined as co-channel interference (CCI) in this thesis. In the MIMO system, the CCI is due to the correlation between the different channel's fading factors, rather than the scrambling codes in the CDMA system. Correspondingly, detection and equalization techniques for CDMA systems can also be transferred to MIMO systems, such as in the MMSE and IC approaches. Meanwhile the iterative receiver structure is also investigated for MIMO systems. Since similar techniques are employed in MIMO and CDMA detection, the MIMO and CDMA receiver can be naturally combined into one receiver for the MIMO-CDMA system, as will be shown in Chapter 5.

Transmitter and receiver models

The transformation $\boldsymbol{D}$ in Figure. 2.1 models the air interface employed to realize a MIMO wireless communication system. Various solutions and schemes have been devised throughout the years to enable effective transceiver architectures for wireless links. However, although they might appear different to each other, they all aim at transforming the source information bits into a set of one or more symbols to be transmitted through the channel from one or more transmit antennas, and to finally be collected at one or more receive antennas. Once received, the transformation applied at the transmitter, i.e., $\boldsymbol{D}$, is reversed at the receiver, i.e., $\boldsymbol{D}^{-1}$, in order to recover the information bits. However, because of the interference and additive noise at the receive antennas, a reconstruction of the information bits cannot be perfectly recovered, hence introducing errors to the recovered data. In addition, the transformations $\boldsymbol{D}$ and $\boldsymbol{D}^{-1}$ are not necessarily linear transformations. Some transceiver structures will be examined later in this chapter.

The fundamental problem is: how should the transformations $\boldsymbol{D}$ and $\boldsymbol{D}^{-1}$ be designed to optimize the performance of the wireless link? The performance might be expressed by the following goals:

1. Data rate maximization: The aim is to provide the highest possible data rate per unit of bandwidth. This is often defined as the spectral efficiency. The ultimate limit or highest possible data rate that can be achieved, with arbitrarily low bit error probability in a Gaussain noise channel, was derived by Shannon [34] and is used as a reference.

2. Reliability: Often conflicting with high data rate is the reliability or robustness of the transmission, which can be measured using the average BER. Since the radio channel is time varying, it is important to choose a communication strategy that can withstand the fading in the received signal caused by the multi-path propagation.

3. Complexity: As one end of the wireless link might be battery powered, it is important to have low complexity architectures since an algorithm with higher complexity will be more power consuming. Hence, it is often desirable to design the transmission/reception schemes so that the complexity is asymmetric, i.e., locating the low complexity algorithms at the battery power side. Therefore, the transformations $\boldsymbol{D}$ and $\boldsymbol{D}^{-1}$ are usually different on the different sides of the channel in a duplex system.

It is generally difficult to achieve simultaneously and optimally all the objectives above, hence, the system designer must carefully choose a trade-off, including the economic as well as the mobility aspects. This work focuses mainly on the complexity aspects and investigates solutions aimed at improving the error rates and/or reduce the overall computational complexity of the receiver. An important factor that has impact on the choice of $\boldsymbol{D}$ is the knowledge of the instantaneous MIMO channel state information (CSI) at the transmitter side. Although CSI at the transmitter improves robustness and spectral efficiency, it consumes system bandwidth and increases the system complexity because of the requirement of a feedback channel.

2.3 Space-Time Architectures

The theoretical work developed by Foschini [33] and Telater [35] highlights the potentially large spectral efficiency of MIMO channels, which grow approximately linearly with the number of antennas, in an idealized propagation context. In general, the ergodic of a given channel is expressed by the maximum achievable average data rate for an arbitrarily low probability of error. The work presented by Foschini [33] and Telater [35] was limited to propagation scenarios in which individual channels between a given pair of transmit and receive antennas are modeled by an independent flat Rayleigh fading channel process. However the potential benefit in capacity promised by MIMO systems mainly depends on the important results given by Foschini [33] and Telater [35]. In fact, MIMO systems have an ergodic capacity growth proportional to min(N,M).

Information-theoretic studies of wireless fading channels have recently accelerated dramatically. The results inspire researchers to find novel, interesting and better ways to transmit data over the wireless channel [36]. This renaissance has already led to interesting results and new coding techniques for MIMO systems. Although the analysis of the MIMO channel's capacity is beyond the scope of this thesis, the discussion motivates the use of specific space-time transmission techniques in a subsequent chapter.

2.3.1 Space-Time Coding

Space-Time Codes (STCs) were first introduced by Tarokh et al. [2] in 1998 as a novel means of providing transmit diversity for multiple antennas in fading channels. Previously, multi-path fading in multiple antenna wireless systems was mostly dealt with by other diversity techniques, such as temporal diversity, frequency diversity and receive antenna diversity, which was the most widely applied technique. However, it is hard to efficiently use receive antenna diversity at the remote units because of the need for keeping them relatively simple, inexpensive and small. Therefore, for commercial reasons, multiple antennas are preferred at the base stations, and transmit diversity schemes are growing increasingly popular as they promise high data rate transmission over wireless fading channels in downlink scenarios while putting the diversity burden on the base station. The space-time coding scheme by Tarokh et al. [2] [37] is essentially a joint design of coding, modulation, transmit and receive diversity. It has been shown that space-time coding is a generalization of other transmit diversity schemes, such as Witneben's bandwidth efficient transmit diversity scheme [38] and the delay diversity scheme introduced by Seshadri and Winters [39].

There are two main types of STCs, namely space-time block codes (STBCs) and space-time trellis codes (STTCs). Space-time block code encoders operate on a block of input symbols, producing a matrix output where the columns represent the time dimension and the rows represent the spatial dimension, i.e., the transmit antennas. In contrast to single antenna block codes for the AWGN channel, STBCs do not provide coding gain, unless concatenated with an outer code. Their main feature is the provision of full diversity with a very simple coding scheme such as the Alamouti scheme [40]. On the other hand, space-time trellis codes operate on one input symbol at a time, i.e., $x(m)$, producing a vector of symbols whose length is equal to the number of transmit antennas, i.e., $\mathbf{x}_c(m) = \left[x_c^1(m), \mathbf{K}, x_c^N(m)\right]^T$. Like traditional trellis coded modulation for a single antenna, STTCs provide coding gain. Since they also provide full diversity gain, their key advantage over STBCs is the provision of coding gain. Therefore, the main motivation is to increase diversity, and thus improve the robustness of the communication link. However, the main drawback of this scheme is the computational complexity, which grows exponentially with the number of bits per symbol, thus limiting achievable data rates.

2.3.2 Spatial Multiplexing

The basic principle of spatial multiplexing (SM) is to transmit essentially independent data from each antenna. Then at the receiver, the multi-antenna signal is separated with appropriate detection techniques. In SM systems, the input data stream is de-multiplexed into N separate streams, using a serial-to-parallel converter, and each stream is transmitted from an independent antenna. The received signal is then passed through the detector, which is similar to a multiuser detector and treats separate streams as separate users of a multiuser channel.

Rayleigh models are realistic for environments with a large number of scatters. In channels with independent Rayleigh fading, a signal transmitted from every individual transmit antenna appears uncorrelated at each of the receive antennas. As a result, the signal corresponding to every transmit antenna has a distinct spatial signature at each receive antenna. The independent Rayleigh fading model can be approximated in MIMO channels if antenna spacing is larger than one half of the carrier wavelength and the antennas are surrounded by a large number of scatterers. An example of such a channel is the downlink in cellular radio.

Let us assume that the channels between any transmit and any receive antennas are uncorrelated from one another. Therefore, the SM technique is utilized. Then, different information data can be allocated to different transmit antennas and transmitted simultaneously through the MIMO channel to the receive antennas. The received signal at the receive antenna is the superposition of the signals coming from all the transmit antennas and additive noise. Because the signal corresponding to every transmit antenna has a particular spatial signature at a receive antenna, it will be able to detect the individual signals transmitted by each of antennas and separate them at the receiver. This operation obviously increases the spectral efficiency of the system by a factor equal to the number of transmit antennas.

As shown by B. Vucetic and J. Yuan [19] and H. Jafarhani [41], space-time codes provide a diversity gain equal to the product of the number of transmit and receive antennas NM. The maximum throughput of space-time codes is one symbol per channel for any number of transmit antennas. The use of multiple antennas results in increasing the capacity of MIMO channel systems. Therefore, one may transmit at a higher throughput, compared to SISO channel systems, for a given probability of error. On the other hand, the throughput of an SM scheme is N symbols per channel for a MIMO channel with N transmit antennas. However, the N-fold increase in throughput will generally come at the cost of a low diversity gain compared to space-time coding. This is the basic idea of the well known Bell Laboratories Layered Space-Time (BLAST) architecture, proposed by Foschini in [42].

Layered Space-Time Transmitter

There are a number of LST architectures, differing in the use of error control coding and the way the modulated symbols are assigned to transmit antennas. An un-coded LST structure, known as vertical layered space-time (VLST) or vertical Bell Laboratories Layered Space-Time (VBLAST) scheme [20], is shown in Figure. 2.2.

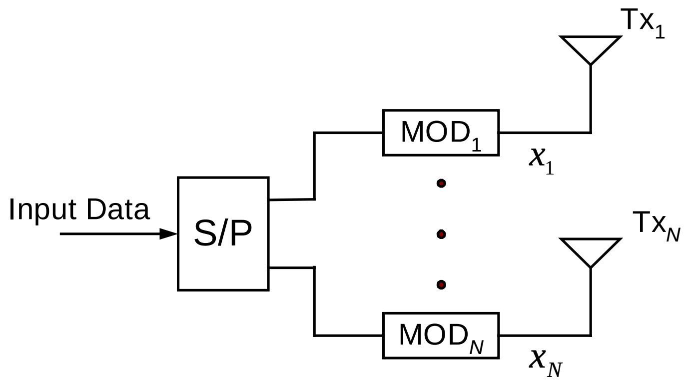

Figure. 2.2 VBLAST architecture

The input information sequence, denoted by **x,** is first de-multiplexed into *N* sub-streams, called layers. The demultiplexing process can be carried out by using a serial to parallel (S/P) converter. Each sub-stream at the output of the S/P converter is then modulated by an ***M-level*** modulation scheme and transmitted in a vertical pattern across the transmit antennas at each time instance. It is possible to use coding schemes such as conventional block or convolutional one-dimension codes for each sub-stream to improve the performance. However, it comes with cost of bandwidth efficiency [43].

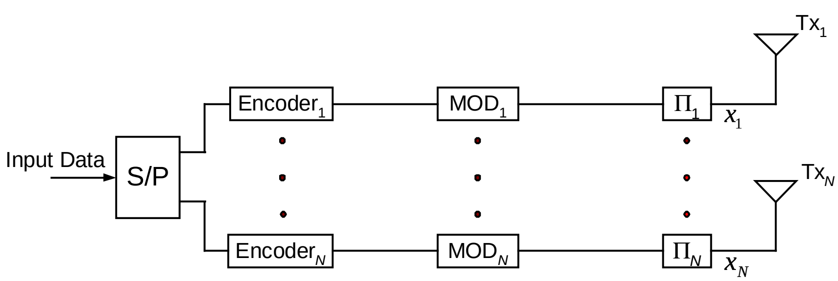

(a) HLST

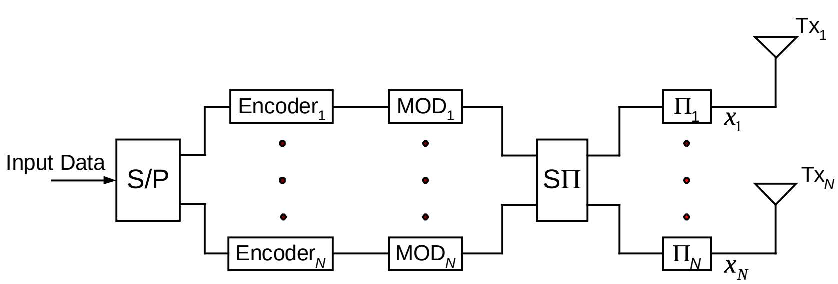

(b) DLST / TLST

Figure 2.3 Different LST architectures

The LST architecture with error control coding is shown in Figure 2.3(a), namely the horizontal layered space-time (HLST) or horizontal BLAST (H-BLAST) structure. In Figure.3 (a), the input data is first de-multiplexed into N sub-streams. Each sub-stream is independently encoded by a 1-D encoder, modulated, interleaved by a time interleaver (Π) and then transmitted by a particular transmit antenna. If the time interleaver output symbols are denoted by x_t^i, where i represents the layer number and t is the time interval. The transmission signal matrix, formed from time interleaver output symbols, denoted by $\mathbf{X}$, is given by

$$\mathbf{X} = \left[x_t^i\right] \tag{2.8}$$

For instance, in a system with four transmit antennas; the transmission signal matrix $\mathbf{X}$ is given by

$$\mathbf{X} = \begin{bmatrix} x_1^1 & x_2^1 & x_3^1 & x_4^1 & x_5^1 & \mathbf{L} \\ x_1^2 & x_2^2 & x_3^2 & x_4^2 & x_5^2 & \mathbf{L} \\ x_1^3 & x_2^3 & x_3^3 & x_4^3 & x_5^3 & \mathbf{L} \\ x_1^4 & x_2^4 & x_3^4 & x_4^4 & x_5^4 & \mathbf{L} \end{bmatrix} \tag{2.9}$$

In this case, the sub-stream of each layer is encoded horizontally. However, utilizing only a 1-D encoder after S/P conversion with time interleaver and simultaneously transmitting the signal from transmit antennas, the HLST scheme will suffer from the presence of sub-channels in deep fade.

To improve the system performance a spatial interleaver is added into the HLST structure, resulting in diagonal layered space-time (DLST) or diagonal BLAST (D-BLAST) and threaded layered space-time (TLST) structures, as shown in Figure. 2.3 (b). In the DLST structure, after modulation, the modulator outputs are distributed among the N antennas along the diagonal of the transmission arrays and followed by time interleaving. The interleaved outputs are then transmitted simultaneously by all transmit antennas. For example, in the DLST system with four transmit antennas, the transmission matrix is formed from matrix $\mathbf{X}$ in Equation (2.9) by delaying the *i*-th row entries by (*i* - 1) time unit, as shown in (2.10)

$$\overline{\mathbf{X}} = \begin{bmatrix} x_1^1 & x_2^1 & x_3^1 & x_4^1 & x_5^1 & x_6^1 & x_7^1 & x_8^1 & \mathbf{L} \\ 0 & x_1^2 & x_2^2 & x_3^2 & x_4^2 & x_5^2 & x_6^2 & x_7^2 & \mathbf{L} \\ 0 & 0 & x_1^3 & x_2^3 & x_3^3 & x_4^3 & x_5^3 & x_6^3 & \mathbf{L} \\ 0 & 0 & 0 & x_1^4 & x_2^4 & x_3^4 & x_4^4 & x_5^4 & \mathbf{L} \end{bmatrix} \tag{2.10}$$

The entries below the diagonal are padded by zeros. Then the first diagonal is transmitted from the first transmit antenna, the second diagonal from the second antenna, the third diagonal from the third antenna, the fourth diagonal from the fourth antenna and the fifth diagonal from the first antenna, and so on. Then, the data in each layer share a balanced presence over all the N paths to the receiver. Therefore, none of the individual sub-streams is hostage to the worst of the N paths. As a consequence, all sub-streams undergo, on average, the same channel. This process can be represented as a spatial interleaver $(\mathbf{S}\Pi)$ as shown in Figure 2.3(b) The DLST utilizes multi-element antenna arrays at both transmitter and receiver and an elegant diagonally layered coding structure in which code blocks are dispersed across diagonals in space and time.

For example, for a D-BLAST system with four layers, the spatial interleaving process for the modulated output matrix, $\overline{\mathbf{X}}$, in Equation (2.10) can be written as

$$\tilde{\tilde{\mathbf{X}}} = \begin{bmatrix} x_1^1 & x_1^2 & x_1^3 & x_1^4 & x_5^1 & x_5^2 & x_5^3 & x_5^4 & \mathbf{L} \\ 0 & x_2^1 & x_2^2 & x_2^3 & x_2^4 & x_6^1 & x_6^2 & x_6^3 & \mathbf{L} \\ 0 & 0 & x_3^1 & x_3^2 & x_3^3 & x_3^4 & x_7^1 & x_7^2 & \mathbf{L} \\ 0 & 0 & 0 & x_4^1 & x_4^2 & x_4^3 & x_4^4 & x_8^1 & \mathbf{L} \end{bmatrix} \begin{matrix} \rightarrow & \mathrm{Tx}_1 \\ \rightarrow & \mathrm{Tx}_2 \\ \rightarrow & \mathrm{Tx}_3 \\ \rightarrow & \mathrm{Tx}_4 \end{matrix} \tag{2.11}$$

where $\tilde{\tilde{\mathbf{X}}}$ represents the spatial interleaver output matrix, x_t^i are the modulator output symbols, i represents the layer number and t is the time interval. Note that successive symbols of every layer follow a diagonal pattern over space and time. This pattern repeats itself after N discrete time instants. However, since at the beginning of the transmission process not all the symbols from all the layers are available, zero padding is necessary to complete the pattern, as shown in Equation (2.11). This reduces the spectral efficiency of the system. However, this scheme introduces space diversity and achieves a better performance than the HLST scheme. In an independent Rayleigh scattering environment, this processing structure leads to theoretical rates that grow linearly with the number of antennas and approach 90% of Shannon capacity [42].

A threaded layered space-time (TLST) structure [44] is obtained from the HLST by introducing a spatial iterleaver $(\mathbf{S}\Pi)$ prior to the time interleaver, as shown in Figure. 2.3(b). The transmitter structure differs from DLST in that the transmitted symbols are not periodically cycled among the N antennas and they are first fed into a spatial interleaver, followed by the time interleaver and then transmitted by all the transmit antennas. In a system with four transmit antennas, the output of $\mathbf{S}\Pi$, denoted by $\overline{\mathbf{X}}$, is given by

$$\overline{\mathbf{X}} = \begin{bmatrix} x_1^1 & x_2^4 & x_3^3 & x_4^2 & x_5^1 & \mathbf{O} \\ x_1^2 & x_2^1 & x_3^4 & x_4^3 & x_5^2 & \mathbf{O} \\ x_1^3 & x_2^2 & x_3^1 & x_4^4 & x_5^3 & \mathbf{O} \\ x_1^4 & x_2^3 & x_3^2 & x_4^1 & x_5^4 & \mathbf{O} \end{bmatrix} \begin{matrix} \rightarrow & \mathrm{Tx}_1 \\ \rightarrow & \mathrm{Tx}_2 \\ \rightarrow & \mathrm{Tx}_3 \\ \rightarrow & \mathrm{Tx}_4 \end{matrix} \tag{2.12}$$

The transmitted symbols appear to have been threaded over time and across the transmit antennas. The spectral efficiency of the HLST and TLST schemes is RmN, where R is the code rate and m is the number of bits in a modulated symbol, while the spectral efficiency of DLST is slightly reduced due to the zero padding in the transmission matrix.

It is shown that the structures of DLST and TLST are very similar. The difference is the spatial interleaving process. The spatial interleaver pattern in Equation (2.11) presents the operation in the case of DLST and the spatial interleaver pattern in Equation (2.12) is an operation of TLST. Finally, the SM has been introduced only with respect to the transmitter structure required for its implementation. However, a SM technique cannot deliver the promised very high spectral efficiency without employing a suitable detection technique at the receiver. Some of these will be described later in this chapter. Moreover, in SM structures, different signals transmitted from different antennas are received simultaneously at each receive antenna and therefore they need an individual detector. As a result, the CCI is the most prominent problem in SM systems. Mitigation is one of the main objectives of the employed detection technique.

Layered Space-Time Receivers

The challenge in the detection of the layered space-time (LST) signal is to design a low complexity detector, which can efficiently remove the co-channel interference (CCI) and approach the interference-free bound. The iterative receiver is one of the effective receivers, which can efficiently suppress and remove the CCI by using suppression and cancellation techniques. The iterative receiver is based on the turbo coding principle [45], which is a joint detection and decoding scheme [9, 46]. Block diagrams of the iterative receivers for LST structures are shown in Figure. 2.4.

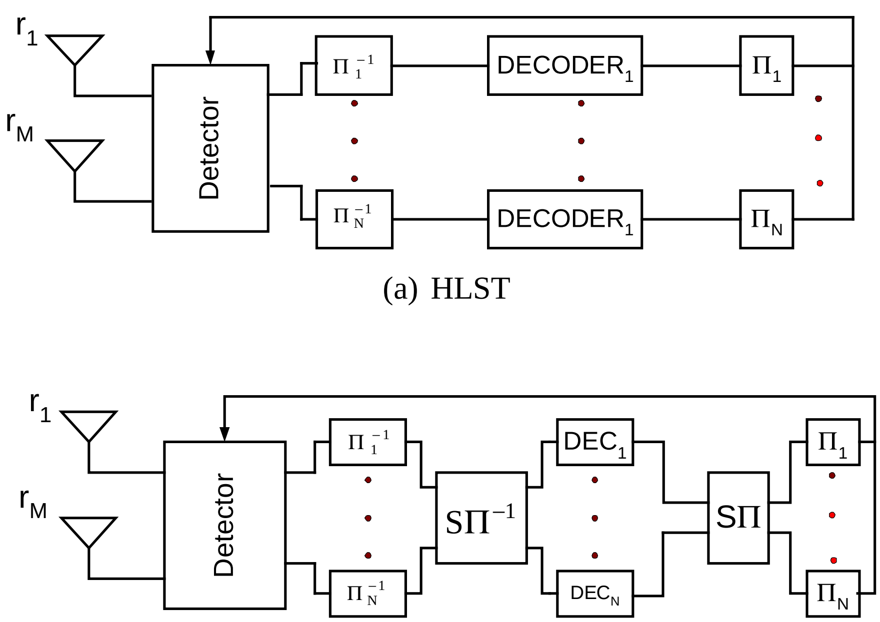

(a) HLST

(b) DLST/TLST

Figure. 2.4 Block diagrams of LST receivers

In Figure. 2.4 (a), each of the detected sequences is decoded by a separate channel decoder with soft inputs/soft outputs. At each iteration, the decoder soft outputs are used to update a priori probabilities of the transmitted signals. These undated probabilities are then used to calculate the symbol estimate in the detector. Each of the coded streams is independently interleaved to enable receiver convergence. Apart from the time interleaving/deinterleaving there is a space interleaving/deinterleaving across transmit antennas as shown in Figure. 2.4 (b).

The decoder can apply a number of soft output decoding algorithms, such as a maximum a posteriori (MAP) algorithm or a soft output Viterbi algorithm (SOVA) [19]. The MAP decoder is optimum in the sense that it minimizes the bit error probability at the decoder output. Although SOVA has a lower complexity, it has a somewhat degraded performance compared to the MAP decoder. This becomes a very important advantage of the MAP algorithm for the iterative decoding algorithm. We also use the MAP decoder in the adaptive iterative receiver structure throughout this thesis. The brief detail of the MAP decoder will be discussed in next section.

2.3.3 Convolutional Codes and MAP Decoding Principles

Most of the materials in this section are adopted from [19]. The (n, k, m) convolutional code can be implemented as a k input n, $(n > k)$ output linear sequence circuit with input memory m. The structure introduced to the signal by the convolutional code is defined by the generator polynomials which describe the connections between the encoder inputs and outputs. The performance of the code depends on a code rate, defined as $R = \frac{k}{n}$, and a code memory m. Figure. 2.5 shows the encoder for the example of binary (2,1,2) code with generator polynomial $(5_8, 7_8)$. The encoder equations can be written as

$$\mathbf{v}^1 = \mathbf{u} * \mathbf{g}^1, \quad \mathbf{v}^2 = \mathbf{u} * \mathbf{g}^2 \tag{2.13}$$

where $*$ denotes the convolution and all operations are modulo-2.

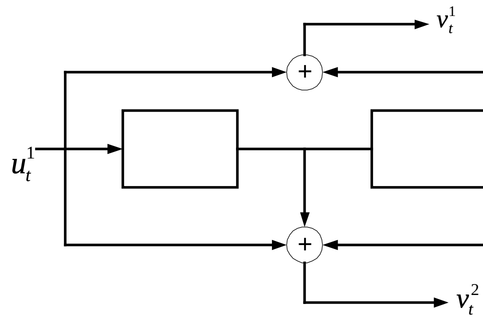

Figure. 2.5 Encoder for a binary (2,1,2) convolutional code.

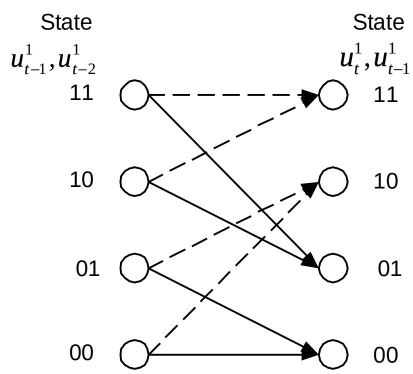

Figure. 2.6 One stage in the trellis diagram for binary (2,1,2) convolutional code

A convenient and common way of describing encoding and decoding operations is using trellis diagrams. A trellis stage for an input at time t for binary (2,1,2) code is shown in Figure. 2.6. A trellis diagram consists of N such stages, where N is the number of input words, each consisting of k input data bits. The stage of the encoder is defined as the content of its shift register. For the encoder with total memory K, the stage number is 2^K. Each new block of k inputs causes the transition to a new stage. That is, there are 2^K branches leaving each stage. Each branch is labeled the k input causing the transition at time unit t, denoted by $\mathbf{u}_t = \lfloor u_{t,1}, u_{t,2}, \mathbf{K}, u_{t,k} \rfloor$ and n corresponding to outputs, denoted by $\mathbf{v}_t = \lfloor v_{t,0}, \mathbf{K}, v_{t,n-1} \rfloor$.

Given that $\mathbf{r}$ is received, the conditional error probability of the decoder is defined as

$$P(E|\mathbf{r}) = P(\hat{\mathbf{u}} \neq \mathbf{u}) = P(\hat{\mathbf{v}} \neq \mathbf{v}) \tag{2.14}$$

The probability of error in the decoder is then given by

$$P(E) = \sum_{\mathbf{r}} P(E|\mathbf{r}) P(\mathbf{r}) \tag{2.15}$$

The term $P(\mathbf{r})$ is independent of the decoding algorithm, so the minimum probability of error in Equation (2.15) is achieved by minimizing $P(E|\mathbf{r}) = P(\hat{\mathbf{v}} \neq \mathbf{v}|\mathbf{r})$ for all **r.** This is equivalent to maximizing the $P(\hat{\mathbf{v}} = \mathbf{v}|\mathbf{r})$. That is, the decoder searches for $\hat{\mathbf{v}}$ which maximizes

$$P(\hat{\mathbf{v}} = \mathbf{v}|\mathbf{r}) = \frac{P(\mathbf{r}|\mathbf{v}) P(\mathbf{v})}{P(\mathbf{r})} \tag{2.16}$$

If the coded sequences are all equally likely, then for a discrete memories channel the optimal decoding maximizes

$$P(\mathbf{r}|\mathbf{v}) = \prod_{i} P(r_i|v_i) \tag{2.17}$$

It is convenient to consider the algorithm of the expression in Equation (2.17) As $\log x$ is a monotone increasing function, maximizing the expression in Equation (2.17) is equivalent to maximizing

$$\log P(\mathbf{r}|\mathbf{v}) = \sum_{i} \log P(r_i|v_i) \tag{2.18}$$

The function $\log P(\mathbf{r}|\mathbf{v})$ is known as log-likelihood function.

Map Decoding Algorithm

The maximum a posteriori probability (MAP) algorithm uses a decoding criteria that minimizes the bit error probability and is usually implemented by using a forward and backward recursion algorithm. It operates on a trellis representation of the code as shown in Figure. 2.6. This decoder algorithm is very important for the iterative decoding algorithm.

The soft-output MAP decoder calculates the a posteriori log-likelihood ratio for data bit u_t as

$$\Lambda(u_t) = \log \frac{P\{u_t = 1|\mathbf{r}\}}{P\{u_t = 0|\mathbf{r}\}} \tag{2.19}$$

Where $P\{u_t = i|\mathbf{r}\},\ i = 0,1$ is the a posteriori probability (APP) of the data bit u_t.
The decoder makes the hard decision by comparing $\Lambda(u_t)$ to zero

$$\Lambda(u_t) = \begin{cases} 1, & \text{if } \Lambda(u_t) > 0 \\ 0, & \text{ortherwise} \end{cases} \tag{2.20}$$

The APPs in Equation (2.19) can be computed from the trellis diagram as

$$P\{u_t = 0|\mathbf{r}\} = \sum_{(m',m)\in B_t^0} P\{S_{t-1} = m', S_t = m|\mathbf{r}\} \tag{2.21}$$

$$P\{u_t = 1|\mathbf{r}\} = \sum_{(m',m)\in B_t^1} P\{S_{t-1} = m', S_t = m|\mathbf{r}\} \tag{2.22}$$

where S_{t-1} and S_t are the encoder stages at time *t*-1 and *t*, respectively, and B_t^0 and B_t^1 are set of transitions from state m' to stage m caused by $u_t = 0$ and $u_t = 1$, respectively. Equation (2.21) and (2.22) can be written as

$$P\{u_t = 0|\mathbf{r}\} = \sum_{(m',m)\in B_t^0} \frac{P\{S_{t-1} = m', S_t = m|\mathbf{r}\}}{P(\mathbf{r})} \tag{2.23}$$

$$P\{u_t = 1|\mathbf{r}\} = \sum_{(m',m)\in B_t^1} \frac{P\{S_{t-1} = m', S_t = m|\mathbf{r}\}}{P(\mathbf{r})} \tag{2.24}$$

where $P(\mathbf{r})$ is a constant. Since it does not affect the maximization, it will be dropped in further derivations.

In order to efficiently calculate the information bits APPs, the following probability functions are defined [19]

$$a_t(m) = P\{S_t = m, \mathbf{r}_1^t\} \tag{2.25}$$

$$b_t(m) = P\{\mathbf{r}_{t+1}^N | S_t = m\} \tag{2.26}$$

$$g_t^i(m', m) = P\{u_t = i, S_t = m, \mathbf{r}_t | S_{t-1} = m'\} \tag{2.27}$$

where
$$\mathbf{r}_t = (r_{t,0}, \mathbf{K}, r_{t,i}, \mathbf{K}, r_{t,n-1}) \tag{2.28}$$

$$\mathbf{r}_t^k = (\mathbf{r}_t, \mathbf{r}_{t+1}, \mathbf{K}, \mathbf{r}_k) \tag{2.29}$$

The joint transition probability, $P\{S_{t-1} = m', S_1 = m, \mathbf{r}\}$, can be expressed as

$$P\{S_{t-1} = m', S_1 = m, \mathbf{r}\} = a_{t-1}(m) \sum_{i\in 0,1} g_t^i(m', m) b_t(m) \tag{2.30}$$

where $a_t(m)$ and $b_t(m)$ are obtained recursively as

$$a_t(m) = \sum_{m'} a_{t-1}(m) \sum_{i\in 0,1} g_t^i(m', m) \tag{2.31}$$

$$b_t(m) = \sum_{m'} b_{t+1}(m) \sum_{i\in 0,1} g_t^i(m', m) \tag{2.32}$$

and $g_t^i(m', m)$ is a channel transition probability weighted by the information bit a priori probability $p_t(u_t = i), i = 0,1$, where u_t is the information symbol associated with transition $S_{t-1} = m' \to S_1 = m$. Coefficient $g_t^i(m', m)$ can be written as

$$g_t^i(m', m) = p_t(u_t = i) \prod_{j=0}^{j=n-1} P\{r_{t,j} | x_{t,j}\} \tag{2.33}$$

$$P\{r_{t,j} | x_{t,j}\} = \frac{1}{\sqrt{2ps}} e^{-\frac{(r_{t,j} - x_{t,j})^2}{2s^2}} \tag{2.34}$$

where $x_{t,j}$, $j = 0, \mathbf{K}, n-1$, is a BPSK modulated symbol in the codeword associated with transition $S_{t-1} = m' \to S_1 = m$.

If we assume that the encoder starts and ends in a zero stage the boundary conditions are

$$a_0(0) = 1, \quad a_0(m) = 0, \text{ for } m \neq 0 \tag{2.35}$$

$$b_N(0) = 1, \quad b_N(m) = 0, \text{ for } m \neq 0 \tag{2.36}$$

The log-likelihood ration now can be written as

$$\Lambda(u_t) = \log \frac{\sum_{(m',m)\in B^1} a_{t-1}(m')g_t^1(m',m)b_t(m)}{\sum_{(m',m)\in B^0} a_{t-1}(m')g_t^0(m',m)b_t(m)} \tag{2.37}$$

The above algorithm is usually referred to as a forward /backward algorithm, since the coefficients $a_t(m)$ are calculated recursively starting from the beginning of the trellis, and the $b_t(m)$ coefficients are calculated recursively starting from the end of the trellis.

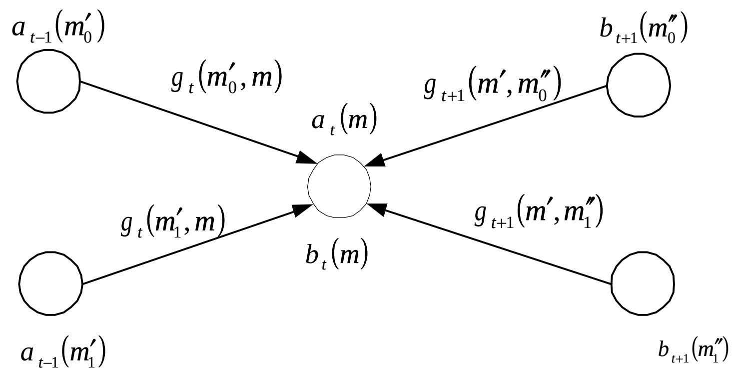

Figure. 2.7 Graphical representation of the forward and backward recursions

Figure. 2.7 shows the graphical representation of the forward and backward recursion. In this figure $a_{t-1}(m_i')$ represents a coefficients for state m_i' in the (t-1)th stage which is connected with stage m in t-th trellis stage and where the transition $S_{t-1} = m' \rightarrow S_1 = m$ is caused by the information bit $u_t = i,\ i = 0{,}1$. Similarly, the $b_{t+1}(m'')$ denotes b coefficient for stage m'' in the (t-1)th trellis stage which is connected with stage m in t-th trellis stage and where the transition $S_{t-1} = m' \rightarrow S_1 = m$ is caused by the information bit $u_t = i,\ i = 0{,}1$. The a posteriori probabilities if the information bits can be calculated as

$$P\{u_t = 1|\mathbf{r}\} = \frac{e^{\Lambda(u_t)}}{1 + e^{\Lambda(u_t)}} \tag{2.38}$$

$$P\{u_t = 0|\mathbf{r}\} = \frac{1}{1+e^{\Lambda(u_t)}} \tag{2.39}$$

The a posteriori probabilities of the transmitted bits can be calculated by adding the probabilities of the codeword that contain a particular transmitted bit. That is,

$$P\{x_{t,j} = 1|\mathbf{r}\} = \sum_{u_t = i, x_{t,j} = 1} P\{u_t = i|\mathbf{r}\} \tag{2.40}$$

$$P\{x_{t,j} = -1|\mathbf{r}\} = \sum_{u_t = i, x_{t,j} = -1} P\{u_t = i|\mathbf{r}\} \tag{2.41}$$

2.4 Multiuser Systems

The description of MIMO wireless systems up to this point has focused on single communication links between a transmitter and a receiver, also called point-to-point communications. However, in reality, in wireless communication systems, where bandwidth is a limited resource, it is necessary to find some solution for sharing this resource amongst multiple users. There are various types of multiple user communication systems, where multiple users can access the channel and transmit information through the channel to the receiver. In this thesis, only two types of multiuser communication systems are considered, multiple access channel (MAC) and broadcast channel (BC). MAC scenario is often referred to as uplink transmission. A number of users share a common channel to transmit information to a receiver. As an example, in a mobile cellular communication system, the users are the mobile transmitter in the cell and the receiver is in the base station. On the other hand, BC scenario is also known as a downlink transmission. A single transmitter transmits information to a number of receivers. In a mobile communication system, the transmitted signal might be sent independently to all users or simultaneously to different users.

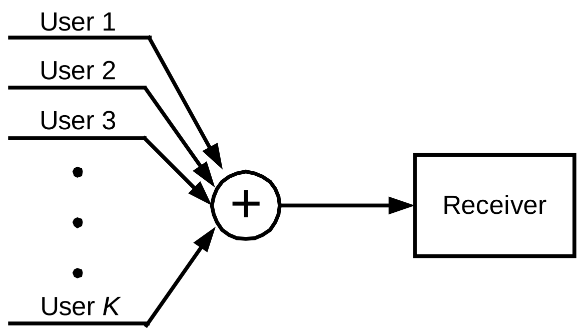

Figure. 2.8 Multiple users communication systems

The multiple user communication scenario is depicted in Figure. 2.8. There are several techniques to accommodate multiple users in a system, whether it is MAC or BC scenarios. The most well known methods, which have been implemented in current wireless communication systems, are Frequency Division Multiple Access (FDMA), Time Division Multiple Access (TDMA) and CDMA techniques.

2.4.1 Multiple Access Techniques

In the FDMA technique, the available channel bandwidth is separated into a number of frequency non-overlapping sub-channels. Each sub-channel is then allocated to each user upon request by the user. However, in a TDMA system, each user who wishes to transmit information is designated a specific time slot within each transmitted frame. In these two schemes the channel is partitioned into independent single-user sub-channels. Therefore, the design methods described in the previous sections of this chapter are directly applicable to multiple access systems employing FDMA and TDMA scenarios, since each user is effectively transmitting and receiving information independently from other users. On the other hand, these two schemes might be strongly inefficient when the nature of data transmitted from users is in bursts. Therefore a user occupies only a fraction of the total assigned time or frequency resources for transmitting information. If the periods of silence become much greater than the transmission periods, the FDMA and TDMA techniques cannot efficiently share the available resources. The alternative to the FDMA and TDMA is to allow all current active users in the system to access the total available channel bandwidth, or part of it, at the same time. This is the basic concept of CDMA systems.

In a CDMA [47] system, each user is assigned a distinct code sequence (signature sequence). Each transmitter sends its data stream by modulating it with their own signature sequence that allows the user to spread the information signal across the available assigned frequency band. Since the signature sequences have fairly low mutual crosscorrelation, a CDMA receiver can detect its own data using the corresponding signature sequence, although the multiple users' signals overlap both in frequency and in time in a random manner. The system model for a CDMA system will be described in detail in the next chapters. However, it is clear that the design of the spreading codes strongly influence the performance of CDMA systems. Therefore, the signature sequence should be carefully designed to achieve low crosscorrelation between users [48]. For ease of generation and synchronization, a signature sequence is pseudo random, meaning that it can be generated by mathematically precise rules, but statistically it satisfies the requirements of a truly random sequence.

A binary sequence, which has zero cross-correlation is the Walsh-Hadamard sequence. However, for a given code length or spreading length L, there are only L distinct and orthogonal sequences, which make it possible to accommodate up to L users in the system. The operation of spreading reduces the data rate of the information bearing by a factor of L, because each information symbol is copied L times and multiplied by the spreading code before transmission. However, the spread signal is transmitted at a higher rate, called the chip rate. Perfect detection of the desired signal can be obtained if all users transmit the spread signals simultaneously and symbols synchronously under a flat fading channel without any delay amongst the signals. Therefore, this technique seems to be suitable to BC scenarios, where the base station can perform synchronization, that is spreading and summation of all the users' signals prior to transmission. However, it is impossible to have the perfect detection even in BC scenarios due to the multi-path fading channel in the system. The signal at the receiver is the summation of all signals arriving at the receive antenna from different directions, which destroys the orthogonality of the spreading sequences. It reduces the auto-correlation of the spreading sequence and increases cross-correlation of the spreading sequence introducing multiple access interference (MAI) into the system. This is a limitation of all types of spreading sequences, especially Walsh-Hadamard sequences. Therefore, the Walsh-Hadamard sequence is not the best solution, for either the MAC or BC. Therefore, the auto-correlation and cross-correlation are two main important properties of spreading sequences. The well known good codes are the Pseudo-Noise (PN) the Gold [49, 50] and the Kasami [51] sequences. The periodic auto-correlation of these codes is very good for high values of spreading sequence length and their periodic cross-correlation is upper bounded by a relatively low value.

There are two types of spreading sequences, namely short and long codes. The spreading sequence is called a short code if it is the same for every data symbol period, where its repetitive period is equal to the symbol period. However, if the period of the PN sequence is larger than the symbol period, this kind of PN sequence is called a long sequence. Long sequences can support more users than short sequences. However, the MMSE multi user detection technique can be only used in short code systems. The Gold sequences with the short code are used throughout this thesis.

In a MIMO frequency selective CDMA communication system, the CCI deteriorates the performance of the system, because in general, different sub-channels between a transmitter and a receiver may have different delay profiles, hence causing additional loss in the orthogonality of the spreading sequences.

DS-CDMA Transmitter

In a K- users synchronous CDMA system, there are K users in the system as shown in Figure(2.9) the received signal, defined by $r(t)$, consists of the sum of all users' spread signals embedded in additive white Gaussian noise (AWGN) is given by

$$r(t) = \sum_{k=0}^{K} s^k(t) A^k x^k + n(t), \qquad t = [0, T] \tag{2.42}$$

where T is the data symbol period. The signature waveform, defined as $s^k(t)$, assigned to the ***k***-th user can be represented as

$$s^k(t) = \sum_{n=1}^{N} s^k(n) q(t-(n-1)T_C) \qquad (2.43)$$

where $s^k(n)$ denoted the ***n***-th chip value of s^k, $q(t)$ is the chip waveform and T_C is the chip interval, $s^k(t)$ is normalized to have unit energy as given by

$$\left\|s^k\right\|^2 = \int_0^T s^{k^2}(t)dt = 1 \qquad (2.44)$$

The signature waveforms are assumed to be zero outside the interval $[0,T]$, and hence there is no inter-symbol interference (ISI). A^k is the received amplitude of the ***k***-th users' signal. A^{k^2} is referred to as the energy of the ***k***-th user. $b^k \in [-1,+1]$ is the symbol transmitted by the ***k***-th user and $n(t)$ is additive white Gaussain noise with zero mean and variance s^2.

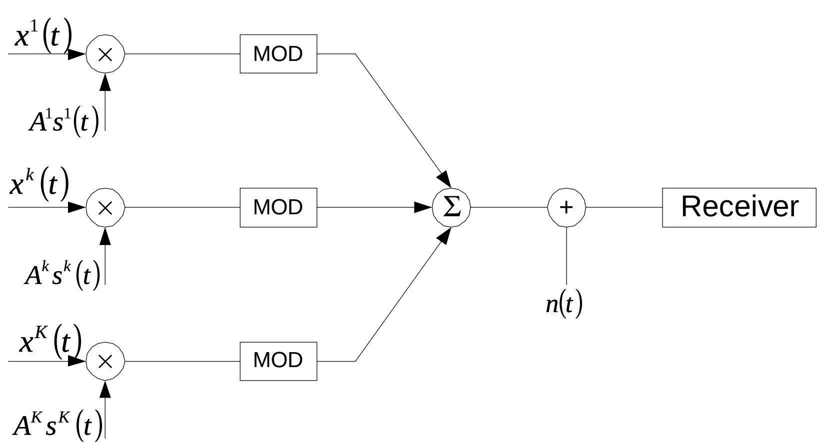

Figure 2.9 DS-CDMA Model

The received signal, denoted by $\mathbf{r}$, can be written in a matrix form as

$$\mathbf{r} = \mathbf{SAx} + \mathbf{n} \tag{2.45}$$

where

$$\mathbf{r} = \left[r(1), r(2), \ldots, r(N)\right]^T \tag{2.46}$$

and

$$\mathbf{S} = \begin{bmatrix} s^1(1) & s^2(1) & \cdots & s^K(1) \\ s^1(2) & s^2(2) & \cdots & s^K(2) \\ \vdots & \vdots & \ddots & \vdots \\ s^1(N) & s^2(N) & \cdots & s^K(N) \end{bmatrix} \tag{2.47}$$

$$\mathbf{A} = diag\left[A^1, A^2, \ldots, A^K\right] \tag{2.48}$$

$$\mathbf{b} = \left[b^1, b^2, \ldots, b^K\right]^T \tag{2.49}$$

$$\mathbf{n} = \left[n(1), n(2), \ldots, n(N)\right]^T \tag{2.50}$$

where N is number of data frame length.

2.5 Detection Techniques

It is well known that the simple receiver for a SISO communication signal corrupted by AWGN is a Matched Filter (MF) sampled periodically at the symbol rate. These samples constitute a set of sufficient statistics for estimating the digital information that was transmitted. If signal samples at the output of the MF are corrupted by ISI, an equalizer will further process the symbol space samples. In the presence of channel distortion, such as channel multi-path, the MF must also be matched to the CIR. However, in practice, the CIR is usually unknown. One approach is to estimate the CIR from the transmission of a sequence of known symbols and to implement the MF using the estimate of the CIR.

Several types of detectors for MIMO channel signal transmission have been studied. Zero-forcing (ZF), MMSE linear receiver and Maximum likelihood sequence estimation (MLSE) techniques can be utilized directly to detect the transmitted signal. However, these techniques use a straight matrix inversion, which requires the knowledge of channel state information at the receiver. Also, the computational complexity is high, especially the computational complexity of MLSE [52] [53] , which grows exponentially with the sum of the channel memory length of each simultaneous user. Another alternative to reducing the computational complexity is an adaptive receiver structure [54] [15] [55]. Moreover, to mitigate the effects of an ISI resulting from a time dispersive channel, such as multi-path fading channels, which are frequency selective, an equalizer is required. The equalizer also effectively reduces MAI in a multiuser system. In addition, transmit diversity techniques are not generally designed for time dispersive channels, where the presence of ISI and MAI introduce unwanted interference from the CCI across the signals transmitted by different antennas. The CCI always occurs in the BLAST system where different data streams are transmitted in the same channel and hence use the same resources in time and frequency.

The conventional detector for CDMA systems over SISO channels is a matched filter. However, the conventional MF detector is not optimal due to the MAI and is also not near-far resistant. Power control is introduced to alleviate the near-far effect. Although ideal power control is difficult to implement, stringent power control is necessary to ensure that users have almost identical signal power at the base station. The conventional detector treats the MAI as AWGN. This is a reasonable approach because CDMA interference consists of contributions from independent interferers. The MAI can be defined through the cross-correlation matrix amongst users. Verdu [56] showed that the near-far effect is overwhelming on other users' signal powers over the desired users' signal power, and is a limitation of the CDMA system. He also showed that this problem could be solved using an optimal multiuser ML detector, and provide a significant capacity improvement over the conventional MF or single-user detector. However, it comes at the cost of huge computational complexity. The computational complexity increases exponentially with the number of active users and the data block length, and leads to impractical implementation. Therefore, a number of sub-optimal multiuser receivers to enhance the detection performance have been studied. Multiuser detectors can be classified into the following two main categories.

Linear detectors – a linear transformation is applied to the soft outputs of the bank of the MFs in order to produce a new set of decision variables with MAI partially or totally decoupled. This is a one-step process, where all the users' signals are simultaneously detected, generally by jointly equalizing the multiple interfering signals.

Interference cancellation detector – a linear or non-linear decision function is applied to the soft outputs of the MFs in order to produce a reliable estimate of MAI. The estimated MAI is then cancelled from the received signals prior to symbol detection of the desired signal. This process is generally repeated in multiple steps, until the MAI is completely or partially removed from the received signal.

However, in designing a multiuser detector for frequency selective MIMO channels, the knowledge of the MAI characteristics, such as the spreading sequences of all users in the CDMA system and the availability of the CSI at the receiver, must be jointly taken into account in order to mitigate MAI, ISI and CCI. A brief description of the most common sub-optimal detectors for a point-to-point transmission communication system is given. An extension to the multiuser systems will be given in detail in the next chapter.

2.5.1 Linear Detectors

Matched Filter for CDMA systems

The simplest approach to demodulate CDMA signal is the single user matched filter (MF). This is the demodulator that first implemented in CDMA receivers. The structure of for single input single output (SISO) CDMA MF [56] is illustrated in Figure (2.10)

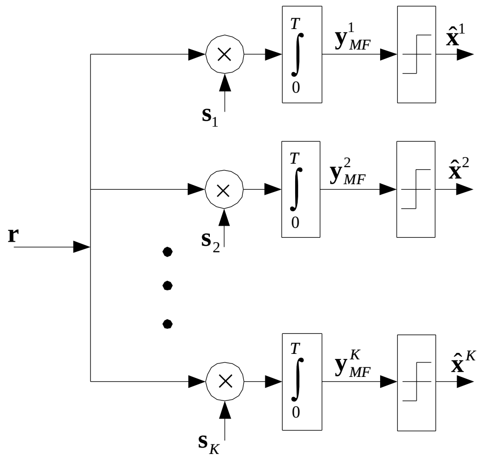

Figure 2.10 Matched filter for CDMA systems

To detect a user's signal that transmitted from the DS-CDMA transmitter shown in Figure (2.11), the filter for a given user is matched to its signal waveform [56].

$$y_{MF}^{k} = \int_{0}^{T} s^{k}(t) r(t) dt \quad = \quad A^{k} b^{k} + \sum_{j \neq k} A^{k} r^{j,k} b^{j} + n'^{k} \tag{2.51}$$

where $r(t)$ and $s^{k}(t)$ are defined in Equation (2.42) and (2.43), respectively.

and

$$n'^{k} = \int_{0}^{T} s^{k}(t) n(t) dt \tag{2.52}$$

$r^{j,k}$ is the crosscorrelation between the ***j***-th and ***k***-th user, given by

$$r^{j,k} = \int_{0}^{T} s^{j}(t) s^{k}(t) dt \tag{2.53}$$

Assuming that hard decisions are made on the received signal, the output of the MF detector is

$$\hat{x}^k = \mathrm{sgn}\left(y_{MF}^k\right) = \mathrm{sgn}\left(A^k b^k + \sum_{j \neq k} A^k r^{j,k} b^j + n'^k\right) \qquad (2.54)$$

where $\sum_{j \neq k} A^k r^{j,k} b^j$ is the multiple access interference (MAI) introduced in the *k*-th user's signal. It is clearly shown that if the summation of the absolute value of noise and MAI is larger than that of the data, an error is possibly occurred.

The MF output in Equation (2.54) can also be express in matrix form

$$\mathbf{y}_{MF} = \mathbf{S}^T \mathbf{r} = \mathbf{S}^T \mathbf{SAb} + \mathbf{n}' = \mathbf{RAb} + \mathbf{n}' \qquad (2.55)$$

where

$$\mathbf{y}_{MF} = \left[y_{MF}^1, y_{MF}^2, \mathbf{L}, y_{MF}^K\right]^T \qquad (2.56)$$

$$\mathbf{n}' = \left[n'^1, n'^2, \mathbf{K}, n'^K\right]^T \qquad (2.57)$$

and

$$\mathbf{R} = \mathbf{S}^T \mathbf{S} = r^{i,j}, \quad i, j = 1,2, \mathbf{K}, K \qquad (2.58)$$

$\mathbf{R}$ becomes correlation matrix if $r^{i,j} = 1$, $i = j$, and $\mathbf{R}$ is a crosscorrelation matrix if $r^{i,j} = r^{j,i}$.

MMSE Detector for CDMA Systems

The linear detectors mainly include the zero-forcing detector [5] and the minimum mean square error (MMSE) [6]. The zero-forcing detector multiplies the output of the conventional MF with the inverse of the correlation matrix. The zero-forcing detector output, defined by $\mathbf{y}^{ZF}$, is given by

$$\mathbf{y}_{ZF} = \mathbf{R}^{-1} \mathbf{S}^T \mathbf{r} = \mathbf{Ab} + \mathbf{R}^{-1} \mathbf{S}^T \mathbf{n} \qquad (2.59)$$

The $\mathbf{y}_{ZF}$ fully decouples the multiuser signal. However, it suffers from the noise enhancement [56] as it is shown in the second term of Equation (2.59). Although, the MAI is perfectly removed, this process increases the noise level. In extreme cases, the additional noise may be higher than the MAI. Therefore, the zero-forcing detector performance deteriorates more than the MF.

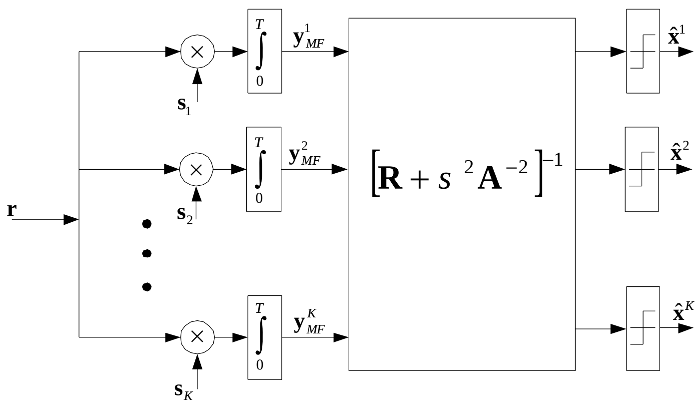

Figure 2.11 MMSE detector for CDMA systems

The MMSE detector can solve the noise enhancement problem of the zero-forcing detector. The structure of the MMSE detector can be depicted in Figure (2.11). The output of the linear MMSE filter [56] for user *k*-th is

$$\mathbf{y}_{MMSE}^{k} = \mathbf{W}^{T}\mathbf{y}_{MF} \tag{2.60}$$

where $\mathbf{W}$ is a matrix of MMSE filter coefficients, and $\mathbf{y}_{MF}$ is the matched filter output vector. The MMSE filter coefficients can be obtained by minimizing the mean square error between the transmitted signal and the detector output

$$z = \min E\left\{\left\|\mathbf{Ab} - \mathbf{W}^{T}\mathbf{y}_{MF}\right\|^{2}\right\} \tag{2.61}$$

Verdu [56] has proved that the solution for the coefficients is

$$\mathbf{W} = \left[\mathbf{R} + s^{2}\mathbf{A}^{-2}\right]^{-1} \tag{2.62}$$

The MMSE detection can be written as

$$\mathbf{y}_{MMSE} = \left[\mathbf{R} + s^{2}\mathbf{A}^{-2}\right]^{-1}\mathbf{S}^{T}\mathbf{r} \tag{2.63}$$

The MMSE detector takes the background noise into account, it generally provides better performance than the zero-forcing detector. However, both the zero-forcing and MMSE detectors require matrix inversion of the correlation matrix. Hence, the computational complexity is very high, especially when the number of user is increased.

Zero-Forcing Detector for MIMO Channel

In the MIMO channel with N transmit and M receive antennas, the zeros-forcing (ZF) detector equalizes the received signal by applying the linear transformation. The output of the ZF receiver , defined by $\mathbf{y}$, [57] is obtained as

$$\mathbf{y} = \mathbf{H}^{\dagger}\mathbf{r} = \mathbf{x} + \mathbf{H}^{\dagger}\mathbf{n} \tag{2.64}$$

where $\mathbf{r}$ is defined by Equation (2.2) and $\mathbf{n}$ is $(M \times 1)$ vector of the AWGN noise with zero mean and noise variance of s^{2}. $\mathbf{H}^{\dagger}$ denotes the Moore-Penrose inverse of the channel matrix $\mathbf{H}$, defined by Equation (2.3). $\mathbf{H}^{\dagger}$ is given by [57]

$$\mathbf{H}^{\dagger} = \begin{cases} \left(\mathbf{H}^{H}\mathbf{H}\right)^{-1}\mathbf{H}^{H} & if \;\; M \geq N \\ \mathbf{H}^{H}\left(\mathbf{H}\mathbf{H}^{H}\right)^{-1} & if \;\; M < N \end{cases} \tag{2.65}$$

where N and M are transmit and receive antennas, respectively.

In MIMO systems, the correlation between the transmit antennas in the system introduces co-channel interference (CCI) as shown in Equation (2.7). Although, the ZF receiver removes the CCI completely, the noise level is increased as shown in the last term in (2.64).

Linear MMSE detector

In the MMSE detection algorithm, the expected value of the mean square error between the transmitted vector $\mathbf{x}$ and linear combination of the received vector $\mathbf{w}^H\mathbf{r}$ is minimized by

$$\min E\left(\mathbf{x}-\mathbf{w}^H\mathbf{r}\right) \tag{2.66}$$

where $\mathbf{w}$ is an $M \times N$ matrix of linear combination coefficients given by [56]

$$\mathbf{w}^H = \left[\mathbf{H}^H\mathbf{H} + s^{\,2}\mathbf{I}_N\right]^{-1}\mathbf{H}^H \tag{2.67}$$

where s is noise variance and $\mathbf{I}_N$ is an $N \times N$ identity matrix. The decision statistics for the symbol sent from antenna ***i*** at time ***t*** is obtained as [20]

$$y_t^i = \mathbf{w}_i^H\mathbf{r} \tag{2.68}$$

where $\mathbf{w}_i^H$ is the ***i***-th row of $\mathbf{w}^H$ consisting of M components. The estimate of the symbol sent by antenna ***i***, denoted by $\tilde{x}_t^i$, is obtained by making a hard decision on y_t^i

$$\tilde{x}_t^i = Q\left(y_t^i\right) \tag{2.69}$$

The above linear equalization methods are based on multiplying the received vector by a detection matrix and then detect the symbols separately. It is obviously shown that the detector only suppresses the interference and calculates the hard decision outputs of all transmit antennas by using Equation (2.69).

To further improve the system performance, a combined interference suppression and interference cancellation techniques is required. For example of the linear MMSE detector, the receiver begins from the antenna N and computes its signal estimate by using Equation (2.68) and Equation (2.69). The received signal form the antenna N is denoted by $\mathbf{r}^N$. To calculate the received signal of the next antenna $(N-1)$, the interference contribution of the hard estimate $\tilde{x}_t^N$ is subtracted from the received signal $\mathbf{r}^N$, and the result, denoted by $\mathbf{r}^{N-1}$ is used to calculate the decision statistic for antenna $(N-1)$ in (2.68), and its hard estimate from (2.69). The process is repeated until the signal for the first antenna is obtained. After detection of the hard estimate $\tilde{x}_t^i$, the received signal for the level $i-1$, denoted by $\mathbf{r}^{i-1}$, is calculated by [20]

$$\mathbf{r}^{i-1} = \mathbf{r}^i - \tilde{x}_t^i \mathbf{h}_i \tag{2.70}$$

where $\mathbf{h}_i$ is the ***i***-th column in the channel matrix $\mathbf{H}$.

Both the MMSE and the decorrelation detector require inversion of the correlation matrix, which costs a significant computational complexity. Therefore, an adaptive detection will be an alternative for a receiver design.

2.5.2 Interference cancellation detectors

Besides the linear detection schemes, researchers have also proposed non-linear detectors that use the interferers' data to detect that of the desired user. Interference cancellation (IC) detectors employ temporary data estimates to reconstruct the interference, and then subtract it from the received signal. The idea of interference cancellation has been mainly applied to cancel the MAI in CDMA systems [58]. However, the same concept could be applied to MIMO systems to improve the detection of each single data stream transmitted from the different transmit antennas. In MIMO systems, the CCI is one of the crucial problems degrading the system performance. The estimate of the interferers is then required at the receiver to reconstruct and subtract from the received signal to improve to the desired signal's detection. This basic approach generally requires multiple stages to recursively refine the mitigation of the interference. In addition, the reliability of the interference estimation is significant for correct interference cancellation. In particular, if the interference estimation is incorrect, the process might dramatically degrade the performance due to error propagation and instability. The IC detectors include two classes, namely successive interference cancellation (SIC) and parallel interference cancellation (PIC).

The SIC based receiver first detects the symbols of an arbitrarily chosen layer using conventional detector schemes such as ZF or MMSE detectors, assuming that the other symbols from the remaining layers are interferences. Upon detection of the chosen symbol, its contribution from the received signal vector is subtracted and the procedure is repeated until all symbols are detected. In the absence of error propagation the SIC converts the MIMO channel into a set of parallel SISO channels with increasing diversity order at each successive stage [33]. In practice, error propagation will be encountered, especially in the absence of an adequate temporal coding for each layer. The error rate performance will be dominated by the first stream decoded by the receiver.

An improved SIC processor is obtained by choosing the stream with the highest signal to interference plus noise ratio (SINR) at each decoding stage. Such a receiver is known as an Ordered SIC (OSIC) receiver or V-BLAST detector [59-62], since they have been used successfully for BLAST architectures. The OSIC receiver reduces the probability of error propagation by realizing a selection diversity gain at each decoding step. However, the OSIC receiver requires slightly higher complexity than the SIC receiver, resulting from the need to compute and compare the SINRs of the remaining streams at each stage. A main problem with the SIC or the OSIC methods for CCI cancellation is the delay inherent in the implementation of the canceller, since it requires one symbol delay per layer [10]. This problem may be alleviated to some extent by devising methods that perform interference cancellation in parallel [11].

As in the SIC receiver, the interference estimates are generated and removed from the received signal before making decisions on the transmitted symbol estimates. On the other hand, the PIC detectors perform the interference estimation and cancellation simultaneously at each stage for all the layers. In [11], P. Patel and J. Holtzman showed that for asynchronous DS-CDMA systems, SIC receivers are superior to PIC receivers in Rayleigh fading channels without power control. However, the PIC based receiver exhibits better performance under ideal power control, since the parallel scheme treats all users fairly and simultaneously. Therefore, if all the users' powers at the receiver are the same, they all experience the same amount of interference. Furthermore, in point-to-point MIMO communication, it is assumed that the signals transmitted from the different antennas have a similar power at the receiver. Alternatively power control techniques can be easily employed, because only users transmit all the symbols. Therefore, the PIC receiver appears to be a better option than SIC detectors when dealing with the CCI. Furthermore, PIC is performed in parallel for all users, the delay required to complete the process is dramatically reduced in comparison with SIC scheme.

The original work on PICs in [11], P. Patel and J. Holtzman employed standard detection techniques at each stage such as MF or linear detectors (decorrelator or MMSE detectors) to estimate the MAI. The interference was then simultaneously removed from all users for the next stage. Between the two stages, demodulation of the users' data and hard decisions were performed to regenerate the MAI. The iteration can be performed as many times as needed. In general, the performance of the detector should continuously improve with an increasing number of iterations. Hence the PIC detection method has been regarded as a promising MUD technique [63-65]. The disadvantage is that the risk of error propagation still exists. The PIC receiver can fully remove the MAI if the temporary decision is correct. However, if the temporary decision is wrong, the error will be increased after the PIC. Therefore the PIC based on hard decisions in each of the iterations carries the risk of oscillation, which means that the performance becomes worse with an increasing number of iterations, especially in the early stages of the iterative process. Accordingly, some schemes have been developed that attempt to guarantee the convergence of the PIC [8, 66-68].

A straightforward enhancement is to use a soft decision rather than a hard decision in each iteration except the last iteration. If an appropriate algorithm is used, the amplitude of a symbol estimate may represent its reliability. The resulting approach is named soft-in soft-out PIC. A similar soft decision-based approach, partial PIC, is proposed in [66-68].

Another approach to the oscillation problem encourages us to try to improve the performance in the first iteration, which is the weakest link. The decorrelating and MMSE detectors are both considered as the first stage of the process.

2.5.3 Adaptive Detectors

Another alternative detection technique is an adaptive signal processing scheme, based on recursive solutions such as the least mean square (LMS) [18, 69] algorithms. The advantages of using adaptive signal processing technique are its capacity to track the channel variations without prior knowledge of channel state information and its simplicity and robustness to the signal.

The LMS algorithm can be attributed to its simplicity and robustness to the signal statistic. Moreover, the LMS algorithm does not require matrix inversion, which has a high computational complexity.

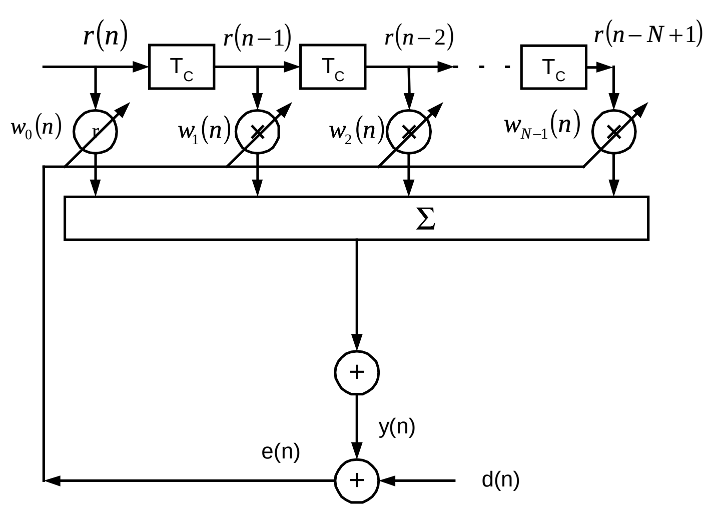

Figure. 2.12 An N-tap transversal adaptive filter.

Consider a transversal filter as in Figure. 2.12. The filter input and tap-weight vector are defined, respectively, by the column vectors [69]

$$\mathbf{r}(n) = [r(n),\ \ r(n-1)\ ,\mathbf{K}, r(n-N+1)]^T \tag{2.71}$$

$$\mathbf{w}(n) = [w_o(n),\ \ w_1(n)\ ,\mathbf{K}, w_{N-1}(n)]^T \tag{2.72}$$

where n denotes the time index and the superscript T stands for transpose. The filter output [18, 69] is

$$y(n) = \sum_{i=0}^{N-1} w_i(n) r(n-i) = \mathbf{w}^T \mathbf{r}(n) \tag{2.73}$$

The optimum tap coefficient vector $\mathbf{w}_0$ is the one that minimizes the mean square error function

$$z\,(n) = E\left[e^2(n)\right] \tag{2.74}$$

where

$$e(n) = d(n) - y(n) \tag{2.75}$$

To adapt the tap coefficient $\mathbf{w}(n)$, $e(n)$ is minimized in the mean square sense. By using a conventional LMS algorithm, which is a stochastic implementation of the steepest descent algorithm, the tap coefficient can be obtained by

$$\mathbf{w}(n+1) = \mathbf{w}(n) - m\nabla e^2(n) \tag{2.76}$$

where m is the algorithm step-size parameter and ∇ is the gradient operator defined as a column vector [69]

$$\nabla = \left[\frac{\partial}{\partial w_0}, \frac{\partial}{\partial w_1}, \mathbf{K}, \frac{\partial}{\partial w_{N-1}} \right]^T \tag{2.77}$$

Note that the *i*-th element of the gradient vector $\nabla e^2(n)$ is

$$\nabla e^2(n) = 2e(n)\frac{\partial e(n)}{\partial w_i} \tag{2.78}$$

Substituting Equation (2.75) in the last factor on the right-hand side of Equation (2.78) and $d(n)$ is independent of w_i, we obtain

$$\frac{\partial e^2(n)}{\partial w_i} = -2e(n)\frac{\partial y(n)}{\partial w_i} \tag{2.79}$$

Substituting for $y(n)$ from Equation (2.73), we get

$$\frac{\partial e^2(n)}{\partial w_i} = -2e(n)r(n-i) \tag{2.80}$$

Using the gradient operator in Equation (2.77), we obtain

$$\nabla e^2(n) = -2e(n)\mathbf{r}(n) \tag{2.81}$$

where $\mathbf{r}(n)$ is defined in Equation (2.71). Therefore the tap coefficient $\mathbf{w}(n)$ can be recursively calculated by [69]

$$\mathbf{w}(n+1) = \mathbf{w}(n) + 2me(n)\mathbf{r}(n) \tag{2.82}$$

Although, the LMS algorithm is simple to implement with low computational complexity, it has a slow convergence speed. To improve the convergence speed of the LMS algorithm, several adaptive algorithms based on the least square error algorithm have been proposed. The partially filtered gradient LMS (PFGLMS) [21] algorithm based on an exponentially weighted least square error is one of the adaptive algorithms, which improve the convergence speed of the LMS algorithm with a slight increase in complexity.

A more accurate estimate of the minimum error function in Equation (2.74) is introduced with exponentially weighted least square errors and defined by [21]

$$z(n) = \frac{1}{2}\sum_{l=0}^{n} l^{t-l} e^{2}(l) \tag{2.83}$$

where l is a forgetting factor ($0 \leq l < 1$). The MSE estimate of Equation (2.83) can be represented as

$$z(n) = l\, z(n-1) + \frac{1}{2} e^{2}(n) \tag{2.84}$$

By taking the derivative of Equation (2.84) with respect to filter tap coefficients, $\mathbf{w}(t)$, then the negative gradient vector, defined by $\mathbf{g}(t)$, can be represented by [21]

$$\mathbf{g}(n) = -\nabla z(n) = l\,\mathbf{g}(n-1) + \frac{1}{2}\mathbf{r}(n)e(n) \tag{2.85}$$

To achieve a more effective estimate of the MSE, the weighted least mean square error is modified as follows

$$z(n) = \frac{1}{2}\left(e^{2}(n) + \sum_{l=0}^{n} l^{n-l} g e_{l}^{2} \right) = \frac{1}{2} e^{2}(n) + \hat{z}(n) \tag{2.86}$$

where

$$\hat{z}(n) = \frac{\left(\sum_{l=0}^{n} l^{n-l} g z_{l}^{2} \right)}{2} \tag{2.87}$$

and γ is a scaling factor ($0 \leq \gamma < 1$), which is required to take a fractional portion of square errors. The negative gradient vector is then given by

$$\mathbf{g}(t) = -\nabla z\ (n) = \mathbf{r}(n)e(n) + \hat{\mathbf{g}}(n) \tag{2.88}$$

with

$$\hat{\mathbf{g}}(n) = \ l\,\hat{\mathbf{g}}(n-1) + g\,\mathbf{r}(n)e(n) \tag{2.89}$$

Therefore the tap coefficient $\mathbf{w}(n)$ can be recursively calculated by

$$\mathbf{w}(n+1) = \mathbf{w}(n) + m_f\,\mathbf{g}(n) \tag{2.90}$$

It is obvious that the LMS adaptive filter scheme is simple to implement with low computational complexity and capable to track the channel variation by recursively updating the filter tap coefficients. The adaptive LMS filter only requires a training sequence to adapt the tap coefficients of the filter. The partially filtered gradient LMS (PFGLMS) [21] algorithm, which has a faster convergence speed, is also applicable to improve the performance of the LMS algorithm with a slight increase in computational complexity. Therefore, the LMS and PFGLMS algorithms will be applied to use for the design of the proposed low complexity adaptive iterative receivers in this thesis.

Chapter 3

Time-domain Adaptive Iterative Receivers for Space-time Coded MIMO Systems

As mentioned in the previous chapter, the performance of layered space-time coding systems is limited by the co-channel interference (CCI), caused by the interference from other layers in the system. To solve this limitation, two main types of receivers, namely non-adaptive iterative and adaptive iterative receivers have been investigated. In this chapter, we consider a communication structure for layered space-time architectures. We focus only on the threaded layered space-time (TLST) structure, in this thesis. A joint iterative detection and decoding scheme based on the turbo principle is described.

An adaptive iterative receiver for threaded layered space-time coded (TLSTC) systems is proposed. The proposed receiver is based on a joint adaptive iterative detection and a decoding algorithm that adaptively suppresses and cancels co-channel interference. The LMS algorithm and Maximum A Posteriori (MAP) algorithm are utilized in the receiver structure. A partially filtered gradient LMS (PFGLMS) algorithm is also applied to improve the convergence speed and tracking ability of the adaptive detector with a slight increase in complexity. The aim of this thesis is to design an adaptive iterative receiver using the turbo decoder, not to design coders or decoders. The reader can obtain a comprehensive introduction to the turbo codes from many research articles [45]. The proposed receiver is analyzed in a slow and fast Rayleigh fading channels in multiple-input multiple-output (MIMO) systems.

3.1 Introduction

Multiple-input multiple output (MIMO) systems have recently emerged as one of the most significant technical advances in modern communications. This technology promises to solve the capacity bottleneck in wireless communication systems [35]. G. J. Foschini. and M. J. Gans showed in [42] that a Diagonal Bell Laboratories Layered Space-Time (DBLAST) MIMO system using a combination of forward error control (FEC) codes can exploit spatial diversity to asymptotically achieve outage capacity. El Gamal et.al., [70] proposed a threaded layered space-time code (TLSTC) structure, which has an improved bandwidth efficiency compared to the DBLAST structure.

In LSTC systems, co-channel interference from adjacent layers limits the system performance. To reduce the co-channel interference, S. Marinkovic et. al., [7] and Gamal et.al in [70] have proposed iterative receivers in which combined detection and decoding are proposed, based on the turbo principle. The receiver scheme, proposed by Gamal et.al., [70], implements Minimum Mean Square Error (MMSE) detection with soft-output Viterbi Algorithm (SOVA) decoding in the iterative receiver. In [7], S. Marinkovic et. al., proposed a combination of Parallel Interference Cancellation (PIC) detection with MAP decoding. Both approaches depend on additional channel estimation, and exhibit near interference-free single user performance for certain ranges of the signal to noise ratio (SNR) under the assumption of perfect channel state information (CSI) at the receiver.

Recently, an adaptive co-channel interference cancellation scheme for an STC system was proposed by J. Li et. al., [15]. However, the adaptive receiver design is based on linear detection, which could suffer performance degradation in a high interference environment. Therefore, non-linear adaptive detection is necessary for improving the performance of the receiver.

In this chapter, a new adaptive iterative TLSTC receiver is proposed based on a joint adaptive iterative detection and decoding algorithm. The proposed receiver does not require channel state information (CSI) as the non-adaptive iterative receivers presented by S. Marinkovic et. al., [7] and Gamal et.al [70]. Therefore, the proposed receiver does not require a matrix inversion process in the system. As a result, the complexity of the proposed receiver is less than that of the non-adaptive iterative receiver. Moreover, this adaptive iterative receiver has the advantage of combining co-channel interference suppression and cancellation. In this chapter, we are mainly concerned with the performance gain due to interference cancellation and the tracking ability of the adaptive iterative structures. We show that the adaptive iterative receiver provides a significant performance improvement compared to a single iteration linear adaptive receiver. The computational complexity of the adaptive iterative receiver is also lower than that of the non-adaptive iterative receiver.

This chapter is organized as follows: Section 3.2 describes the LSTC systems and channel models as well as the proposed adaptive iterative receiver structure. An analysis of the computational complexity is investigated in Section 3.3. The simulation results are discussed in Section 3.4, followed by the conclusion in Section 3.5.

3.2 System Model

A layered space-time coding system transmission through a Rayleigh slow and fast fading channel is analyzed. A threaded layered space-time coding (TLST) system is used in this thesis. The transmitter and receiver structures for a single user are described.

3.2.1. Transmitter structure

A TLST transmitter structure is depicted in Figure. 3.1, consisting of N transmit and M receive antennas. The binary information stream is converted by a serial to parallel converter and encoded by a convolutional encoder to produce a coded data stream for each layer, corresponding to each of the N transmit antennas. The layered coded data streams are then modulated and fed into a spatial interleaver, $(\mathbf{S}\Pi)$, to distribute a coded stream for all layers among N transmit antennas. After time interleaving, (Π), the coded symbols of each layer are simultaneously and synchronously transmitted from the N transmit antennas through the MIMO channel.

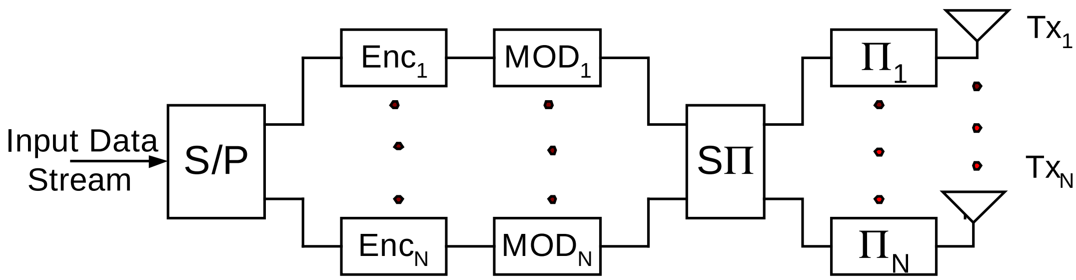

Figure.3.1 Layered space-time transmitter structure

Let $\mathbf{x}_t$ be an N×1 vector of the transmitted symbols across the N transmit antennas, defined by

$$\mathbf{x}_t = \left[x_t^1, x_t^2, \mathbf{K}, x_t^N\right]^T \tag{3.1}$$

where x_t^i is the coded symbol of the ***i***-th antenna, at time interval ***t***. The transmitted symbols vector $\mathbf{x}_t$**,** is then transmitted simultaneously through a MIMO channel. The received signal at each of the M receive antennas can be considered as a superposition of all N transmitted symbols and additive white Gaussian noise (AWGN). The received signal vector, denoted by $\mathbf{r}_t$, at the time interval ***t*****,** can be represented as [20]

$$\mathbf{r}_t = \mathbf{H}_t \mathbf{x}_t + \mathbf{n}_t \tag{3.2}$$

where $\mathbf{r}_t$ is an M×1 column vector of the received signals across the M receive antennas, at time interval ***t*****,** defined by $\mathbf{r} = \left[r_1, r_2, \mathbf{K}, r_M\right]^T$. $\mathbf{H}_t$ is an $M \times N$ complex channel matrix gain for time interval *t*, given by [20]

$$\mathbf{H}_t = \begin{bmatrix} h_{11}^t & \cdots & h_{1N}^t \\ \vdots & \ddots & \vdots \\ h_{M1}^t & \cdots & h_{MN}^t \end{bmatrix} \tag{3.3}$$

The element of $\mathbf{H}_t$, denoted by h_{ji}^t, is a fading attenuation coefficient at time *t* from the *i*-th transmit antenna, $i = 1, \ldots, N$, to the *j*-th receive antenna, and $j = 1, \ldots, M$. We assume synchronous transmission from various transmit antennas. The transmitted power of each layer is assumed to be *P/N*, where the *P* is total transmitted power and *N* is the number of transmit antennas. The fading coefficient amplitudes are Rayleigh distributed with the mean square value normalized so that the received power for each of *M* receive antennas is equal to the total transmitted power. That is

$$E\left\{\left(\sum_{i=1}^{N} h_{ji} x_{ji}\right)\left(\sum_{i=1}^{N} h_{ji} x_{ji}\right)^H\right\} = P \tag{3.4}$$

This imposes the following restriction on the channel coefficients

$$E\left(\sum_{i=1}^{N} h_{ji} h_{ji}^H\right) = 1 \tag{3.5}$$

The phases of the channel coefficients are uniformly distributed between $(0,2\pi)$.

$\mathbf{n}_t$ is an $M \times 1$ vector of the AWGN noise with a zero mean and the noise variance of σ^2 at time t, given by

$$\mathbf{n}_t = [n_1, n_2, \ldots n_M]^T \tag{3.6}$$

3.2.2 Receiver Structures

The challenge in detection of space-time signals is to design a low-complexity detector, which efficiently removes the CCI and approaches the interference bound. The iterative processing principle, as applied in turbo coding [45, 71], has been successfully extended to joint detection and decoding [7, 9, 70, 72]. The block diagram of an iterative LSTC receiver structure is shown in Figure. 3.2. It consists of two stages: a soft-input soft-output (SISO) detector followed by N parallel SISO channel decoders. Time and spatial deinteleavers and spatial and time interleavers separate the two stages.

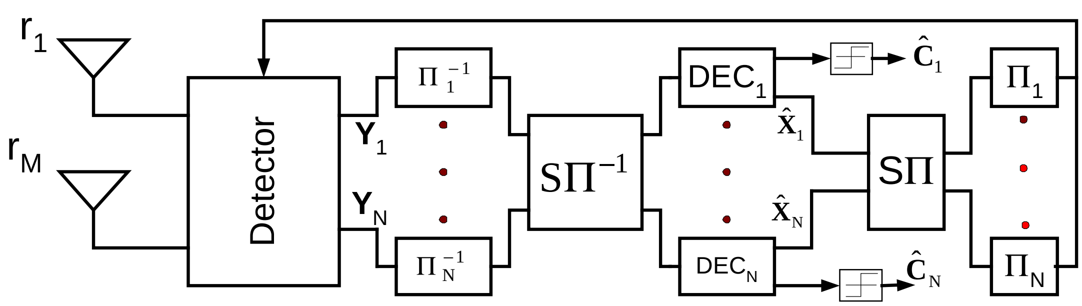

Figure.3.2 Block diagram of a threaded layered space-time receiver structure

The decoder can apply a number of the soft output decoding algorithms. However, the maximum a posteriori (MAP) approach [73], which minimizes the bit error probability at the decoder output, is employed in this structure. The detail of the MAP algorithm will be described later. For the detectors, two receiver structures are investigated in this chapter. They are based on a non-adaptive iterative receiver, and adaptive iterative receiver algorithms.

3.2.2.1 Non-adaptive Iterative Receiver

A non-adaptive iterative receiver or iterative receiver based on a joint minimum mean square error decision feedback (MMSE-DF) detection and decoding scheme is described. An iterative MMSE-DF detector consists of a soft-input soft-output (SISO) feed-forward and feedback filters, as shown in Figure. 3.3.

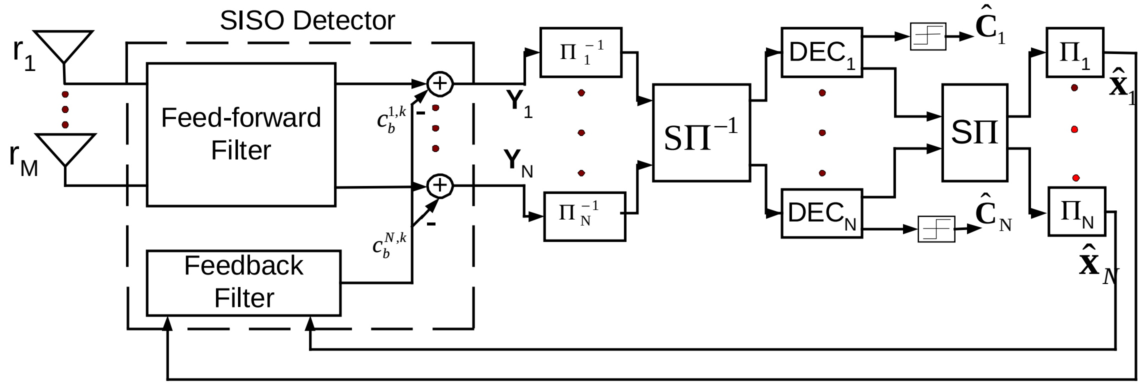

Figure. 3.3 Block diagram of iterative MMSE Receiver

In the first iteration, the feed-forward filter performs interference suppression without the interference cancellation process because there are no estimated symbols from the output of the MAP decoder. After the first iteration, the feedback filter is included into the detection process. The estimated symbols from the output of the decoder are fed back to the feedback filter to cancel the interference from other antennas in the detection process. The detected symbol obtained at the output of the MMSE detector in the *k*-th iteration at time *t*, for layer *i*, denoted by $y_t^{i,k}$, is given by [9]

$$y_{t,MMSE}^{i,k} = \mathbf{w}_f^{i,k\,H}(t)\mathbf{r}_t + \mathbf{w}_b^{i,k\,H}(t)\hat{\underline{\mathbf{x}}}_t^{i,k} \tag{3.7}$$

where $\mathbf{w}_f^{i,k}(t)$ is an $M\times1$ feed-forward coefficient vector, represented as

$$\mathbf{w}_f(t) = \left[w_{f,0}(t), w_{f,1}(t), \ldots, w_{f,M-1}(t)\right]^T \tag{3.8}$$

and $\mathbf{w}_b^{i,k}(t)$ is an $(N\text{-}1)\times1$ feedback coefficient vector, that can be written in the form

$$\mathbf{w}_b(t) = \left[w_{b,0}(t), w_{b,1}(t), \mathbf{K}, w_{b,i-1}(t), w_{b,i+1}(t), \mathbf{K}, w_{b,N-1}(t)\right]^T \tag{3.9}$$

$\underline{\hat{\mathbf{x}}}_t^{i,k}$ is an $(N-1)\times 1$ vector of the estimated symbols from the output of the SISO MAP decoders at the k-th iteration at time t for other antennas, given as

$$\underline{\hat{\mathbf{x}}}_t^{i,k} = \left(\hat{x}_t^{1,k}, \hat{x}_t^{2,k}, \ldots, \hat{x}_t^{i-1,k}, \hat{x}_t^{i+1,k}, \ldots, \hat{x}_t^{N,k}\right)^T \tag{3.10}$$

The decoder calculates the log-likelihood ratio (LLRs) for the transmitted symbols at a particular time instant for each transmit antenna. The LLRs values then are used to calculate the transmitted symbol estimates, $\underline{\hat{x}}_t^{l,k}, l = 1,\ 2,\ \mathbf{K},\ i-1, i+1, \mathbf{K}, N$.

The second term in Equation (3.7) represents the cancelled interference, denoted by a scalar feedback coefficient $c_b^{i,k}(t)$ and given by [9]

$$c_b^{i,k}[t] = \mathbf{w}_b^{i,k\,H}(t)\underline{\hat{\mathbf{x}}}_t^{i,k} \tag{3.11}$$

Therefore, the detected symbol, $y_t^{i,k}$, can be written as

$$y_{t,\,MMSE}^{i,k} = \mathbf{w}_f^{i,k\,H}(t)\mathbf{r} + c_b^{i,k}(t) \tag{3.12}$$

The values of $\mathbf{w}_f^{i,k}(t)$ and $c_b^{i,k}(t)$ are calculated by minimizing the mean square error between the transmitted symbol and its estimate, given by

$$z\,(t) = E\left[\left|y_{t,\,MMSE}^{i,k} - x_t^{i,k}\right|^2\right] \tag{3.13}$$

Let us assume that there is perfect knowledge of the channel coefficients matrix $\mathbf{H}_t$ during time t. Define $\mathbf{H}_{t,i}$ as the i-th column of the channel matrix $\mathbf{H}_t$, representing an $M \times 1$ vector of the complex channel gains for the i-th transmit antenna, $\mathbf{H}_{t,i}^H$ is a conjugate transpose of $\mathbf{H}_{t,i}$ and $\underline{\mathbf{H}}_t^i$ is an M×(N-1) matrix composed of the complex channel gains for the other (N-1) transmit antennas at time t. Also define

$$\mathbf{A}_t = \mathbf{H}_{t,i}\mathbf{H}_{t,i}^H \tag{3.14}$$

$$\mathbf{B}_t = \underline{\mathbf{H}}_t^i \left[\mathbf{I}_{N-1} - diag\left(\hat{\underline{\mathbf{x}}}_t^{i,k} \hat{\underline{\mathbf{x}}}_t^{i,k^T} \right) + \hat{\underline{\mathbf{x}}}_t^{i,k} \hat{\underline{\mathbf{x}}}_t^{i,k^T} \right] \underline{\mathbf{H}}_t^{i\,\mathrm{H}} \tag{3.15}$$

$$\mathbf{D}_t = \underline{\mathbf{H}}_t^i \hat{\underline{\mathbf{x}}}_t^{i,k} \tag{3.16}$$

$$\mathbf{R}_t = s_t^2 \mathbf{I}_M \tag{3.17}$$

where $\mathbf{I}_{N-1}$ and $\mathbf{I}_M$ are $(N-1)\times(N-1)$ and $M \times M$ identity matrices, respectively. The optimum feed-forward and feedback coefficients are given by [9]

$$\mathbf{w}_f^{i,k^T}(t) = \mathbf{H}_{t,i}^H \left(\mathbf{A}_t + \mathbf{B}_t + \mathbf{R}_t - \mathbf{D}_t \mathbf{D}_t^H \right)^{-1} \tag{3.18}$$

$$c_b^{i,k^T}(t) - \mathbf{w}_f^{i,k^T}(t)\mathbf{D}_t \tag{3.19}$$

From (3.18), it is obvious that the complexity of computing an $M \times M$ inverse matrix is approximately in the order of M^3 [74]. Another drawback of the non-adaptive iterative MMSE receiver is the requirement of the CSI at the receiver. In practice, there is no knowledge of the CSI at the receiver. Therefore, an adaptive algorithm, which requires only a training sequence, is proposed in this thesis to reduce a high computational complexity. Detail of the adaptive algorithm will be discussed in the next section.

3.2.2.2 Adaptive Iterative Receiver

As we mentioned in the previous section that the computational complexity of a non-adaptive iterative MMSE receiver is very high due to a matrix inversion process. The adaptive algorithm is an alternative algorithm, used to reduce such a high computational complexity workload. The adaptive structure based on SISO feedback equalization is employed, as shown in Figure. 3.4. Training sequences are transmitted at the start of the transmission. The adaptive structure consists of two linear filters, one for the feed-forward filter and one for the feedback filter.

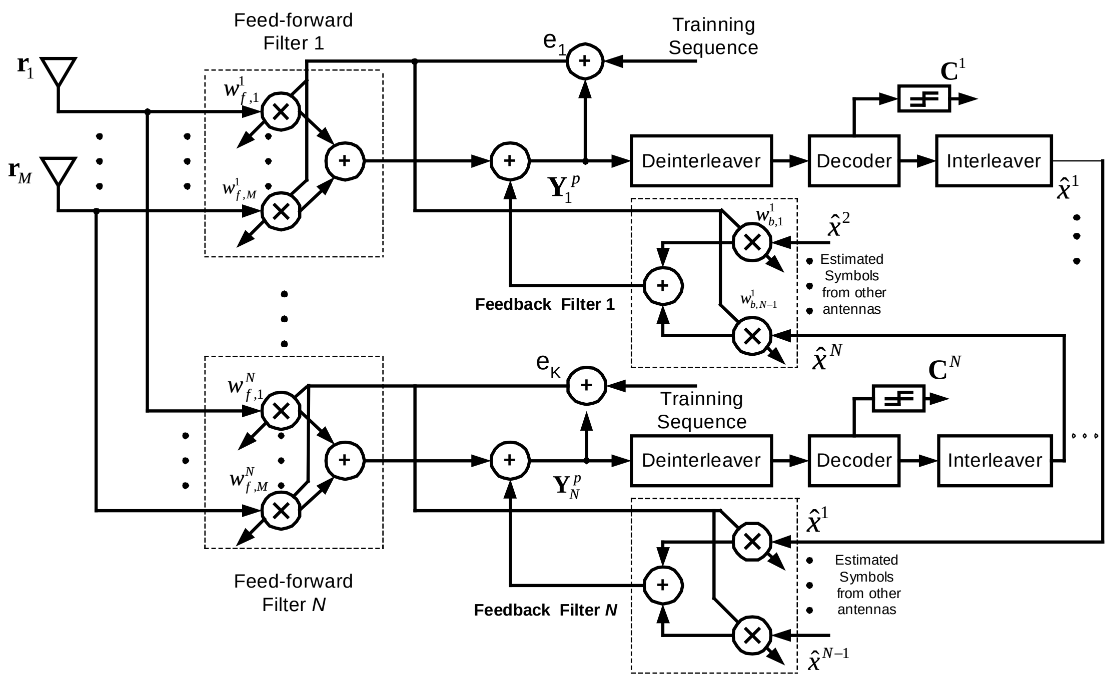

Figure. 3.4 Block diagram of adaptive iterative MMSE Receiver

A well-known least mean square (LMS) algorithm [18] is used in the feed-forward and feedback filter because of its simplicity and numerical stability. The detected symbol obtained at the output of the SISO detector in the *k*-th iteration at time *t*, for layer *i*, denoted by $y_{t,LMS}^{i,k}$, is given by [9]

$$y_{t,LMS}^{i,k} = \mathbf{w}_f^{i,k^H}(t)\mathbf{r}_t + \mathbf{w}_b^{i,k^H}(t)\underline{\hat{\mathbf{x}}}_t^{i,k} \tag{3.20}$$

The feed-forward coefficient vector $\mathbf{w}_f^{i,k}(t)$ and feedback coefficient vector $\mathbf{w}_b^{i,k}(t)$ are defined in (3.8) and (3.9), respectively, and determined recursively by an adaptive Least Mean Square (LMS) algorithm [18]. To calculate the coefficients $\mathbf{w}_f^{i,k}(t)$ and $\mathbf{w}_b^{i,k}(t)$ adaptively for a particular time instant t, the mean squared error, defined by $z(t)$, for the LMS algorithm is given by [18]

$$z(t) = E\left[\left|\mathbf{w}_f^{i,k^T}(t)\mathbf{r}_t + \mathbf{w}_b^{i,k^T}(t)\hat{\underline{\mathbf{x}}}_t^{i,k} - x_t^{i,k}\right|^2\right] \tag{3.21}$$

where

$$\mathbf{w}_f^{i,k}(t+1) = \mathbf{w}_f^{i,k}(t) + \mu_f e(t)\mathbf{r}_t \tag{3.22}$$

$$\mathbf{w}_b^{i,k}(t+1) = \mathbf{w}_b^{i,k}(t) + \mu_b e(t)\hat{\underline{\mathbf{x}}}_t^{i,k} \tag{3.23}$$

μ_f and μ_b are the step sizes for the feed-forward and feedback adaptations respectively.

As the LMS algorithm has slow convergence and may not track in a non-stationary environment very well, the partially filtered gradient LMS (PFGLMS) [21] algorithm based on an exponentially weighted least square error is used to improve the convergence speed of the LMS algorithm with a slight increase in complexity. The conventional LMS algorithm requires 2M+1 multiplications and the same number of additions for each received data symbol. However, the PFGLMS algorithm requires 4M+1 multiplications and the same number of additions for each received data symbol. Therefore, the computation complexity is approximately in the order of M for both the LMS and PFGLMS algorithm.

To apply the PFGLMS algorithm, as mentioned in Chapter 2, to the adaptive iterative detector, as proposed in this thesis, the detected symbol obtained at the output of the SISO detector in the *k*-th iteration at time *t*, for layer *i*, denoted by $y_{t,PFGLMS}^{i,k}$, is given by [21]

$$y_{t,PFGLMS}^{i,k} = \mathbf{w}_f^{i,k\,H}(t)\mathbf{r}_t + \mathbf{w}_b^{i,k\,H}(t)\underline{\hat{\mathbf{x}}}_t^{i,k} \tag{3.24}$$

the modified feed-forward and feedback coefficients of the PFGLMS algorithm for MIMO systems can be expressed by [21]

$$\mathbf{w}_f^{i,k}(t+1) = \mathbf{w}_f^{i,k}(t) + m_f \mathbf{g}_f^{i,k}(t) \tag{3.25}$$

and

$$\mathbf{w}_b^{i,k}(t+1) = \mathbf{w}_b^{i,k}(t) + m_b \mathbf{g}_b^{i,k}(t) \tag{3.26}$$

where μ_f and μ_b are the step sizes for the feed-forward and feedback adaptations, respectively.

and

$$\left.\begin{aligned} \mathbf{g}_f^{i,k}(t) &= e(t)\mathbf{r}_t + \hat{\mathbf{g}}_f^{i,k}(t) \\ \hat{\mathbf{g}}_f^{i,k}(t) &= l_f \hat{\mathbf{g}}_f^{i,k}(t-1) + g_f e(t)\mathbf{r}_t \end{aligned}\right\} \tag{3.27}$$

$$\left.\begin{aligned} \mathbf{g}_b^{i,k}(t) &= e(t)\underline{\hat{\mathbf{x}}}_t^{i,k} + \hat{\mathbf{g}}_b^{i,k}(t) \\ \hat{\mathbf{g}}_b^{i,k}(t) &= l_b \hat{\mathbf{g}}_b^{i,k}(t-1) + g_b e(t)\underline{\hat{\mathbf{x}}}_t^{i,k} \end{aligned}\right\} \tag{3.28}$$

where (l_f, l_b) and (g_f, g_b) are the forgetting factors and the scaling factors, respectively, and $\hat{\mathbf{g}}_f^{i,k}(0) = \hat{\mathbf{g}}_b^{i,k}(0) = 0$.

3.2.3 MAP decoding Algorithm

In the proposed receiver structure, the detection outputs for layer *i* for a whole block of transmitted symbols from vector, $\mathbf{y}^{i,k}$, are passed to time de-interleaved , followed by a spatial deinterleaver. The well-known SISO MAP [19] decoder takes the spatial de-interleaver output as a soft-input to the decoder. Based on the turbo principle, the soft-output from the decoder is used to calculate the interference, which is subtracted from the detector output in the next iteration. This iterative detection/decoding process is performed until the symbol estimate converges to the optimal performance. The soft-output from the decoder in the last iteration is then fed into a decision device to produce a decision.

Let $l_t^{i,k}$ be log-likelihood ratios (LLR) for the transmitted modulated symbols 1 and –1 for the ***k***-th iteration for the ***i***-th transmit layer, at the particular time instants, given by [20]

$$l_t^{i,k} = \log\left(\frac{P\left(x_t^{i,k} = 1 \middle| \mathbf{y}_t^{i,k}\right)}{P\left(x_t^{i,k} = -1 \middle| \mathbf{y}_t^{i,k}\right)}\right) \tag{3.29}$$

The soft-output symbols estimate in the ***i***-th layer and ***k***-th iteration can be determined as functions of the LLR, given in Equation (3.30) [20]

$$\hat{x}_t^{i,k} = \frac{e^{l_t^{i,k}} - 1}{e^{l_t^{i,k}} + 1} \tag{3.30}$$

3.3 Complexity Analysis

In this section, we define the receiver computation complexity as the required number of signal processing operations per coded symbol and per layer. As we want to compare the receiver complexity between the non-adaptive and adaptive iterative receiver, we will consider only the complexity of the detector since the decoder is the same for both implementations.

The computational complexity of a non-adaptive detector is very high due to the matrix inversion process. In a non-adaptive algorithm, we only consider the complexity based on the total multipliers requires in the receiver. For each coded symbol per layer and per iteration, the non-adaptive feed-forward filter, corresponding to Equation (3.12) and Equation (3.14) to Equation (3.18), requires $M^3 + 4M + 4(N-1)$ multipliers to perform interference suppression, where N and M are a number of transmit and receive antennas. The feedback filter, corresponding to Equation (3.19), requires M multipliers to perform interference cancellation. As a result, the total complexity of the non-adaptive iterative receiver consists of $NI\left(M^3 + 5M + 4(N-1)\right)$ multipliers for N layers and M receive antennas at I iterations.

On the other hand, the computational requirement for the adaptive iterative receiver based on the conventional LMS algorithm requires $2M + 1$ multiplications for a feed-forward filter and $2(N-1) + 1$ multiplications for a feedback filter. The total computational requirement for the LMS algorithm is $NI(2M + 2N)$ multiplications for N transmit and M receive antennas at I iterations.

The PFGLMS algorithm requires $4M + 1$ multiplications and $4(N - 1) + 1$ for a feed-forward filter and feedback filter, respectively. Therefore, the total computational requirement for PFGLMS algorithm is $NI(4M + 4N - 2)$ multiplications for N transmit and M receive antennas at I iterations. The comparison of the complexity amongst these detectors is shown in Table 1.

Table 1. Complexity comparison between non-adaptive receivers
and the proposed adaptive detectors

Algorithm	Number of multiplications	Computational Complexity ($N = 4$, $M = 4$, and $I = 10$)
Iterative MMSE receiver	$NI\left(M^3 + 5M + 4(N-1)\right)$	3840
LMS algorithm	$NI(2M + 2N)$	640
PFGLMS algorithm	$NI(4M + 4N - 2)$	1200

N = number of transmit antennas, M = number of receive antennas,

I = number of iteration.

It can be observed from Table 1 that the computational complexity of the non-adaptive iterative MMSE receiver is very high compared to the adaptive LMS and PFGLMS detectors. For example, assuming the system consists of four transmit and four receive antennas, and performs 10 iterations, the computational complexity of a non-adaptive iterative receiver is equal to 3840; the computational complexities for the conventional LMS and PFGLMS detectors are 640 and 1200, respectively. The receiver based on the conventional LMS algorithm can save about 83% of computational complexity compared to the non-adaptive iterative MMSE receiver, and the reduction of the computational complexity in the receiver based on the PFGLMS algorithm is about 69% compared to the non-adaptive iterative MMSE receiver.

Therefore, the proposed adaptive iterative receivers, based on both the conventional LMS and PFGLMS algorithms, offer a significant reduction in computational complexity. Although, the PFGLMS algorithm has a slightly higher complexity compared to the conventional LMS algorithm, the convergence speed of the PFGLMS algorithm is faster than that of the conventional LMS. In addition, the PFGLMS algorithm provides the tracking ability to the system in a fast fading channel as shown in the next section.

3.4 Performance Results

This section presents simulation results for the LSTC non-adaptive and adaptive iterative receivers with BPSK modulation in slow and fast Rayleigh fading channels. The system operates in the training mode until the mean square error (MSE) approaches the minimum mean square error (MMSE), then it switches to the decision directed mode. The constituent codes are nonsystematic convolutional codes with the code rate R of 1/2, memory order of 3, and the generating polynomial $g_1 = 15_8$ and $g_2 = 17_8$. [19] The proposed system is simulated with various numbers of transmit and receive antennas, i.e., 2×2 and 4×2 MIMO systems, with 130 information bits per layer in each frame. After serial to parallel conversion, each layer of the LSTC system consists of 130 information bits, followed by 266 encoded symbols per layer. The data rate is 1 Mbps at the carrier frequency f_c, of 2 GHz. The simulation results are represented in terms of the average bit error rate (BER) versus the ratio of the averaged energy per bit, denoted by E_b, to the power spectral density of the AWGN, denoted by N_o.

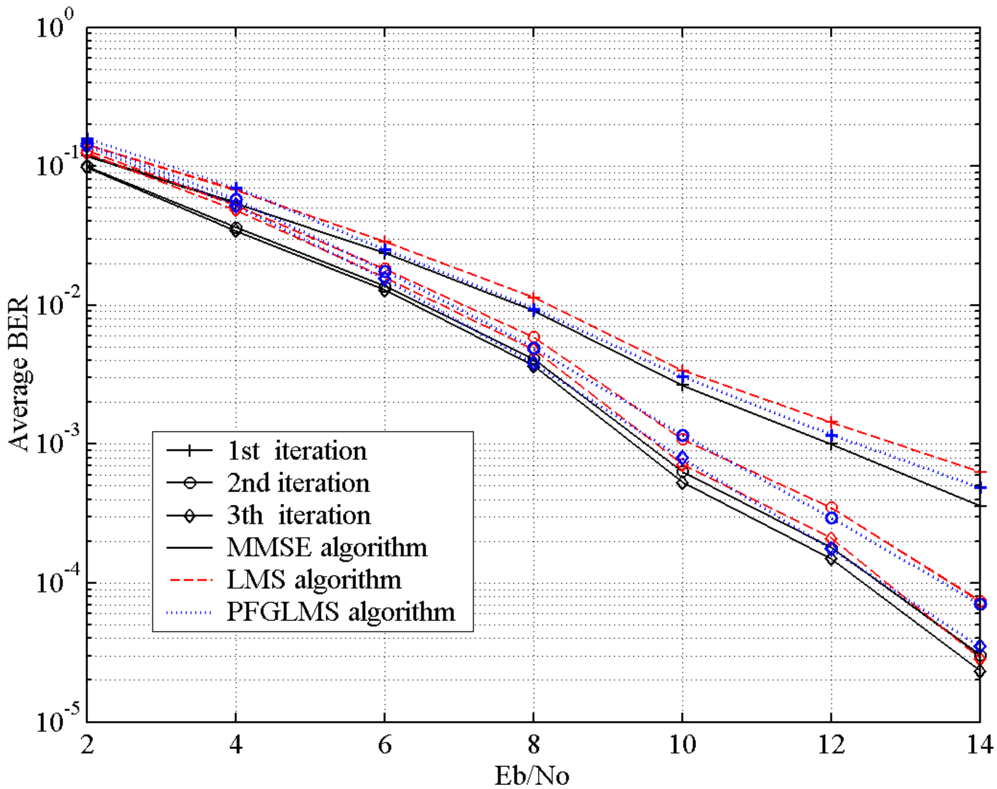

Figure. 3.5 Performance comparison between Adaptive Iterative and Non-adaptive Iterative MMSE algorithm in a quasi-static Rayleigh fading channel with 2×2 antennas system

3.4.1. Performance Results on Slow Fading Channels

The slow fading channel is modeled as a quasi-static fading channel, where each fading coefficient is constant within a frame, but changes from one frame to another and for each sub-channel. The average BER of the non-adaptive iterative MMSE receiver for various numbers of iterations under the perfect channel knowledge assumption is shown in Figure. 3.5. The system performance is significantly improved for the second iteration compared to the first iteration and gradually increases for higher iterations. The BER curves also show that the performance converges to a steady state after the third iteration. The performance of the adaptive iterative receiver based on the LMS algorithm and the non-adaptive iterative MMSE receiver are shown in Figure. 3.5. The results show that the average BER of the adaptive iterative structure approaches the performance results of the non-adaptive iterative MMSE receiver.

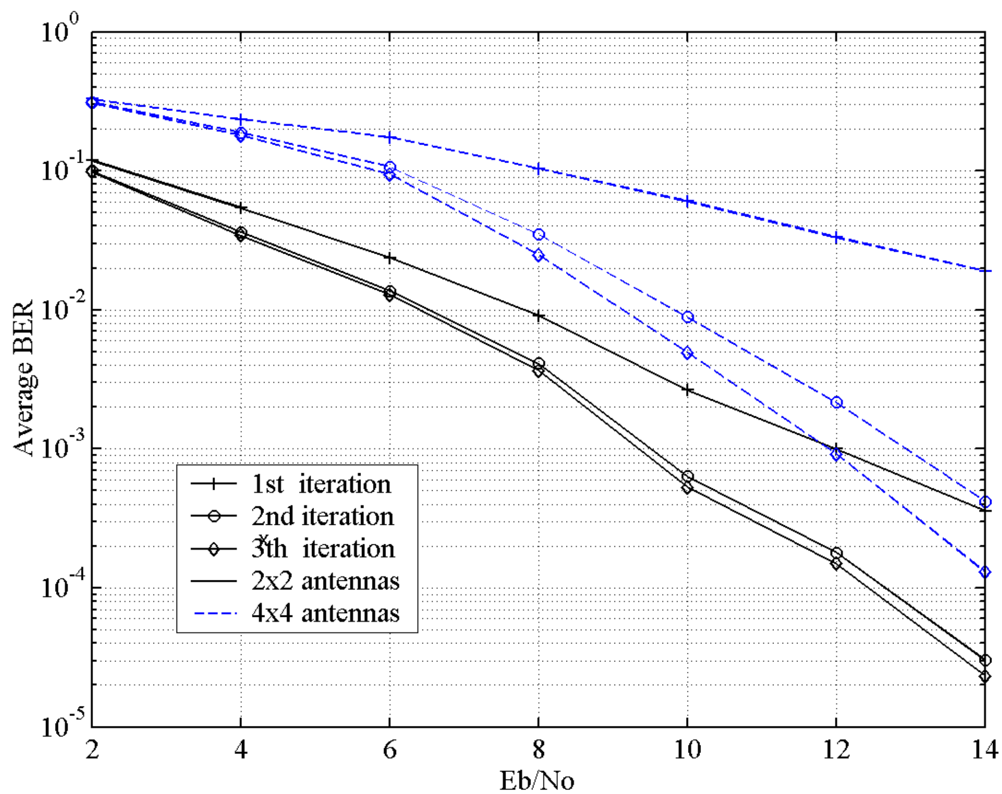

Figure. 3.6 Performance comparison between 2×2 antennas and 4×2 antennas Non-adaptive Iterative MMSE algorithm in a quasi-static Rayleigh fading channel

Figure.3.6 presents the performance of the systems between a 2×2 antennas system and $4{\times}2$ antennas system. Since the system with $4{\times}2$ antennas utilizes more transmit antennas, the interference caused by other transmit antennas is increased corresponding to the number of transmit antennas in use. Consequently, the performance of the system of $4{\times}2$ antennas is decreased compared to a 2×2 antennas system.

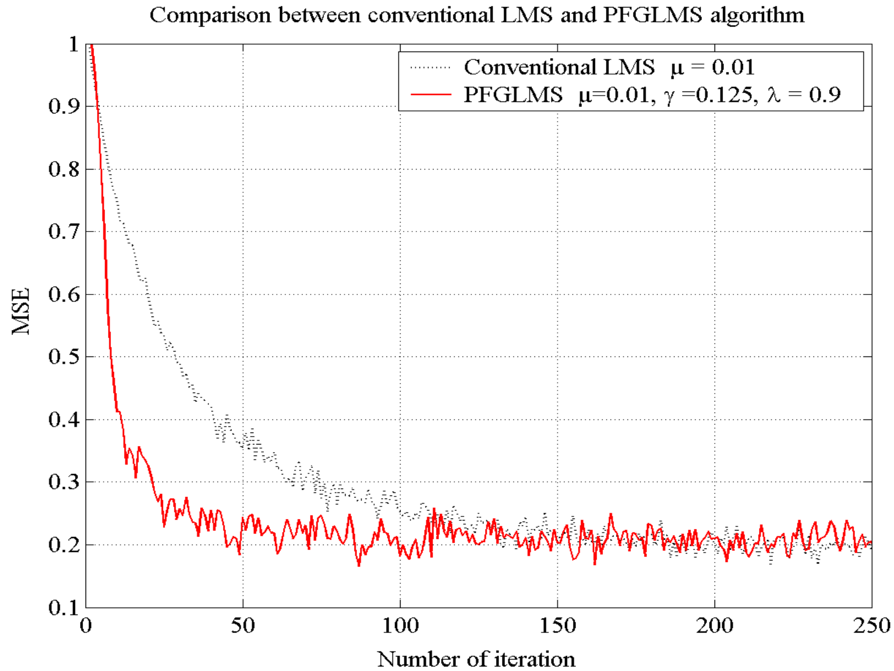

Figure. 3.7 The convergence speed of the conventional LMS and PFGLMS algorithm

Figure. 3.7 presents a comparison of the convergence speeds of the LMS and PFGLMS receiver at the first iteration. The figure shows that the convergence speed of the PFGLMS receiver outperforms that of the conventional LMS receiver. The convergence rate of the PFGLMS algorithm is about three times faster than that of the conventional LMS algorithm. The average BER of both structures, non-adaptive and adaptive receivers, is presented in Figure. 3.8. The result shows that the PFGLMS algorithm has a good tracking ability compared to the LMS algorithm on rich scattering environments. The average BER of the PFGLMS receiver is close to the average BER of the MMSE receiver in the last iteration. Therefore, the PFGLMS receiver is more convenient for rich scattering environments.

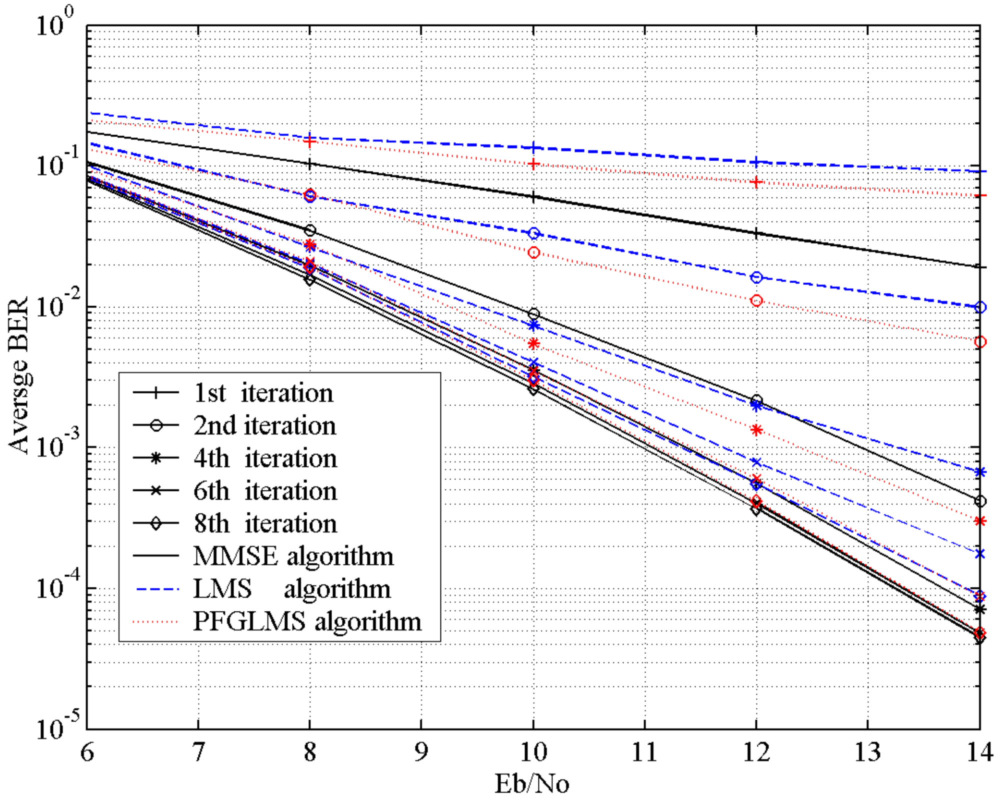

Figure. 3.8 Performance between Adaptive Iterative and Non-adaptive Iterative MMSE algorithm in a quasi-static Rayleigh fading channel with a 4×2 antennas system

3.4.2. Performance Results on Fast Fading Channels

In the fast fading channel, the fading coefficients are constant within each symbol period and vary from one symbol to another. The performance of the proposed receiver with perfect knowledge of CSI at various fading rates is shown in Figure. 3.9. The figure shows that the average BER decreases when the fading rate is increased, since the MAP decoder performance is sensitive to the fade rates. When the fade rate is increased, the inputs to the MAP decoder are less correlated and the decoder has a better performance. On the other hand, the LMS adaptive detector is sensitive to the channel estimation accuracy [75]. Therefore the average BER of the LMS adaptive iterative receiver is increased because of inaccurate channel estimation in the fast fading channel. Therefore, the average BER of the LMS receiver increases when the fade rate is increased as shown in Figure 3.10. Figure. 3.11 presents the comparison of the MMSE, LMS and PFGLMS receivers at the normalized fading rate of 0.0002. The result shows that the PFGLMS algorithm has good tracking ability compared to the LMS algorithm on a fast fading channel. The average BER of the PFGLMS receiver is close to the average BER of the MMSE receiver in the first iteration. Therefore, the PFGLMS receiver is more convenient for the fast fading channels.

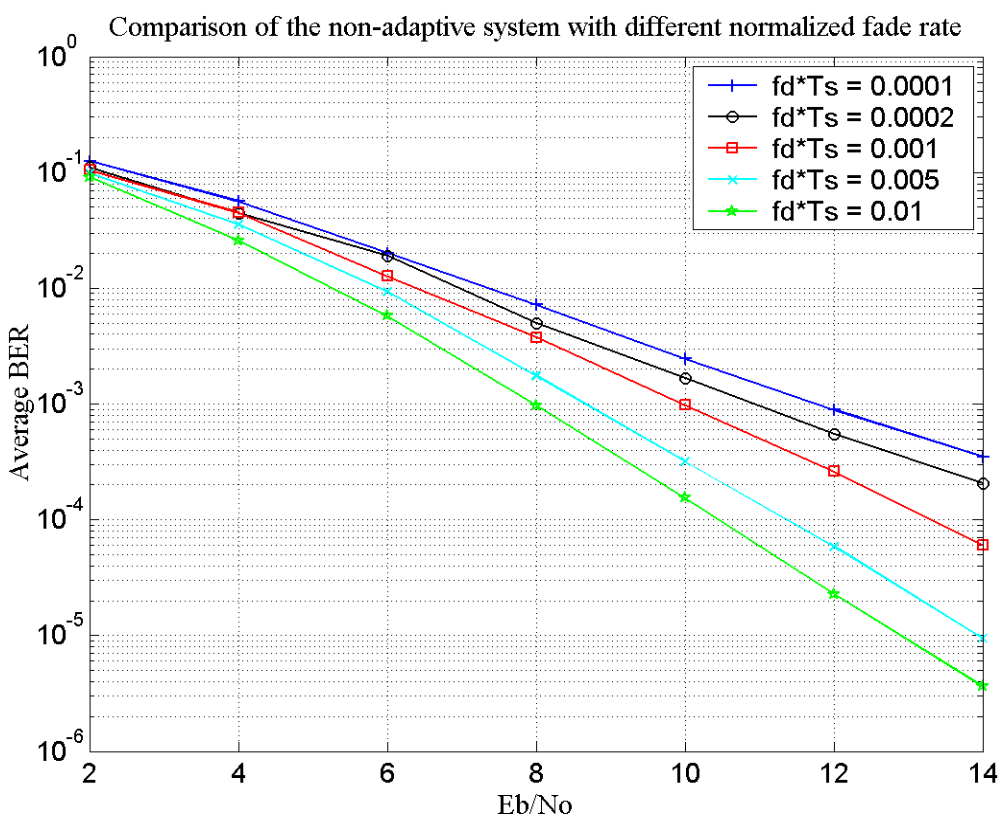

Figure. 3.9 Performance of the non-adaptive iterative MMSE receiver in various normalized fading rates with perfect channel knowledge

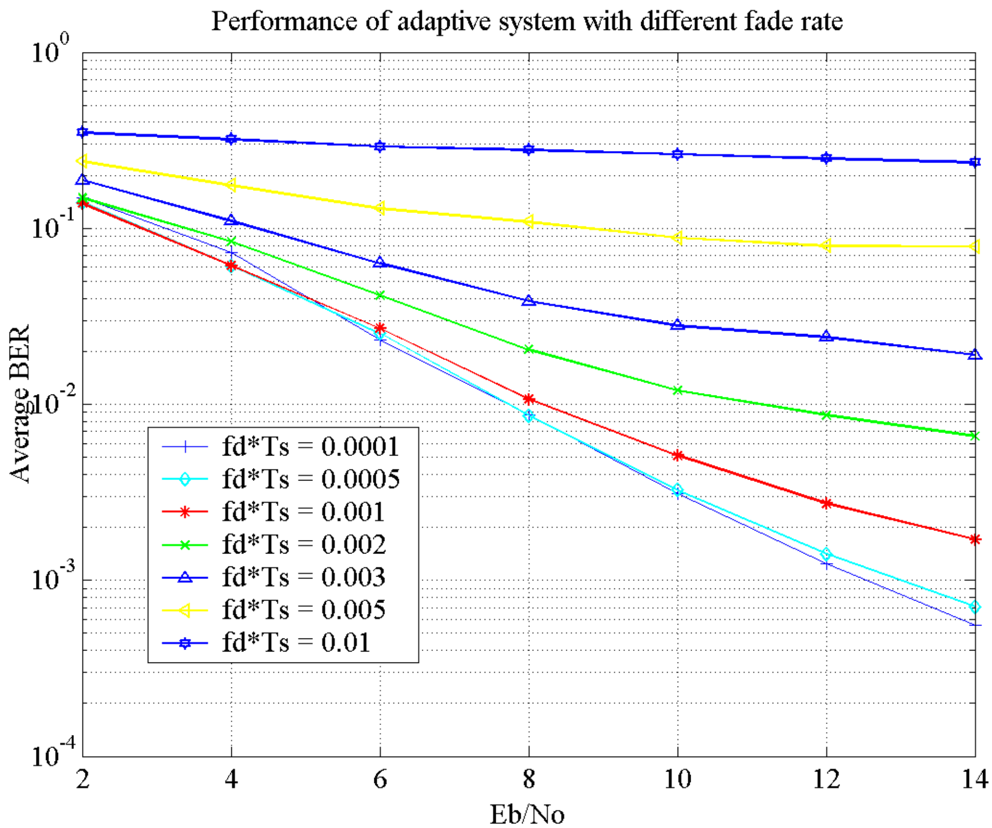

Figure. 3.10 Performance of the LMS adaptive iterative receiver in various normalized fading rates with imperfect channel knowledge

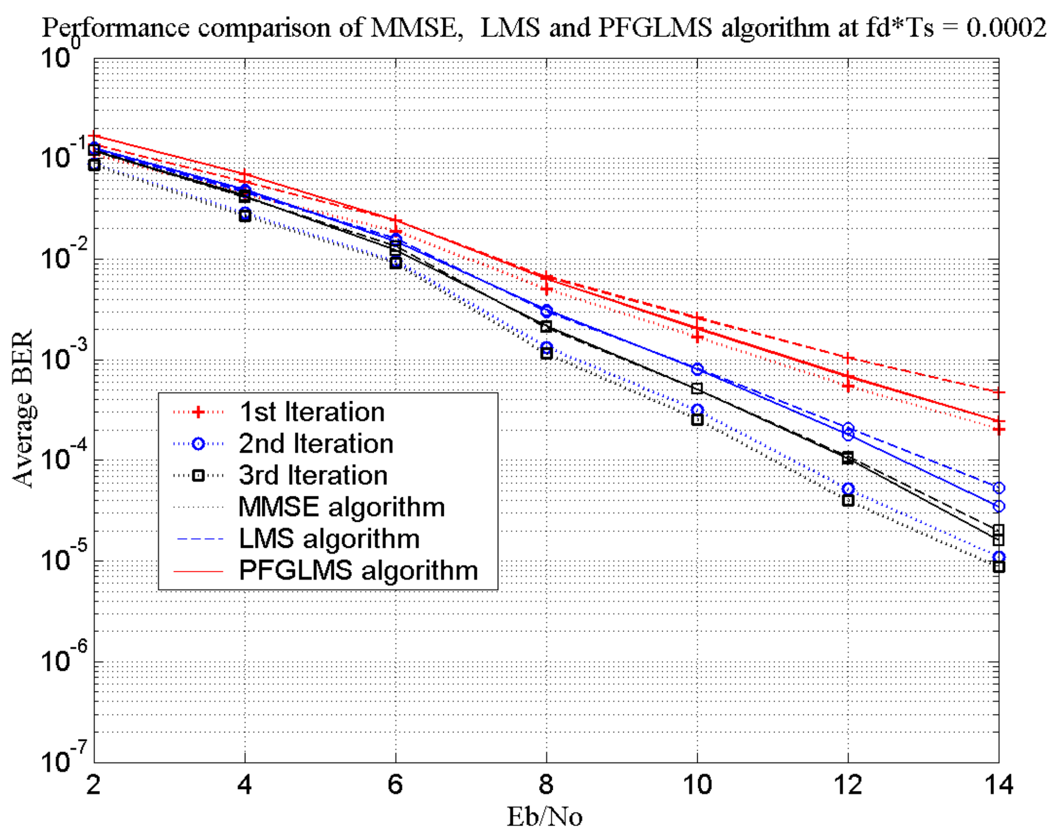

Figure. 3.11 Comparison between the non-adaptive iterative MMSE algorithm and adaptive (LMS and PFGLMS) iterative algorithm at the 0.0002 normalized fading rate

3.5 Conclusions

In this chapter, the receiver structure of the proposed adaptive iterative receiver for MIMO systems based on a joint adaptive iterative detection and decoding structure has been investigated. It is shown that when dealing with multiple transmit antennas, effective detection techniques are required to avert the detrimental effect of the interference. The non-adaptive iterative receiver, such as the iterative MMSE receiver, was able to mitigate the interference caused by other antennas. The use of a decoding stage at each iteration allowed a greater performance improvement over multistage detectors, due to the higher reliability of the co-channel interference (CCI) estimation. However the computational complexity of the non-adaptive receiver is significantly high, due to the matrix inversion process.

To reduce the computational complexity, the adaptive iterative receiver is proposed. The adaptive iterative receiver reduces co-channel interference (CCI) by using interference suppression and cancellation techniques. The comparison of the complexity is considered only the complexity of the detector since the MAP decoder has been used with all detectors in the receiver structures. The complexity of the proposed receiver is lower than that of the non-adaptive receiver because there is no matrix inversion operation in adaptive detectors. The complexity is reduced from the order of M^3 in the non-adaptive receiver to the order of M in the adaptive receiver in each received data symbol. However, there is a need for transmission of training sequences at the beginning of each simulation. Moreover, the proposed receiver based on the PFGLMS algorithm has a faster convergence speed and better tracking ability compared to the LMS receiver in both a rich scattering environment and fast fading channels with a slight increase in the complexity in terms of the number of multipliers and adders. Therefore the PFGLMS receiver needs a shorter training period than the LMS receiver. The performance of the proposed receiver approaches that of the non-adaptive iterative receiver.

Chapter 4

Frequency-domain Adaptive Iterative Receiver for Space-time Coded MIMO Systems

It is well known that a linear convolution process can be carried out either in the time domain or in the frequency domain, based on the time-frequency duality principle. As a result, a linear convolution of two vectors in the time domain can be performed in the frequency domain by using the element-wise multiplication because of the time-frequency duality principle [97]. Therefore, the equalization in the time domain can be performed in the frequency domain by using the element-wise multiplication of their frequency transform.

The frequency domain approach has been shown to have a lower computational complexity [22] . Therefore, if equalization is carried out in the frequency domain, the convolution can be avoided and thus the complexity is reduced. Therefore, in this chapter, a new low complexity adaptive iterative receiver structure employing frequency domain conventional LMS (FD-LMS) and PFGLMS (FD-PFGLMS) algorithms is explored. The adaptive iterative receiver structure in the frequency approach is modified in the time domain receiver structure as described in Chapter 3. As we mentioned in Chapter 3, page 80, the computational complexity in the time domain approach is defined as the required number of signal processing operations per coded symbol and per layer. The number of signal operations is referred to the number of multiplications required for the convolution process in the time domain. Therefore, the computational complexity of the time domain conventional least mean square (LMS) and partially filtered gradient LMS (PFGLMS) is proportional to (N+ M), where N and M are a number of transmit and receiver antennas, respectively. Thus, the computational complexity of these algorithms is also proportional to (N+ M).

In contrast to the time domain receivers, the number of signal operations is referred to the number of multiplications required for the element-wise multiplication process in the frequency domain. Therefore, the number of the element-wise multiplication operations for the frequency domain is proportional to $\log_2(N+M)$. Consequently, the complexity of the frequency domain LMS and PFGLMS algorithms is proportional to $\log_2(N+M)$. To reduce the computational complexity, the equalization is performed in the frequency domain approach by using the element-wise multiplication instead of using the linear convolution in the time domain. As a result, the computational complexity of the frequency domain approaches is significantly reduced compared to that of the time domain approaches. The simulation results also show that the system performance of the adaptive frequency domain LMS and PFGLMS receivers is identical to that of the adaptive time domain LMS and PFGLMS receivers.

4.1 Introduction

In the previous chapter, the adaptive iterative receiver based on the LMS and PFGLMS algorithms is described. The advantages of the LMS based receiver are the implementation simplicity and numerical stability. In addition, the computational complexity of the adaptive LMS detector is significantly lower than that of the non-adaptive iterative receiver. However, the LMS often converges slowly and the tracking ability may not work very well in a non-stationary environment. A partially filtered gradient LMS (PFGLMS) algorithm is then applied to improve the convergence speed and the tracking ability of the adaptive structures. The total computation complexity of the adaptive iterative receiver based on the PFGLMS algorithm is still higher than that of the adaptive iterative receiver based on the conventional LMS receiver. As mentioned in the Chapter 3, the computational complexity is proportional to the number of transmit and receive antennas. Recently, a frequency domain equalizer (FDE) structure was proposed for single-input and single-output structure [76-78]. The FDE, proposed by the authors in [79-83], has been applied to MIMO systems. Such a technique offers a significant reduction in the computational complexity in comparison to the time domain approach.

In this chapter, new low complexity adaptive iterative TLSTC receivers are proposed based on a joint frequency domain adaptive iterative detection and decoding algorithm. The frequency domain adaptive iterative detectors apply the FD-LMS and FD-PFGLMS algorithms into the receiver system. The structure of the transmitter and receiver of the system is the same as the one in Chapter 3. However, at the detector end, instead of performing the convolution in the time domain, it performs the convolution in the frequency domain. These frequency domain adaptive iterative receivers also have the advantage of combining co-channel interference suppression and cancellation with a significant reduction of the complexity compared to time domain approaches. In this chapter, we are mainly concerned with the performance gain due to interference suppression and cancellation and tracking ability of the adaptive iterative structures in the frequency domain approaches. We show that the performance of the frequency domain adaptive iterative receiver is identical to the time domain adaptive receiver with a lower computation complexity.

This chapter is organized as follows: Section 4.2 describes the LSTC systems and channel models as well as the proposed adaptive iterative receiver structure. The computational complexity analysis is given in Section 4.3. The simulation results are discussed in Section 4.4, followed by the conclusion in Section 4.5.

4.2 System Model

We utilize the threaded layered space-time coded transmitter structure for a single user, as shown in Figure. 3.1. Therefore, the transmitted signals of all N transmit antennas are the same transmitted signals as given in Chapter 3, which is repeated here for the reader's convenience.

Let $\mathbf{x}_t$ be an $N\times1$ vector of the transmitted symbols across the N transmit antennas, defined by

$$\mathbf{x}_t = \left[x_t^1, x_t^2, \ldots, x_t^N\right]^T \tag{4.1}$$

where x_t^i is the coded symbol of the i-th antenna, at time interval t. The transmitted symbol vector $\mathbf{x}_t$, is then transmitted simultaneously through a MIMO channel. The received signal at each of the M receive antennas can be considered as a superposition of all N transmitted symbols and additive white Gaussian noise (AWGN). The received signal vector, denoted by $\mathbf{r}_t$, at time t can be represented as

$$\mathbf{r}_t = \mathbf{H}_t\mathbf{x}_t + \mathbf{n}_t \tag{4.2}$$

where $\mathbf{r}_t$ is an $M\times1$ column vector of the received signals across the M receive antennas, as defined by $\mathbf{r} = \left[r_1, r_2, \ldots, r_M\right]^T$. $\mathbf{H}_t$ is an $M \times N$ complex channel matrix gain for time interval t, given by

$$\mathbf{H}_t = \begin{bmatrix} h_{11}^t & \cdots & h_{1N}^t \\ \vdots & \ddots & \vdots \\ h_{M1}^t & \cdots & h_{MN}^t \end{bmatrix} \tag{4.3}$$

where h_{ji}^t, is the fading attenuation coefficients at time t from the i-th transmit antenna, $i = 1, \ldots, N$, to the j-th receive antenna, $j = 1, \ldots, M$. $\mathbf{n}_t$ is a $M\times1$ vector of the AWGN noise with a zero mean and the noise variance of σ^2, given by

$$\mathbf{n}_t = [n_1, n_2, \ldots n_M]^T \tag{4.4}$$

4.2.1 Frequency Domain Adaptive Iterative Receiver

The frequency domain adaptive iterative LSTC receiver structure is shown in Figure. 4.1. It consists of a soft-input soft-output (SISO) detector and N parallel SISO channel decoders. Deinteleavers and interleavers separate the two modules. The SISO detector employs an adaptive iterative MMSE interference canceller consisting of frequency domain feed-forward and feedback filters. The deinterleaver module consists of time and spatial deinterleavers, which perform a reverse process of time and spatial interleavers corresponding to the transmitter structure. After the SISO decoding process, the SISO estimated signals from the decoder are interleaved by the spatial interleaver and then the time interleaver, respectively. The outputs of the time interleaver are used to regenerate the interference for the interference cancellation process in the next iteration, which will be described later in this chapter.

4.2.1.1 Frequency domain adaptive LMS detector

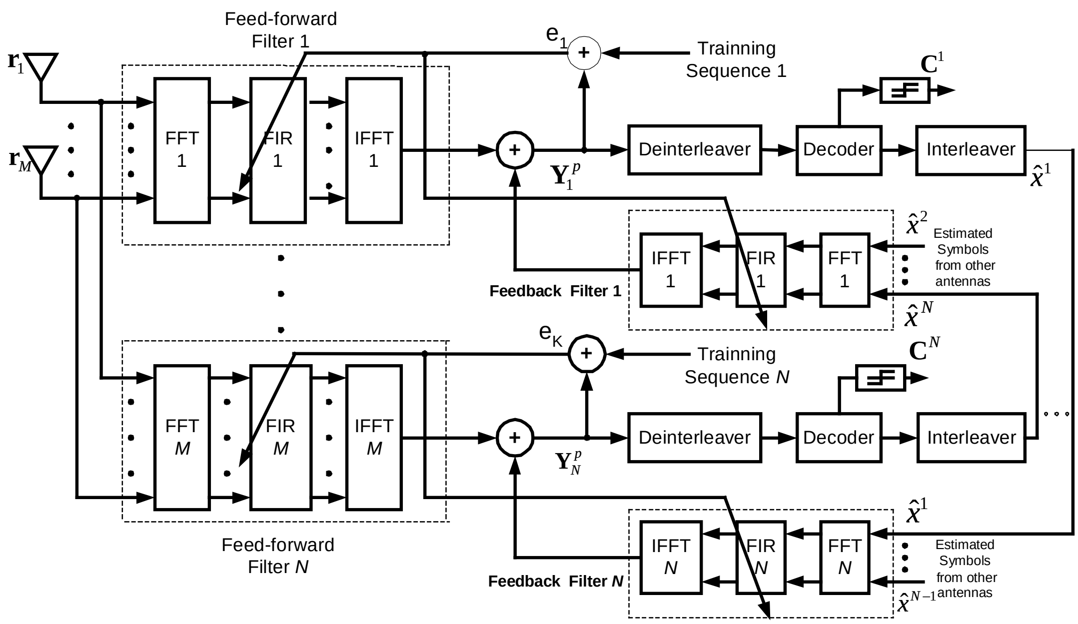

Figure. 4.1 Block diagram of frequency domain the adaptive iterative LST Receiver

As can be seen in Figure.4.1, the received signals from all receive antennas are first transformed into the frequency domain using the fast Fourier transform (FFT). The frequency domain output signals from the FFT module are then passed to the feed-forward filter to perform the convolution in the frequency domain. The inverse fast Fourier transform (IFFT) transforms the feed-forward filter output signals from the frequency domain into the time domain signals, and the desired time domain outputs of the feed-forward filter are then collected for further processing.

The received signals, $\mathbf{r}_t$, across M receive antennas, defined in (4.2), at time interval t, are transformed into the frequency domain using FFT. The outputs of the FFT module, denoted by $\mathbf{\Omega}_t$, where $\mathbf{\Omega}_t$ is the received signal vector at time instance t in the frequency domain, is given by [84]

$$\mathbf{\Omega}_t = fft(\mathbf{r}_t) \tag{4.5}$$

where

$$\mathbf{\Omega}_t = \left[\Omega_t^1, \Omega_t^2, \mathbf{K}, \Omega_t^q, \mathbf{K}, \Omega_t^M\right] \tag{4.6}$$

and

$$\Omega_t^q = \sum_{l-0}^{M-1} r_t^l e^{\frac{-j2pql}{M}} \tag{4.7}$$

$\mathrm{FFT}(\cdot)$ represents the fast Fourier transform, and Ω_t^q, $q = 1, \mathbf{K}, M$, is the FFT transform of the receive signal across the M receive antennas, at time instant t.

Let $\mathbf{w}_f^{i,k}(t)$ be the $M \times 1$ time domain feed-forward tap coefficients vector for the i-th transmit antenna during the k-th iteration at time instance t, given by

$$\mathbf{w}_f^{i,k}(t) = \left[w_{f,0}^{i,k}(t), \mathbf{K}, w_{f,q}^{i,k}(t), \mathbf{K}, w_{f,M-1}^{i,k}(t)\right]^T \tag{4.8}$$

where $w_{f,q}^{i,k}(t)$, q = 1,…,M, is the feed-forward tap coefficient corresponding to the q-th receive antenna.

Let $\mathbf{\Psi}_{f,t}^{i,k}$ represent the FFT transform signals of $\mathbf{w}_f^{i,k}(t)$, defined by

$$\mathbf{\Psi}_{f,t}^{i,k} = fft\left(\mathbf{w}_f^{i,k}(t)\right) \tag{4.9}$$

where

$$\mathbf{\Psi}_{f,t}^{i,k} = \left[\Psi_{f,t}^{i,k}(0), \mathbf{K}, \Psi_{f,t}^{i,k}(q), \mathbf{K}, \Psi_{f,t}^{i,k}(M-1)\right] \tag{4.10}$$

and

$$\Psi_{f,t}^{i,k}(q) = \sum_{l=0}^{M-1} w_{f,t}^{i,k}(l) e^{\frac{-j2pql}{M}} \tag{4.11}$$

where $\Psi_{f,t}^{i,k}(q)$ is the FFT of the feed-forward tap coefficient for the *i*-th transmit antenna corresponding to the *q*-th receive antenna during the *k*-th iteration at time *t*. $\mathbf{\Omega}_t$ is then sent to the feed-forward filter to perform the element-wise multiplication with the feed-forward tap coefficient $\mathbf{\Psi}_{f,t}^{i,k}$ in the frequency domain.

The output of the feed-forward filter for the *k*-th iteration at time *t*, for the *i*-th antenna, denoted by $\overline{\mathbf{F}}_t^{i,k}$, is given by

$$\overline{\mathbf{F}}_t^{i,k} = diag(\mathbf{\Omega}_t)^H \cdot \mathbf{\Psi}_{f,t}^{i,k} \tag{4.12}$$

where $diag(\cdot)$ and $(\cdot)^H$ are a diagonal matrix and the conjugate transpose function.

$\overline{\mathbf{F}}_t^{i,k}$ is then transformed back into the time domain by the inverse fast Fourier transform (IFFT). The feed-forward filter output for the *i*-th antenna during the *k*-th iteration at time *t*, is given by

$$\mathbf{F}_t^{i,k} = ifft\left(\overline{\mathbf{F}}_t^{i,k}\right) \tag{4.13}$$

where

$$\mathbf{F}_t^{i,k} = \frac{1}{M} \sum_{l=0}^{M-1} \overline{\mathbf{F}}_t^{i,k} e^{\frac{-j2pl}{M}} \tag{4.14}$$

Let $F_t^{i,k}$ be the time domain feed-forward filter output for *i*-th antenna at the *k*-th iteration at time *t*, denoted by

$$F_t^{i,k} = \mathbf{I_F} \cdot \mathbf{F}_t^{i,k} \tag{4.15}$$

where $\mathbf{I_F}$ is defined by $\mathbf{I_F} = [1 \;\; \mathbf{0}_{M-1}]$ and $\mathbf{0}_{M-1}$ is a row vector of length (M –1) containing all zeros. In the first iteration, the feed-forward filter only performs interference suppression without the interference cancellation process since there are no estimated symbols from the output of the MAP decoder.

After the first iteration, the feedback filter is included in the detection process. The estimated symbols from the output of the decoder are fed back to the feedback filter to generate and cancel the interference from other antennas in the detection process.

The symbol estimates from the output of the decoders are first transformed into the frequency domain using the FFT and then passed to the feedback filter. The output of the FFT, denoted by $\mathbf{\Lambda}_t^{i,k}$, at symbol interval *t*, is given by

$$\mathbf{\Lambda}_t^{i,k} = fft\left(\underline{\hat{\mathbf{x}}}_t^{i,k}\right) \tag{4.16}$$

where

$$\mathbf{\Lambda}_t^{i,k} = \left[\Lambda_{t,1}^{i,k}, \mathbf{K}\, \Lambda_{t,b}^{i,k}, \mathbf{K}, \Lambda_{t,N-1}^{i,k}\right] \tag{4.17}$$

and

$$\Lambda_{t,b}^{i,k} = \sum_{m=1}^{KN-1} \hat{x}_{t,m}^{i,k} e^{\frac{-j2pam}{KN-1}}; \quad a \in (1\mathbf{K}\, N-1) \tag{4.18}$$

where $\underline{\hat{\mathbf{x}}}_t^{i,k}$ is an $(N-1)\times 1$ vector of the estimated soft symbols, at the *k*-th iteration, from MAP decoders, except the *i*-th antenna, during the time *t*, given by

$$\underline{\hat{\mathbf{x}}}_{t,p}^{i,k} = \left(\hat{x}_t^{1,k}, \hat{x}_t^{2,k}, \ldots, \hat{x}_t^{i-1,k}, \hat{x}_t^{i+1,k}, \ldots, \hat{x}_t^{N,k}\right) \tag{4.19}$$

Let $\mathbf{w}_b^{i,k}(t)$ be the (N-1) $\times$ 1 time domain feedback filter coefficients of the transmit antennas, except the ***i***-th antenna at time *t*, given by

$$\mathbf{w}_b^{i,k}(t) = \left[w_b^{1,k}(t), \ldots, w_b^{i-1,k}(t), w_b^{i+1,k}(t), \mathbf{K} w_b^{N,k}(t)\right] \quad (4.20)$$

Let $\mathbf{\Psi}_{t,b}^{i,k}$ represent the FFT of $\mathbf{w}_b^{i,k}(t)$, defined by

$$\mathbf{\Psi}_{t,b}^{i,k} = fft\left(\mathbf{w}_b^{i,k}(t)\right) \quad (4.21)$$

where

$$\mathbf{\Psi}_{t,b}^{i,k} = \left[\Psi_{t,b}^{i,k}(0), \mathbf{K}, \Psi_{t,b}^{i,k}(a), \mathbf{K}\, \Psi_{t,b}^{i,k}(N-2)\right] \quad (4.22)$$

and

$$\Psi_{t,b}^{i,k}(a) = \sum_{m=0}^{N-2} w_{t,b}^{i,k}(m) e^{\frac{-j2pam}{N-1}} \quad (4.23)$$

The output of the FFT, denoted by $\mathbf{\Lambda}_t^{i,k}$, is then applied to the feedback filter with the frequency domain feedback tap coefficients $\mathbf{\Psi}_{t,b}^{i,k}$ to perform the element-wise multiplication in frequency domain. The feedback filter output signals, defined by $\overline{\mathbf{F}}_{t,b}^{i,k}$, at symbol interval *t*, is given by

$$\overline{\mathbf{F}}_{t,b}^{i,k} = \left(diag\left(\mathbf{\Lambda}_t^{i,k}\right)^H \cdot \mathbf{\Psi}_{t,b}^{i,k}\right) \quad (4.24)$$

$\overline{\mathbf{F}}_{t,b}^{i,k}$ is then transformed back into time domain by the IFFT. The feedback filter output for the ***i***-th antenna of the ***p***-th user, during the ***k***-th iteration, at symbol interval *t*, is given by

$$\mathbf{F}_{t,b}^{i,k} = ifft(\overline{\mathbf{F}}_{t,b}^{i,k}) \quad (4.25)$$

where

$$\mathbf{F}_{t,b}^{i,k} = \frac{1}{N-1}\sum_{m=0}^{N-2}\overline{\mathbf{F}}_{t,b}^{i,k} e^{\frac{-j2pm}{KN-1}} \tag{4.26}$$

Let $F_{t,b}^{i,k}$ represent the time domain feedback filter output for the ***i***-th antenna during the ***k***-th iteration at time *t*, defined by

$$F_{t,b}^{i,k} = \mathbf{I}_{\mathrm{B}} \cdot \mathbf{F}_{t,b}^{i,k} \tag{4.27}$$

where $\mathbf{I}_B = [1 \ \mathbf{0}_{N-1}]$, and $\mathbf{0}_{N-1}$ is a row vector with length *N*-1 containing all zeros. The detected output in (4.27) represents the CCI, the interference from other antennas in the system.

The detected symbol obtained at the output of the adaptive detector in the time domain for the ***i***-th antenna during the ***k***-th iteration at symbol interval *t*, denoted by $y_{t,}^{i,k}$, given by

$$y_t^{i,k} = F_t^{i,k} + F_t^{p,k} \tag{4.28}$$

where $F_t^{i,k}$ and $F_t^{p,k}$ represent the feed-forward and the feedback filter outputs in the time domain, given in (4.15) and (4.27), respectively. The feed-forward coefficient vector $\mathbf{w}_f^{i,k}(t)$ and feedback coefficient vector $\mathbf{w}_b^{i,k}(t)$ defined in (4.8) and (4.20) are determined recursively by an adaptive Least Mean Square (LMS) algorithm [18]. Thus the mean squared error is given by

$$z = E\left[\left|e(t)\right|^2\right] = E\left[\left|y_t^{i,k} - x_t^{i,k}\right|^2\right] \tag{4.29}$$

where $y_t^{i,k}$ is the soft detector output in the time domain and can be expressed in a time domain expression based on the conventional LMS algorithm as defined in (4.30)

$$y_t^{i,k} = \mathbf{w}_f^{i,k\,H}(t)\mathbf{r}_t + \mathbf{w}_b^{i,k\,H}(t)\underline{\hat{\mathbf{x}}}_t^{i,k} \tag{4.30}$$

By using (4.29) and (4.30) to calculate the coefficients $\mathbf{w}_f^{i,k}(t)$ and $\mathbf{w}_b^{i,k}(t)$ adaptively for a particular time instant *t*, the mean squared error for the LMS algorithm is given by [18]

$$z(t) = E\left[\left|\mathbf{w}_f^{i,k^T}(t)\mathbf{r}_t + \mathbf{w}_b^{i,k^T}(t)\underline{\hat{\mathbf{x}}}_t^{i,k} - x_t^{i,k}\right|^2\right] \tag{4.31}$$

where
$$\mathbf{w}_f^{i,k}(t+1) = \mathbf{w}_f^{i,k}(t) + m_f e(t)\mathbf{r}_t \tag{4.32}$$

and
$$\mathbf{w}_b^{i,k}(t+1) = \mathbf{w}_b^{i,k}(t) + m_b e(t)\underline{\hat{\mathbf{x}}}_t^{i,k} \tag{4.33}$$

μ_f and μ_b are the step sizes for the feed-forward and feedback adaptations respectively.

As mentioned in the Chapter 3., it is obvious that the convolution process in the PFGLMS is performed in the same manner as the LMS algorithm. The only difference is the method of calculating the feed-forward and feedback coefficients. The modified feed-forward and feedback coefficients of the PFGLMS algorithm for MIMO systems can be expressed by [21]

$$\mathbf{w}_f^{i,k}(t+1) = \mathbf{w}_f^{i,k}(t) + m_f \mathbf{g}_f^{i,k}(t) \tag{4.34}$$

and
$$\mathbf{w}_b^{i,k}(t+1) = \mathbf{w}_b^{i,k}(t) + m_b \mathbf{g}_b^{i,k}(t) \tag{4.35}$$

where μ_f and μ_b are the step sizes for the feed-forward and feedback adaptations, respectively.

where
$$\left.\begin{aligned} \mathbf{g}_f^{i,k}(t) &= e(t)\mathbf{r}_t + \hat{\mathbf{g}}_f^{i,k}(t) \\ \hat{\mathbf{g}}_f^{i,k}(t) &= l_f \hat{\mathbf{g}}_f^{i,k}(t-1) + g_f e(t)\mathbf{r}_t \end{aligned}\right\} \tag{4.36}$$

and
$$\left.\begin{aligned} \mathbf{g}_b^{i,k}(t) &= e(t)\underline{\hat{\mathbf{x}}}_t^{i,k} + \hat{\mathbf{g}}_b^{i,k}(t) \\ \hat{\mathbf{g}}_b^{i,k}(t) &= l_b \hat{\mathbf{g}}_b^{i,k}(t-1) + g_b e(t)\underline{\hat{\mathbf{x}}}_t^{i,k} \end{aligned}\right\} \tag{4.37}$$

where (l_f, l_b) and (g_f, g_b) are the forgetting factors and the scaling factors, respectively, and $\hat{\mathbf{g}}_f^{i,k}(0) = \hat{\mathbf{g}}_b^{i,k}(0) = 0$.

In the proposed receiver structure, the well-known SISO MAP decoder takes the detection output of the detector, $y_t^{i,k}$, as a soft-input to the decoder. The soft-output from the decoder is used to calculate the interference, which is subtracted for the decoder input in the next iteration. This iterative detection/decoding process is performed until the symbol estimate converges to the optimal performance. The soft-output from the decoder in the last iteration is then fed into a decision device to produce a decision. For the BPSK modulation scheme, the likelihood ratios (LLR) in the *k*th iteration for the *i*th transmit layer, denoted by $l_t^{i,k}$, are given by [20]

$$l_t^{i,k} = \log\left(\frac{P\left(x_t^{i,k} = 1 \middle| y_t^{i,k}\right)}{P\left(x_t^{i,k} = -1 \middle| y_t^{i,k}\right)}\right) \tag{4.38}$$

The soft-output symbols estimated in the *i*th layer and *k*th iteration can be determined as

$$\hat{x}_t^{i,k} = \frac{e^{l_t^{i,k}} - 1}{e^{l_t^{i,k}} + 1} \tag{4.39}$$

4.3 Complexity Analysis

In this section, the computational complexity of the adaptive algorithm based on the frequency domain and time domain approaches is analyzed. We define the receiver computation complexity as the required number of signal processing operations per coded symbol and per layer. As we want to compare the receiver complexity between the time domain and the frequency domain adaptive iterative receivers, we will consider only the complexity of the detector since the decoder is the same for both implementations.

As mentioned in Chapter 3, the computational requirement for the adaptive iterative receiver, based on the conventional time domain LMS algorithm for N transmit and M receive antennas, requires $2M$ +1 multiplications for the feed-forward filter and $2(N\text{-}1)$ +1 multiplications for the feedback filter. The total computational requirement for the LMS algorithm is $NI(2M + 2N)$ multiplications for the N transmit and M receive antennas at I iterations for every detected output symbol.

The PFGLMS algorithm requires $4M$ +1 multiplications and $4(N - 1)$ +1 for the feed-forward filter and feedback filter, respectively. Therefore, the total computational requirement for the PFGLMS algorithm is $NI(4M+4N-2)$ multiplications for the N transmit and M receive antennas at I iterations for every detected symbol.

On the other hand, the frequency domain adaptive LMS algorithm requires $\log_2(2M+1)$ multiplications for the feed-forward filter and $\log_2(2(N-1)+1)$ multiplications for the feedback filter. The total computational requirement for the frequency domain LMS algorithm is $NI(\log_2(2M+1)+\log_2(2N-1))$ multiplications for the N transmit and M receive antennas at I iterations for every detected coded symbol. The frequency domain PFGLMS also requires $\log_2(4M+1)$ multiplications for the feed-forward filter and $\log_2(4(N-1)+1)$ multiplications for the feedback filter. The total computational requirement for the frequency domain LMS algorithm is $NI(\log_2(4M+1)+\log_2(4N-3))$ multiplications for the N transmit and M receive antennas at I iterations for every detected coded symbol. The comparison of the complexity amongst these detectors is shown in table 1.

Table 1. Complexity comparison between time- domain adaptive receivers and the proposed frequency-domain adaptive detectors

Algorithm	LMS algorithm		PFGLMS algorithm	
	Time domain	Frequency domain	Time domain	Frequency domain
Number of multiplications	$NI(2M+2N)$	$NI(\log_2(2M+1)+\log_2(2N-1)$	$NI(4M+4N-2)$	$NI(\log_2(4M+1)+\log_2(4N-3))$
Computational Complexity	640	239	1200	304

N = number of transmit antennas, M = number of receive antennas,
I = number of iteration.

It can be observed from Table 1 that the computational complexity of the time domain adaptive iterative PFGLMS receiver is very high compared to the time domain adaptive iterative LMS and PFGLMS detector. For example, for four transmit (N) and four receive (M) antennas, where the number of iterations I is10, the computational complexity of the time domain adaptive PFGLMS receiver is equal to 1200; the computational complexities for the conventional time domain LMS receiver is 640. Therefore, the computation requirement of the time domain PFGLMS receiver is almost double the requirement of the time domain LMS receiver.

Nevertheless, using the frequency domain filter, we can reduce the computational complexity of these time domain receivers. The computational complexity of the frequency domain LMS and PFGLMS receivers is about 239 and 304, respectively. The reduction of the computational complexity in the receiver based on the frequency domain LMS algorithm compared to the time domain LMS algorithm is about 63 %. In addition, the frequency domain PFGLMS receiver can save about 75% in computational requirement compared to the time domain PFGLMS approach. Moreover, the complexity of the frequency domain PFGLMS is slightly higher than the frequency domain LMS receiver.

It is obvious that the proposed frequency domain adaptive iterative receivers, based on both the conventional LMS and PFGLMS algorithms, offer a significant reduction in computational complexity. Although, the PFGLMS algorithm has a slightly higher complexity compared to the conventional LMS algorithm, the convergence speed of the PFGLMS algorithm is faster than that of the conventional LMS. In addition, the PFGLMS algorithm provides the tracking ability in the system in the slow fading channel as shown in the next section.

4.4 Performance Results

This section presents simulation results for the LSTC frequency domain adaptive iterative receivers with BPSK modulation in a quasi-static fading channel where each fading coefficient is constant within a frame, but changes from one frame to another and for each sub-channel. The system operates in the training mode until the mean square error (MSE) approaches the minimum mean square error (MMSE), then switches to the decision directed mode. The constituent codes are nonsystematic convolutional codes with the code rate R of 1/2, memory order of 3, and the generating polynomial [19] $g_1=15_8$ and $g_2 = 17_8$. The proposed system is simulated with two transmit and two receive antennas, two transmit and four receive antennas, and four transmit and two receive antennas system with 130 information bits in each transmit antennas. Each layer of the LSTC system consists of 130 information bits and these are encoded by the channel encoder. The simulation results are represented in terms of the average bit error rate

(BER) versus the ratio of the averaged energy per bit, denoted by E_b, to the power spectral density of the AWGN, denoted by N_o.

The average BER of the time and frequency domain LMS adaptive iterative receiver of a 2×2 MIMO system for various numbers of iterations is shown in Figure. 4.2. The results show that the performance of the time and frequency domain LMS approach is identical. The system performance is significantly improved for the second iteration compared to the first iteration and gradually increases for higher iterations. The BER curves also show that the performance converges to a steady state after the third iteration.

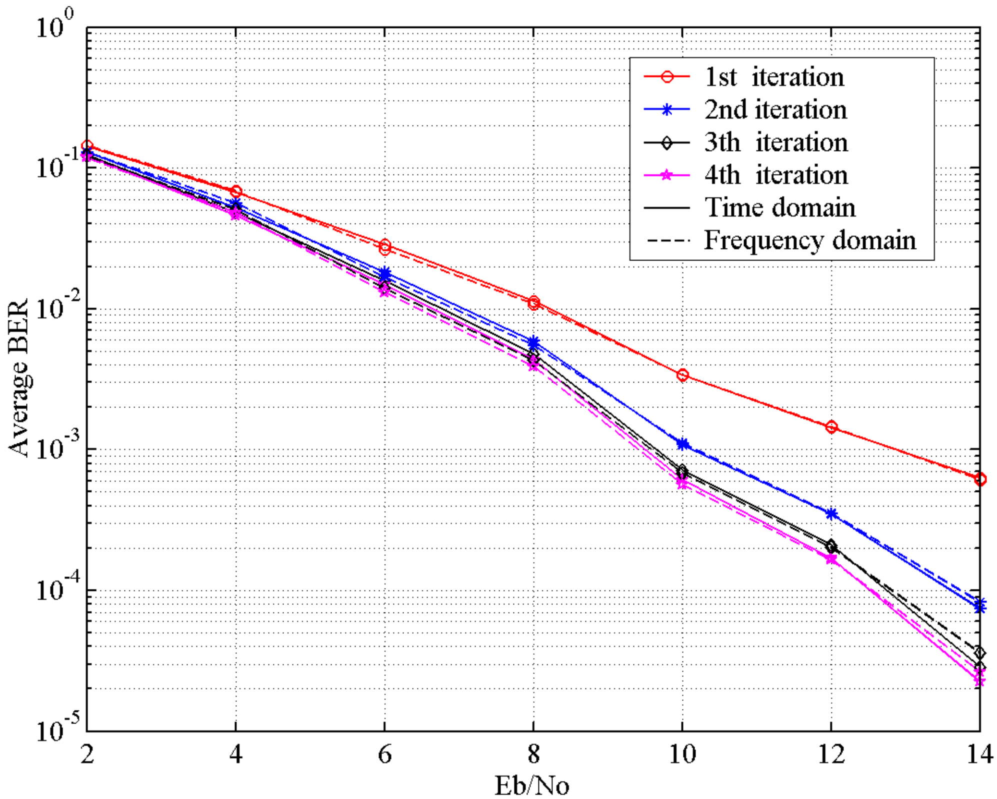

Figure.4.2 Performance comparison between the time and frequency domain LMS adaptive iterative in a quasi-static Rayleigh fading channel with 2×2 antennas system

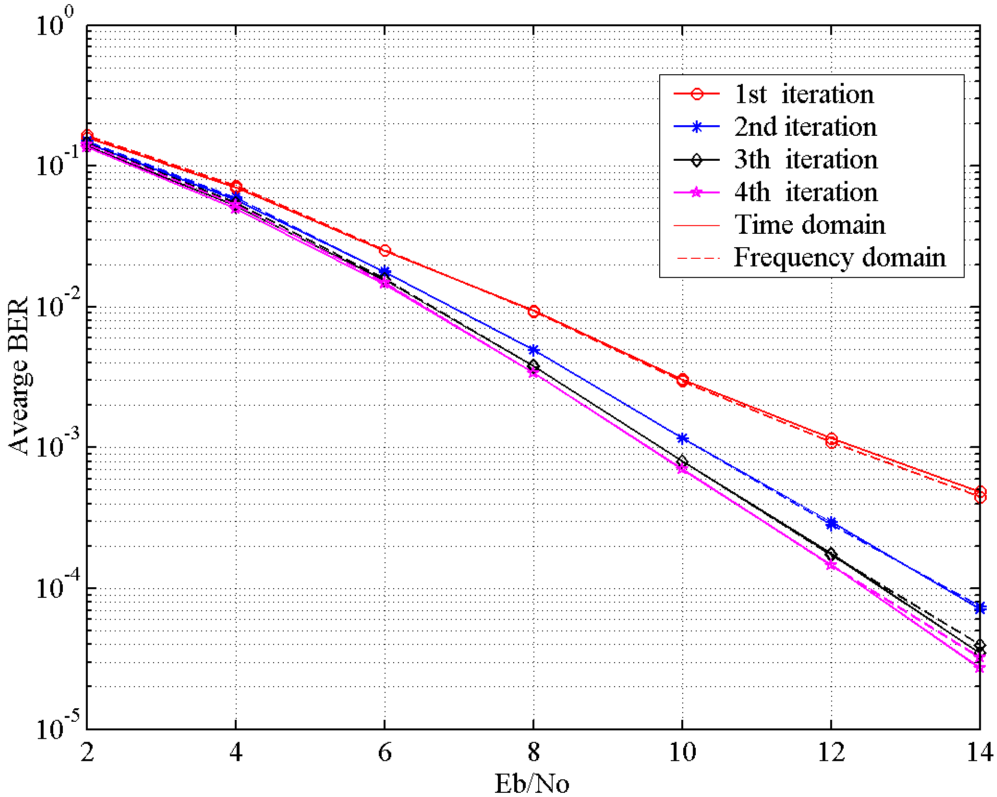

Figure. 4.3 Performance comparison between the time and frequency domain PFGLMS adaptive iterative in a quasi-static Rayleigh fading channel with 2×2 antennas system

The performance of adaptive iterative receiver based on the time and frequency domain PFGLMS algorithms is also shown in Figure. 4.3. Similarly, the results in Figure.4.3 show that the performance of the time and frequency domain PFGLMS algorithms is the same.

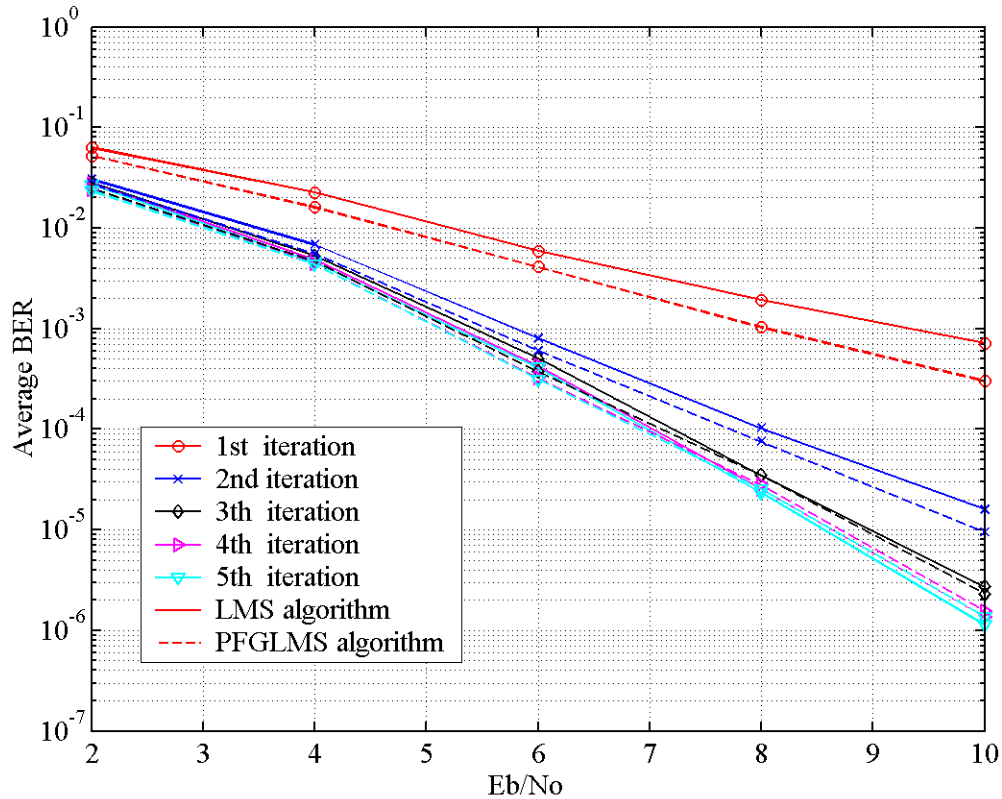

Figure. 4.4 Performance comparison between the frequency domain LMS and PFGLMS adaptive iterative in a quasi-static Rayleigh fading channel with 2×4 antennas system

The performance of the two transmit and four receive antennas under the frequency domain approach is presented in Figure. 4.4. The results show that the performance of the adaptive iterative receiver based on the frequency domain PFGLMS algorithm has a significant improvement in the first iteration and gradually improves for the higher iterations compared to the adaptive iterative receiver based on the frequency domain LMS algorithm. The BER curves also show that the PFGLMS based receiver has an excellent tracking ability in the scattering environment.

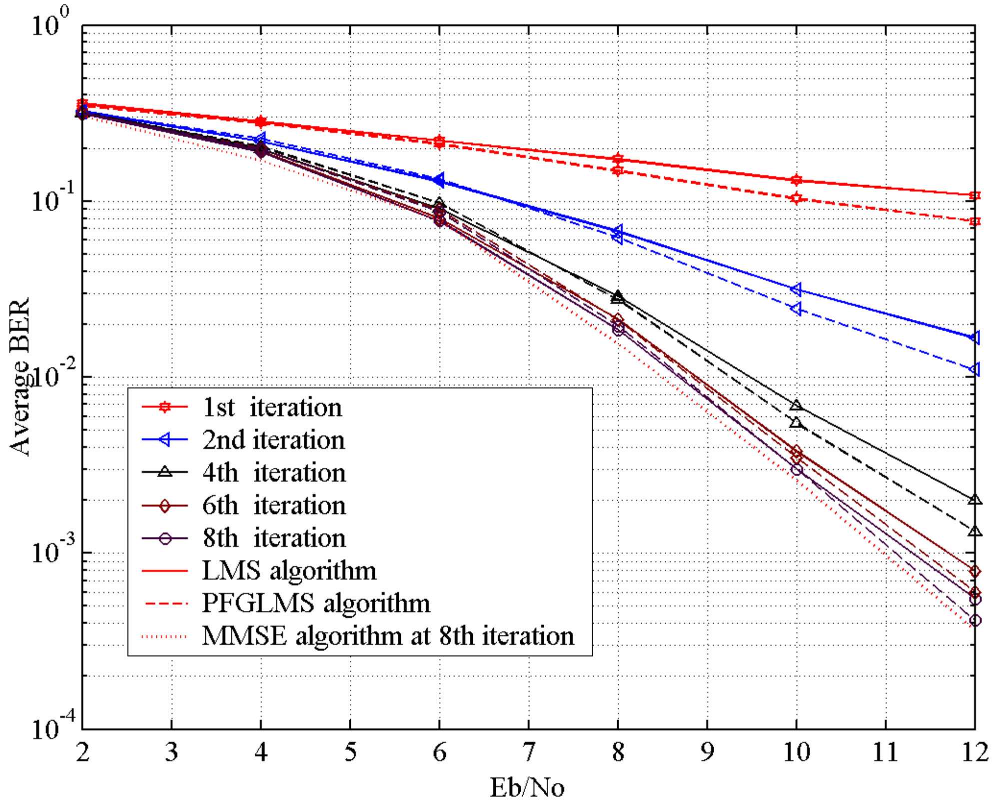

Figure. 4.5 Performance comparison between frequency domain LMS and PFGLMS adaptive iterative in a quasi-static Rayleigh fading channel with 4×2 antennas system

Figure. 4.5 presents the performance of the frequency domain adaptive iterative receivers, including the performance of the time domain non-adaptive iterative MMSE receiver at the 8^{th} iteration for the four transmit and two receive antennas system. It is obvious that the system performance is degraded compared to 2×2 or 2×4 antennas system because of the additional co-channel interference due to an increasing of the number of transmit antennas. The average BER shows that the performance of the frequency domain adaptive receivers is improved as the number of iterations is increased. Furthermore, the performance of the frequency domain adaptive receivers approaches the same performance of the non-adaptive iterative MMSE receiver at the 8^{th} iteration. Therefore, the proposed frequency domain adaptive receiver can suppress and remove the CCI from the system.

4.5 Conclusion

A new frequency domain adaptive iterative receiver for MIMO systems based on a joint adaptive iterative detection and decoding structure has been discussed. The adaptive iterative receiver reduces co-channel interference by interference suppression and cancellation techniques. The computational complexity is considered only the complexity of the detector. In comparison to the time domain receiver, the proposed frequency domain receiver has a significantly lower computational complexity and achieves the same performance. As a given example, the computational complexity of the frequency domain receiver based on the LMS and PFGLMS algorithm is 63 % and 75% lower than that of a time domain receiver, respectively in each received data symbol. However, there is a need for the transmission of training sequences at the beginning of each simulation. Moreover, the proposed receiver based on the PFGLMS algorithm has a faster convergence speed and better tracking ability compared to the LMS receiver in a dense interference environment with a slight increase in the complexity in terms of the number of multipliers. Therefore the PFGLMS receiver needs a shorter training period than the LMS receiver. The performance of the proposed receiver approaches the one of the non-adaptive iterative receiver as shown in Figure. 4.5.

Chapter 5

Time-domain Adaptive Iterative Receivers for Layered Space-time Coded CDMA Systems

In this chapter, a new adaptive iterative receiver for a layered space-time coded CDMA (LSTC-CDMA) system is discussed. The system is based on the assumption that there is no a priori knowledge of channel state information (CSI), spreading sequences and fading coefficients. A normalized least mean square (NLMS) feed-forward filter and a feedback iterative parallel interference canceller operating in the time domain are employed. The system performance is evaluated by using a semi-analytical approach and compared to the simulation results. The results show that there is an excellent agreement between the two approaches. The results indicate that the proposed receiver performance approaches that of the interference-free single user performance for a high signal-to-noise ratio (SNR).

5.1 Introduction

Direct-Sequence CDMA (DS-CDMA) has emerged as a predominant multiple access technique for 3G systems because it efficiently utilizes the radio spectral capacity and facilitates network planning in a cellular environment compared to 2G TDMA systems. MIMO systems have recently emerged as one of the most significant technical advances in modern communications. This technology promises to solve the capacity bottleneck in wireless communication systems [20, 35, 42]. E. Telatar has shown in [35] that the asymptotic capacity of multiple-input multiple-output (MIMO) Rayleigh fading channels grows linearly with the minimum number of transmit and receiver antennas. Space-time coding, for instance, is a technique, which combines the space and time diversity to achieve performance gain without bandwidth expansion. The Bell Lab layered space-time (BLAST) architecture which uses multiple antennas at both the transmitter and receiver end can achieve a channel capacity as high as 10-100 times those for single antenna architectures in rich scattering environments.

In layered space-time (LST) coding algorithm, N data streams are transmitted simultaneously over N antennas over the same frequency band. The receiver uses M receive antennas and interference canceling/suppression techniques to minimize interference caused by simultaneous transmission from N transmit antennas. Therefore, the detection techniques of LST coded systems can also be directly applied in multiuser CDMA systems. The combination of layered space-time coding (LSTC) and CDMA, referred to as LSTC-CDMA, has been intensively studied [85-89] recently. However, such a combination introduces co-channel interference (CCI) [7, 90] from adjacent layers and multiple access interference (MAI) from other users.

To reduce CCI and MAI in LSTC-CDMA systems, an iterative minimum mean square error (MMSE) detection with soft-output Viterbi algorithm (SOVA) decoding was proposed by Gamal et. al., [44]. In [7], S. Marinkovic et. al., proposed an iterative parallel interference cancellation (PIC) detection scheme with decision statistics combining. Both approaches exhibit near interference-free single user performance for certain ranges of the signal-to-noise ratio (SNR). However, both schemes rely on the assumption of perfect channel state information (CSI) at the receiver end. An imperfect CSI will significantly degrade the system performance and the complexity of calculating the channel state information in non-adaptive systems is significantly high due to matrix inversion [20].

To reduce the computational complexity, feed-forward adaptive MMSE receivers for LSTC systems were considered by [15, 23, 54]. However, these receiver structures have a poor performance in high interference environments due to inaccurate channel estimates, we proposed an improved-non-linear adaptive iterative receiver presented in [30, 31]. Such a receiver consists of a feed-forward filter for interference suppression and a feedback filter for interference cancellation. It is shown clearly that the proposed receiver can effectively suppress and remove interference with reduced complexity in comparison to non-adaptive approaches as mentioned in Chapter 3.

Miller, S. L. [91], proposed a single input single output adaptive DS-CDMA receiver, which has the capability of multiuser interference rejection and is near-far resistant. By applying the adaptive receiver, proposed by the C. Teekapakvisit et. al., in [30] and the adaptive DS-CDMA receiver, proposed by Miller, S. L in [91], we propose a multiuser receiver, called a multiuser LSTC-CDMA receiver for MIMO-CDMA systems. Such an adaptive iterative receiver is investigated for a downlink LSTC-CDMA system under a quasi-static fading channel with no a priori knowledge of CSI, spreading sequences and fading coefficients. Training sequences for each user are transmitted at the start of the transmission for each user. For the downlink, we assume that all the users have the same number of antennas and each user can detect all other user's information and suppress them in its receiver, just like a conventional multi-user detection.

Such a receiver can effectively mitigate MAI and thus improve the multiuser system performance. The simulation results show that the adaptive iterative receiver can also achieve the interference-free single user performance for a certain range of the signal-to-noise ratio (SNR).

The rest of this chapter is organized as follows. Section 5.2 describes the system model of an LSTC-CDMA system including the proposed adaptive receiver structure. The computational complexity analysis is given in Section 5.3. The system evaluation of the proposed receiver structure is discussed in Section 5.4. In Section 5.5 the simulation results and discussions are presented. Finally in Section 5.6 conclusions are drawn.

5.2 System Model

5.2.1 Transmitter structure

A downlink LSTC-CDMA system where all user signals are transmitted simultaneously is considered. A general K user threaded LSTC-CDMA transmitter is shown in Figure. 5.1. We assume that each user is equipped with the same number of antennas. A system with N transmit and M receive antennas for each user is considered throughout this chapter. It is assumed that the binary information of each user is transmitted at a data rate of $r_b = 1/T_b$, where T_b is the bit interval. The binary information stream of each user is first passed through a serial to a parallel converter and multiplexed into N layers. The data in each layer is then encoded by a convolutional encoder, followed by a BPSK modulation and a spatial interleaver ($S\mathbf{\Pi}$), which distributes a coded stream of all users and all layers to N transmit antennas. Each layer at the output of the spatial interleaver is then interleaved and spread by a user specific signature sequence, which is the same for all layers. The spreading gain is denoted by L and defined as $L = T/T_c$, where T is the symbol interval and T_c is a chip duration of the spreading sequence. The spread symbols of all users are then combined and simultaneously transmitted through N transmit antennas.

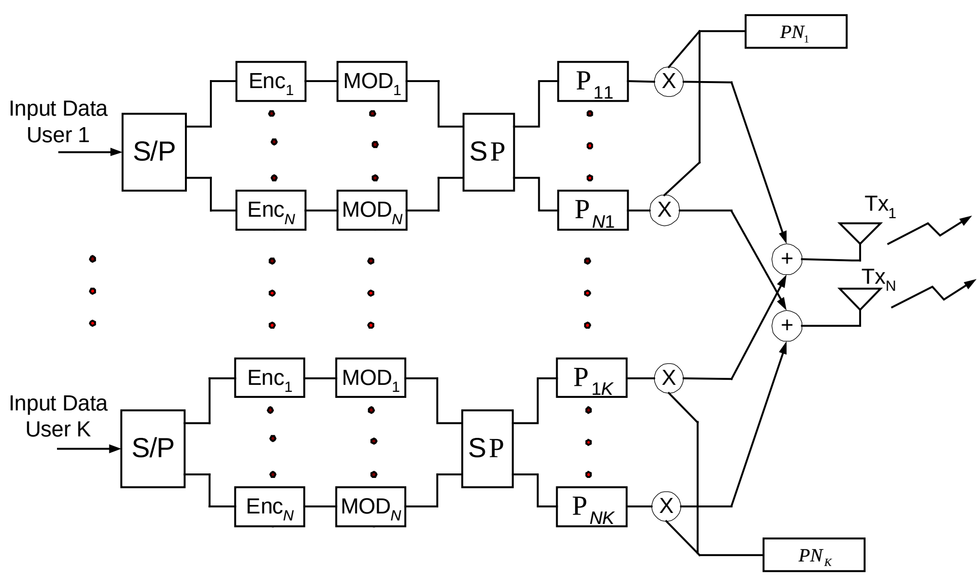

Figure.5.1 Layered space-time CDMA transmitter structure

Let $\mathbf{b}$ be the coded signal vectors transmitted by K users through N transmit antennas, given by

$$\mathbf{b}=[\mathbf{b}_1,\mathbf{b}_2,\mathbf{K},\mathbf{b}_p,\mathbf{K},\mathbf{b}_K]^T \tag{5.1}$$

where

$$\mathbf{b}_p=[b_p^1,\mathbf{K},b_p^n,\mathbf{K},b_p^N] \tag{5.2}$$

$b_p^n, n=1,\mathbf{K},N$, $p=1,\mathbf{K},K$, is the coded information bit of the *p*-th user for the *n*-th transmit antenna, and $[\mathbf{x}]^T$ is the transpose of a vector $\mathbf{x}$.

Let $\mathbf{r}_{t,j}^p$ be the received signal vector for the *p*-th user at the receive antenna *j*, $j=1,\mathbf{K},M$, for symbol *t*, then we can write $\mathbf{r}_{t,j}^p$ as

$$\mathbf{r}_{t,j}^p=\mathbf{S}\mathbf{H}_{t,j}^p\mathbf{b}+\mathbf{n}_{t,j}^p \tag{5.3}$$

where $\mathbf{r}_{t,j}^p=[r_{t,j}^{p,1},\mathbf{K}\,r_{t,j}^{p,q},\mathbf{K},r_{t,j}^{p,L}]^T$ and $r_{t,j}^{p,q}$ is the received signal for the *p*-th user at the *q*-th chip of the *t*-th symbol for *j*-th antenna , $\mathbf{S}$ represents the $L\times KN$ spread transmitted sequence of K users for N transmit antennas, denoted by

$$\mathbf{S}=[\mathbf{s}_1^1,\mathbf{K},\mathbf{s}_1^N,\mathbf{K},\mathbf{s}_p^n,\mathbf{K},\mathbf{s}_K^1,\mathbf{K},\mathbf{s}_K^N] \tag{5.4}$$

where $\mathbf{s}_p^n$ is the spread sequence corresponding to the *p*-th user and *n*-th antenna, represented as

$$\mathbf{s}_p^n=[s_p^{n,1},\mathbf{K},s_p^{n,q},\mathbf{K},s_p^{n,L}]^T \tag{5.5}$$

and $s_p^{n,q}$, $n=1,\mathbf{K},N$, $p=1,\mathbf{K},K$, $q=1,\mathbf{K},L$, is the *q*-th chip of the spreading sequence for the *p*-th user and the *n*-th transmit antenna. For each user the spreading sequences are the same for all sub-streams. $\mathbf{H}_{t,j}^{p}$ is the $KN \times KN$ complex channel matrix for the p-th user, given by

$$\mathbf{H}_{t,j}^{p} = \begin{bmatrix} \mathbf{h}_{t,j}^{p} & \mathbf{0} & \cdots & \mathbf{0} \\ \mathbf{0} & \ddots & \ddots & \vdots \\ \vdots & \ddots & \ddots & \vdots \\ \mathbf{0} & \cdots & \cdots & \mathbf{h}_{t,j}^{p} \end{bmatrix}_{KN \times KN} \tag{5.6}$$

where

$$\mathbf{h}_{t,j}^{p} = \begin{bmatrix} h_{j,1}^{p}(t) & 0 & \cdots & \cdots & 0 \\ 0 & \ddots & \ddots & \ddots & 0 \\ \vdots & \ddots & h_{j,n}^{p}(t) & \ddots & \vdots \\ \vdots & \ddots & \ddots & \ddots & \vdots \\ 0 & 0 & \cdots & \cdots & h_{j,N}^{p}(t) \end{bmatrix}_{N \times N} \tag{5.7}$$

$h_{j,n}^{p}(t)$ is the fading coefficient from the n-th transmit antenna to the j-th receive antenna of the p-th user, $n = 1, \ldots, N$, and $j = 1, \ldots, M$. $\mathbf{n}_{t,j}^{p}$ is an $L \times 1$ noise vector at the receive antenna j of the p-th user, given by $\mathbf{n}_{t,j}^{p} = [n_{j,1}^{p}(t), \ldots, n_{j,q}^{p}(t), \ldots n_{j,L}^{p}(t)]^{T}$, where $n_{j,q}^{p}(t)$ is a Gaussian random variable with a zero mean and two sided power spectral density $N_0/2$ per dimension. Therefore, the received signal at each user's receiver has a different channel matrix and noise vector. The received signals for all receive antennas of the p-th user are arranged in a vector $\mathbf{R}_{t}^{p}$

$$\mathbf{R}_{t}^{p} = [\mathbf{r}_{t,1}^{p}, \ldots, \mathbf{r}_{t,j}^{p}, \ldots, \mathbf{r}_{t,M}^{p}]^{T} \tag{5.8}$$

5.2.2 Receiver Structure

For the downlink system, we assume that all the users have the same number of antennas and each user can detect all other user's information and suppress them in its receiver, just like a conventional multi-user detection. We also assume that the system has no knowledge of CSI, spreading sequences, and the fading coefficients. Training sequences are transmitted for each user at the start of transmission. A block diagram of the proposed adaptive iterative LSTC-CDMA multiuser receiver for the *p*-th user is shown in Figure. 5.2. It consists of *K* adaptive iterative LSTC-CDMA single user receivers, each with an adaptive detector followed by *N* parallel soft-input soft-output channel decoders.

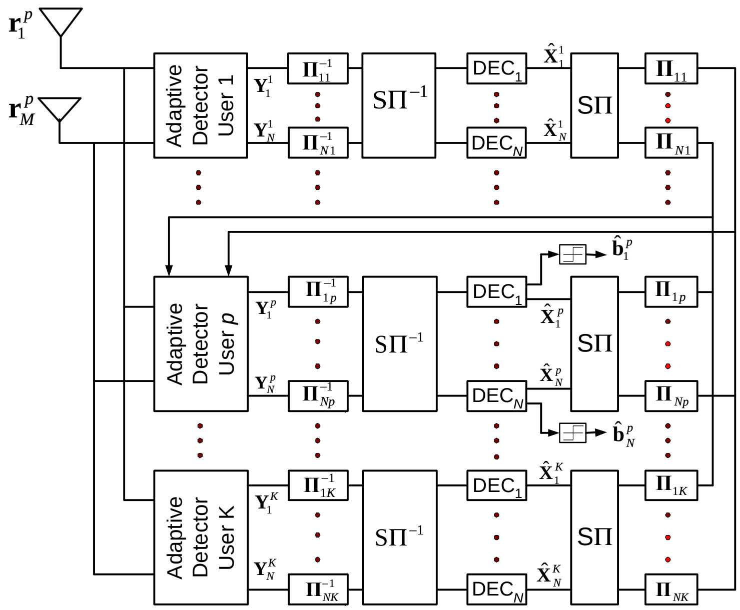

Figure. 5.2 Block diagram of an adaptive iterative TLSTC- CDMA Receiver for the *p*-th user

The received signals are first processed by the adaptive detector. The detector outputs, corresponding to the *N* transmitted antennas for each user, are then fed to the time and spatial deinterleavers, denoted by Π^{-1} and $S\Pi^{-1}$, respectively. The outputs of the deinterleavers are decoded by parallel MAP decoders. The CCI and MAI interferences are cancelled by an iterative technique. The soft output of the MAP decoders from all users are sent to the spatial and time interleavers, and then fed back to the adaptive MMSE detector. A soft estimate of a particular user's signals transmitted from a given antenna is obtained by canceling the interference from other antennas and other users.

5.2.2.1 LSTC-CDMA Receiver

The block diagram of the adaptive iterative TLSTC-CDMA receiver for the ***p***-th user is shown in Figure. 5.3. In the proposed adaptive receiver structure, ***N*** sets of an adaptive detector, consisting of a feed-forward and feedback filter modules, are employed. Each adaptive detector consists of ***M*** equalizers for the feed-forward filter module and an equalizer for the feedback filter module. An equalizer, employed in the proposed adaptive detector, is based on a normalized LMS algorithm. The detector output for each layer is obtained from combining a feed-forward and a feedback filter output. The detector outputs are then passed to the time deinterleaver and the spatial-deinterleaver. The spatial-deinterleaver outputs are decoded by parallel MAP decoders. In the first iteration, there are no estimated symbols from the decoders and then the feedback filter coefficients are zeros, thus the feedback filter output is zero.

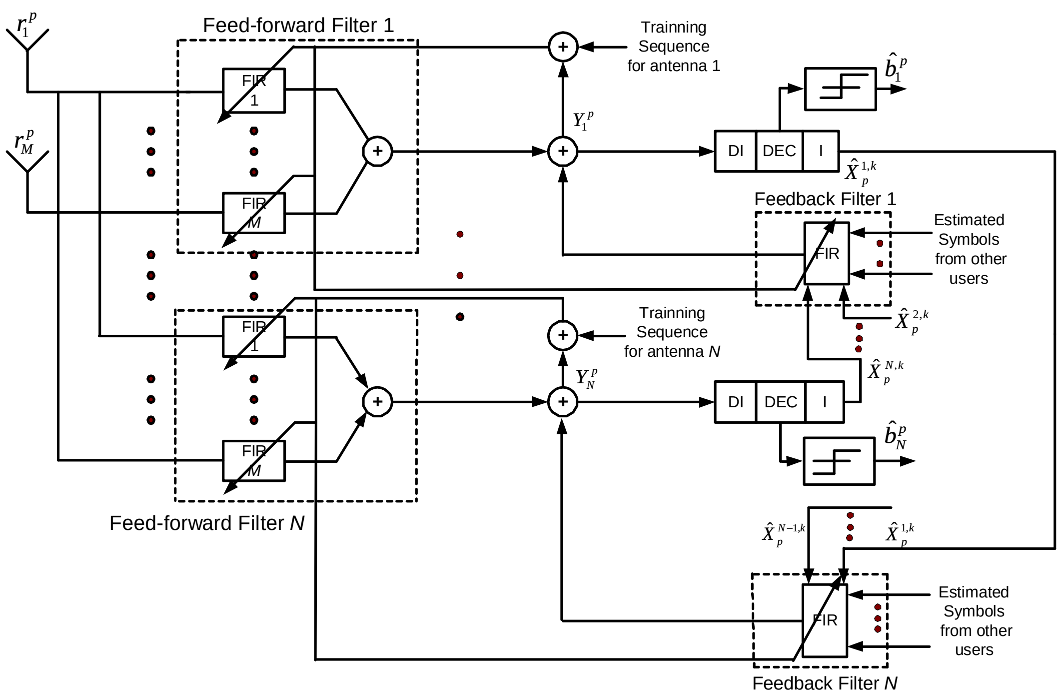

Figure.5.3 Block diagram of the adaptive iterative TLSTC-CDMA receiver for the p-th user

Because of inaccurate channel estimation in the adaptive scheme in a high interference environment, the interference from adjacent antennas (CCI) and other users (MAI) still influence the system performance. As a result, an iterative process is required to remove the interferences. In the iterative process the feed-forward filter compensates for the channel estimation error and the feedback filter is used to cancel the interference from adjacent antennas and other users.

Adaptive Iterative Detector

In the feed-forward filter module, the *M* adaptive equalizers in the feed-forward filter module are used to estimate the channel coefficients and signature sequence for each layer of each user, as well as to suppress the interference in the system. The equalizer outputs from all receive antennas are added to obtain a feed-forward filter output signal for each transmit antenna as shown in Figure. 5.3.

Let $\mathbf{w}_{t,j}^{p,k}$ be an L×1 feed-forward tap coefficients vector for the ***j***-th receive antenna of the ***p***-th user during the ***k***-th iteration at symbol interval ***t***, given by

$$\mathbf{w}_{t,j}^{p,k} = \left[w_{t,j}^{p,k}(0), \mathbf{K}, w_{t,j}^{p,k}(q), \ldots, w_{t,j}^{p,k}(L-1)\right]^{T} \tag{5.9}$$

where $w_{t,j}^{p,k}(q)$ is the feed-forward tap coefficient corresponding to the ***q***-th chip of the spreading sequence. $\underline{\hat{\mathbf{x}}}_{t,p}^{i,k}$ is an (KN – 1)×1 vector of the estimated soft symbols, at the ***k***-th iteration, from MAP decoders of all antennas of all users, except the ***i***-th antenna of the ***p***-th user, at symbol interval ***t***, given by

$$\underline{\hat{\mathbf{x}}}_{t,p}^{i,k} = \left(\hat{\mathbf{x}}_{t,1}^{1,k}, \mathbf{K}, \hat{\mathbf{x}}_{t,1}^{N,k}, \mathbf{K}, \hat{\mathbf{x}}_{t,p}^{i,k}, \mathbf{K}, \hat{\mathbf{x}}_{t,K}^{1,k}, \ldots, \hat{\mathbf{x}}_{t,K}^{N,k}\right)^{\mathrm{T}} \tag{5.10}$$

where

$$\hat{\mathbf{x}}_{t,p}^{i,k} = \left(\hat{x}_{t,p}^{1,k}, \hat{x}_{t,p}^{2,k}, \ldots, \hat{x}_{t,p}^{i-1,k}, \hat{x}_{t,p}^{i+1,k}, \ldots, \hat{x}_{t,p}^{N,k}\right) \tag{5.11}$$

Let $\mathbf{w}_{b}^{i,k}(t)$ be the feedback filter coefficients of all users, except the ***i***-th antenna of the ***p***-th user, at symbol interval ***t*** in time domain, given by

$$\mathbf{w}_{b,p}^{i,k}(t)=\left[\mathbf{w}_{b,1,}^{1,k}(t),\mathbf{K},\mathbf{w}_{b,1}^{N,k}(t),\mathbf{K},\mathbf{w}_{b,p}^{i,k}(t),\mathbf{K}\mathbf{w}_{b,K}^{1,k}(t)\mathbf{K},\mathbf{w}_{b,K}^{N,k}(t)\right]^T \tag{5.12}$$

where

$$\mathbf{w}_{b,p}^{i,k}(t)=\left[w_{b,p}^{1,k}(t),\ldots,w_{b,p}^{i-1,k}(t),w_{b,p}^{i+1,k}(t),\mathbf{K}w_{b,p}^{N,k}(t)\right] \tag{5.13}$$

The detected symbol of the *p*-th user obtained at the output of the adaptive detector for the *i*-th antenna during the *k*-th iteration at symbol interval *t*, denoted by $y_{t,p}^{i,k}$, is given by

$$y_{t,p}^{i,k}=\sum_{j=0}^{M}\mathbf{w}_{t,j}^{p,k}(t)^H\mathbf{r}_{t,j}^{p}+\mathbf{w}_{b,p}^{i,k}(t)^H\hat{\underline{\mathbf{x}}}_{t,p}^{i,k} \tag{5.14}$$

The detector soft output $y_{t,p}^{i,k}$ in the time domain is then compared to the training symbol, denoted by $x_{t,p}^{i,k}$, and the difference between them, referred to as the detection error, is calculated. The detection error for the *p*-th user in the *k*-th iteration at symbol interval *t*, for *i*-th antenna, denoted by $e_{t,p}^{i,k}$, is given by

$$e_{t,p}^{i,k}=y_{t,p}^{i,k}-x_{t,p}^{i,k} \tag{5.15}$$

The detection error is then used to adapt the feed-forward filter and feedback filter tap coefficients in the time domain. After the mean square error (MSE) approaches a specified value, the training mode is switched to the decision directed mode, in which the training sequence is replaced by the hard decision output of each user detector. In the decision directed mode, the detection error is given by the difference between the detector output and the hard decision of the detector output.

The values of feed-forward filter tap coefficients, $\mathbf{w}_j^{p,k}(t)$, in Equation (5.9) and feedback filter tap coefficients, $\mathbf{w}_{b,p}^{i,k}(t)$, in Equation (5.12) are calculated by minimizing the mean square error, defined as z, between the training sequence and the detector soft output, given by

$$z = \text{mim}\left(E\left| e_{t,p}^{i,k} \right|^2 \right) = \min\left(E\left[\left| y_{t,p}^{i,k} - x_{t,p}^{i,k} \right|^2 \right] \right) \tag{5.16}$$

They can be determined recursively by the adaptive Least Mean Square (LMS) algorithm [18] as follows

$$\mathbf{w}_j^{p,k}(t+1) = \mathbf{w}_j^{p,k}(t) + \frac{m_f}{a_f + \mathbf{r}_{t,j}^{p\;H} \mathbf{r}_{t,j}^p} e_{t,p}^{i,k} \mathbf{r}_{t,j}^p \tag{5.17}$$

$$\mathbf{w}_{b,p}^{i,k}(t+1) = \mathbf{w}_b^{i,k}(t+1) + \frac{m_b}{a_b + \hat{\underline{\mathbf{x}}}_{t,p}^{i,k\;H} \hat{\underline{\mathbf{x}}}_{t,p}^{i,k}} e_{t,p}^{i,k} \hat{\underline{\mathbf{x}}}_{t,p}^{i,k} \tag{5.18}$$

where $\mathbf{r}_{t,j}^p$ and $\hat{\underline{\mathbf{x}}}_{t,p}^{i,k}$ are defined in (5.3) and (5.10), respectively. μ_f and μ_b are the step sizes for the feed-forward and feedback adaptations, respectively and α_f and α_b are positive constants to prevent division by zero.

In the proposed receiver structure, detector output for user *p*, denoted by $y_{t,p}^{i,k}$, is applied to the MAP decoder. The soft-output from the decoder is used to cancel interference in the feedback filter in the next iteration. This adaptive iterative detection/decoding process is performed k times where k is the number of iterations, determined by simulation. The soft-output from the decoder in the last iteration is fed into a decision device. For BPSK, the likelihood functions for the transmitted modulated symbols 1 and –1 can be written as [19]

$$P\left(y_{t,p}^{i,k} \middle| x_{t,p}^{i,k} = \pm 1 \right) = \frac{1}{\sqrt{2ps^2}} \exp \frac{-\left(y_{t,p}^{i,k} \mathbf{m} 1 \right)^2}{2s^2} \tag{5.19}$$

The log-likelihood ratios (LLR) determined in the *k*-th iteration for the *i*-th transmit layer of the *p*-th user, denoted by $l_{t,p}^{i,k}$, are given by [19]

$$l_{t,p}^{i,k} = \log\left(\frac{P\left(x_{t,p}^{i,k} = 1 \middle| y_{t,p}^{i,k} \right)}{P\left(x_{t,p}^{i,k} = -1 \middle| y_{t,p}^{i,k} \right)} \right) \tag{5.20}$$

The *a posteriori probabilities* (APP), $P\left(x_{t,p}^{i,k}=q \middle| y_{t,p}^{i,k}\right)$, $q=1,-1$, conditioned on the output variable $y_{t,p}^{i,k}$ for the *p*-th user can then be obtained as

$$P\left(x_{t,p}^{i,k}=1 \middle| y_{t,p}^{i,k}\right)=\frac{e^{l_{t,p}^{i,k}}}{e^{l_{t,p}^{i,k}}+1} \tag{5.21}$$

$$P\left(x_{t,p}^{i,k}=-1 \middle| y_{t,p}^{i,k}\right)=\frac{1}{e^{l_{t,p}^{i,k}}+1} \tag{5.22}$$

The soft-output symbol estimate in the ***i***-th layer and ***k***-th iteration for ***p***-th user can be calculated as

$$\hat{x}_{t,p}^{i,k}=\frac{e^{l_{t,p}^{i,k}}-1}{e^{l_{t,p}^{i,k}}+1} \tag{5.23}$$

5.3 Complexity Analysis

In this section, the system computational complexity defined as the required number of signal processing operations per coded symbol and per user is considered. As we want to investigate the receiver complexity of adaptive iterative receivers, we will consider only the complexity of the detector.

In the time domain adaptive detector [28], for each coded symbol per user per iteration in the equalization process, each feed forward filter requires *ML* multiplications and *ML* additions while the feedback filter requires (*KN* –1) multiplications and (*KN* –1) additions. The coefficient-updating process requires *M*(2*L*+1) multiplications and *M*(2*L*+1) additions for the feed-forward tap coefficients, as well as 2*KN* –1 multiplications and 2*KN* –1 additions for the feedback tap coefficients. Therefore the total number of operations is *KNI*(3*ML*+*M*+ 3*KN* - 2) multiplications and *KNI*(3*ML*+ *M*+*3 KN*- *2*) additions for each coded symbol for *K* users, *N* transmit and *M* receive antennas at *I* iterations with the spreading sequence length *L*.

Table 1. Complexity of the proposed adaptive iterative detector

Algorithm	Number of multiplications	Number of Additions
Time-domain detector	$KNI(3ML+M+3KN-2)$	$KNI(3ML+M+3KN-2)$

K = number of users, L = processing gain, N = number of transmit antennas,
M = number of receive antennas, and I = number of iteration

5.4 SEMI-Analytical Performance Evaluation

In this section, we analyze the performance of the proposed adaptive iterative receiver. Since an analytical expression for the adaptive iterative receiver is difficult to derive, a semi-analytical approach using an extrinsic information transfer chart (EXIT chart) [92] is utilized. The results show an excellent agreement between the semi-analytical and simulation approaches.

As the number of users increases, based on the law of large numbers and central limit theorem [93] , we can approximate multi-user interference by an additive Gaussian noise with zero mean and variance σ_k [94, 95]. Obviously, σ_k varies with the number of users, K. Moreover, in a system with the proposed adaptive iterative receiver, the multiuser interference will decrease as the number of iterations, k, increases. Therefore, σ_k is a function of K and k, denoted by $\sigma_k(K, k)$.

As observed by S. ten Brink and H. El Gamal et al., [92, 96], if the input to a MAP decoder is an independent Gaussian random variable, then the output log-likelihood ratio (LLR), defined by (5.20), can be tightly approximated by a Gaussian random variable.

Figure. 5.4. shows the signal-to-noise ratio (SNR) input-output relationship of the proposed adaptive iterative receiver, where SNR_{in} and SNR_{out1} are the input and output SNRs of the adaptive detector, respectively, and SNR_{out2} is the output SNR of the decoder. The convergence of the adaptive iterative receiver can be characterized by tracking the SNR changes at the output of the adaptive detector and decoder for each iteration.

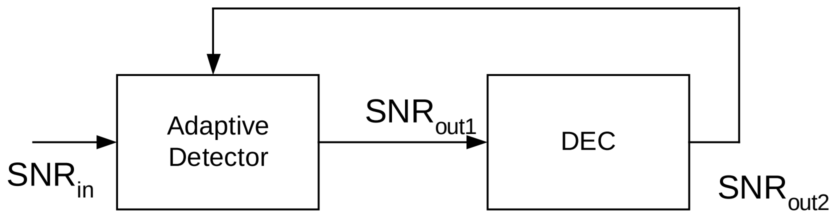

Figure.5.4 Block diagram of the SNR input-output relationship of the proposed receiver

Let $y_{t,p}^{i,k}$ represent the input statistics to the decoder at the k-th iteration for the i-th transmit antenna of the p-th user at symbol interval t. Due to the symmetry of the channel, and for the sake of simplicity, we may drop off subscripts i and p, and use y_t^k to denote $y_{t,p}^{i,k}$.

Based on a Gaussian approximation of multiuser interference, y_t^k can be expressed as

$$y_t^k = u_s(t)s(t) + \tilde{n}^k(t) \tag{5.24}$$

where $u_s(t)$ is the amplitude of signal $s(t)$ at the output of the detector and $\tilde{n}^k(t)$ is the equivalent noise at the k-th iteration with zero mean and variance $\sigma_k(K, k)$. The signal to interference noise ration (SINR) at the output of the detector at the k-th iteration denoted by SINR(K, k), can be calculated from Equation (5.24) as follows

$$SINR(K,k) = \frac{(u_s)^2}{s_k^2(K,k)} \tag{5.25}$$

where u_s is the mean of the signal $u_s(t)s(t)$.

To evaluate the performance of the detector and decoder in the proposed receiver, we run simulations of the proposed receiver for various numbers of users *K* and iteration *k*. From the simulation results, the amplitude of signal $u_s(t)$ and the variance $\sigma_k(K\ ,\ k)$ can be calculated. As a result, SINR(*K*, *k*) in (5.25) is determined. Figure. 5.5. shows variations of SINR(*K*, *k*) as a function of *K* for various numbers of iterations at E_b/N_o = 10 dB. For a fixed number of users, SINR(*K*, *k*) increases as the number of iterations increases but SINR(*K*, *k*) goes down when the number of users, K, increases.

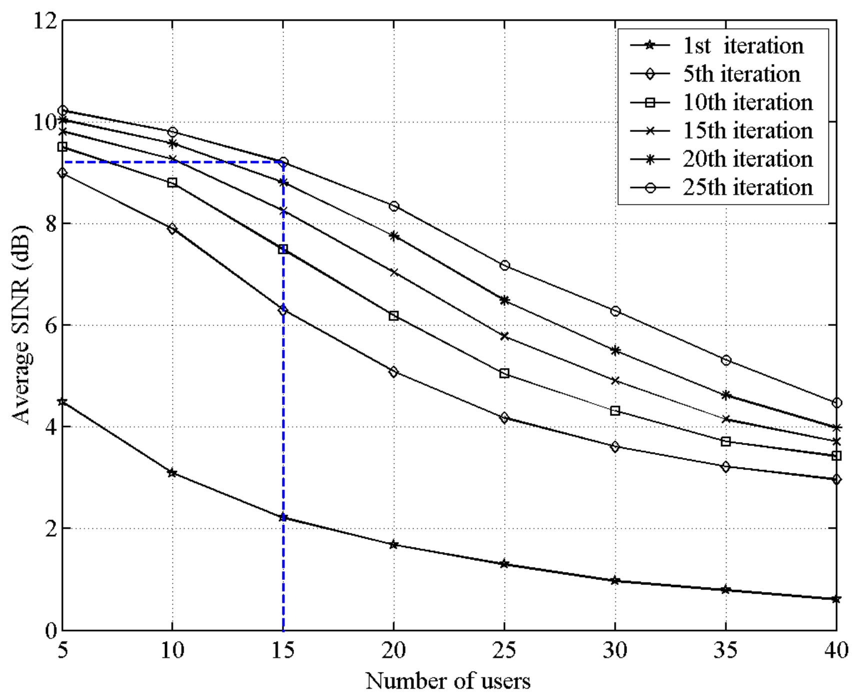

Figure. 5.5. SINR as a function of the number of users
for various numbers of iterations at E_b/N_o at 10dB

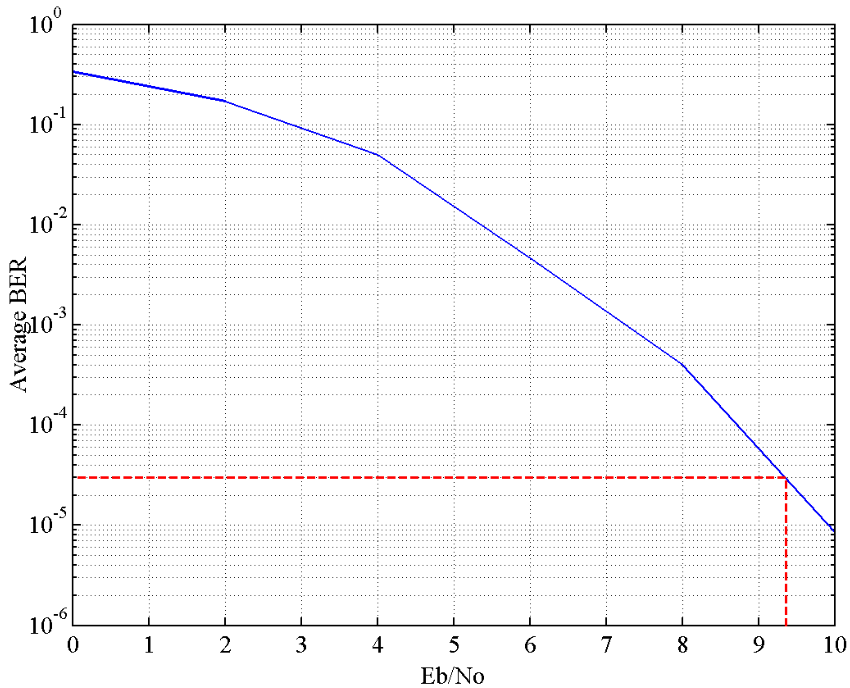

Figure. 5.6 BER performance of a single decoder in the system

To investigate the performance of the MAP decoder module in the proposed receiver, the detector output, y_t^k, is passed to a set of decoders. By symmetry of the general MAP decoder model, the decoder behavior can be considered from one decoder of a single user system [92]. Figure.6 shows the simulated BER performance of one decoder of a single user system for various values of E_b/N_o.

By relating the SINR curve in Figure. 5.5 and the BER curve in Figure. 5.6, we can obtain a semi-analytical BER behavior for various numbers of users at a fixed number of iterations. For instance, using the plot from Figure. 5.5 to obtain the average SINR for 15 users with 25 iterations, the average SINR is about 9.3 dB. In Figure. 5.6, we calculate the BER value of the decoder at E_b/N_o = 9.3 dB. The BER at 9.3 dB is about 3×10^{-5}. Therefore, the BER of a system with 15 users at the 25th iteration at E_b/No 10 dB is about 3×10^{-5}. Similarly, we can obtain the average BER for various numbers of users and iterations by using the above semi-analytical approach.

To verify the predicted performance, we compare the performance obtained by the semi-analytical approach to the simulation results. It can be observed from Figure. 5.7 that the semi-analytical and simulation results are identical. The benefit of this method is to predict the system performance without actually simulating data transmission, which significantly reduces the system simulation time.

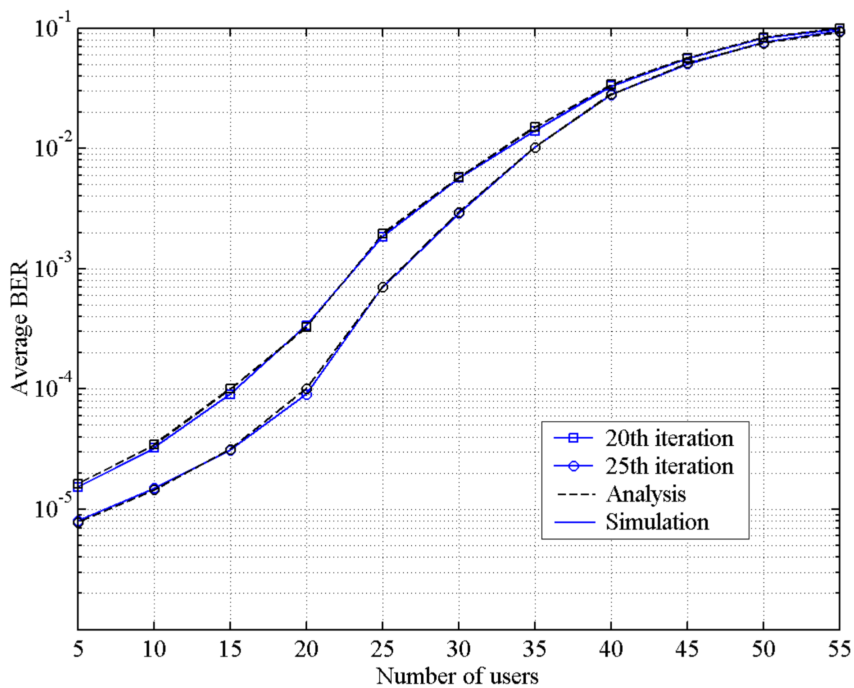

Figure. 5.7 BER performance determined by simulation and semi-analysis approach for E_b/N_o of 10 dB

5.5 Performance Results

This section presents simulation results for the adaptive iterative LSTC-CDMA receiver operating in the frequency domain. We consider BPSK modulation and a quasi-static fading channel, for which the fading coefficients are constant within a frame, but change independently from one frame to another. The system operates in the training mode until the MSE reaches the minimum, at which point it switches to the decision directed mode.

The constituent codes are non-systematic convolutional codes with the code rate of 1/2, memory order of 3 and the generating polynomials $g_1 = 15_8$ and $g_2 = 17_8$. The spreading sequences used are Gold sequences with the processing gain of 7. The proposed system is simulated with four transmit and four receive antennas, i.e., a 4 × 4 LSTC-CDMA system, with 130 information symbols in each frame per layer for each user. Therefore, each layer of the LSTC-CDMA system consists of 266 encoded symbols per frame.

The bit error rates (BER) of the adaptive iterative MMSE receivers for a single user with various numbers of iterations are shown in Figure. 5.8. It can be observed that the system performance is significantly improved in the second iteration compared to the first iteration, and approaches the interference free bound in the 5th iteration.

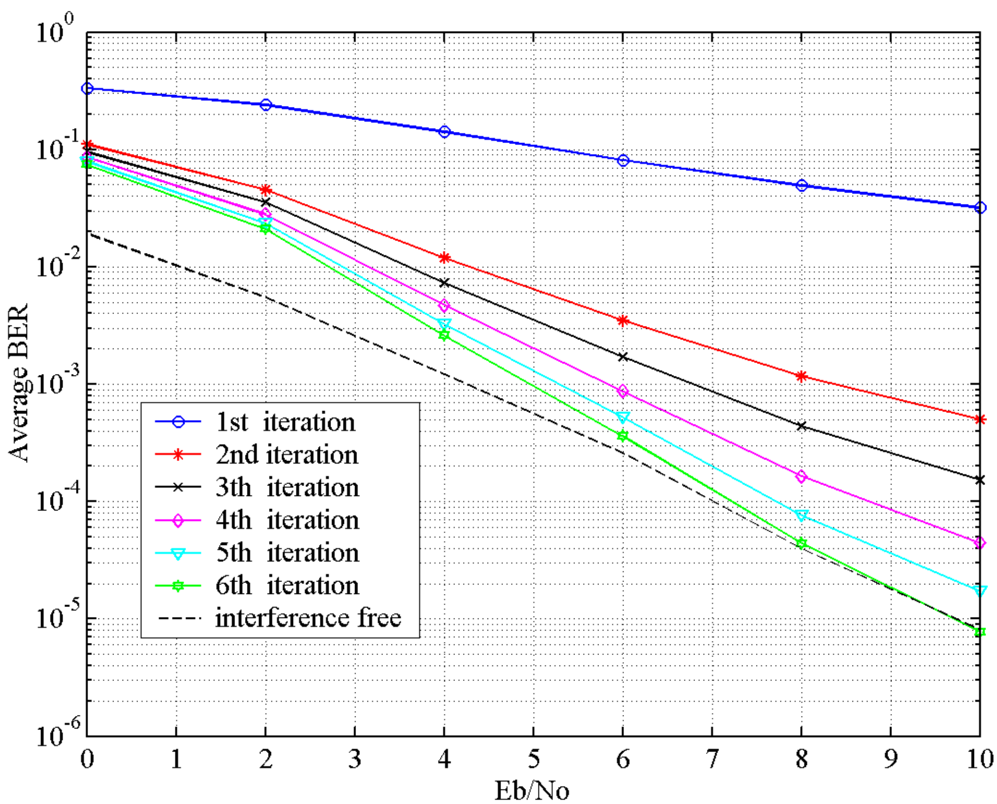

Figure. 5.8 Performance of adaptive iterative MMSE receiver for a single user in a quasi-static Rayleigh fading channel.

Figure. 5.9 presents the system performance with 20 users for the adaptive receiver. The average BER plot shows that the performance is significantly improved after the second iteration, in comparison to the first iteration. It gradually increases for higher numbers of iterations. Because of the influence of the interference from the co-channel interference (CCI) and the multiple access interference (MAI) to the system, the receiver requires a number of the iteration processes to remove interferences out of the system. As shown in Figure. 5.9, the performance of the proposed adaptive receiver approaches the single user performance at the 30^{th} iteration.

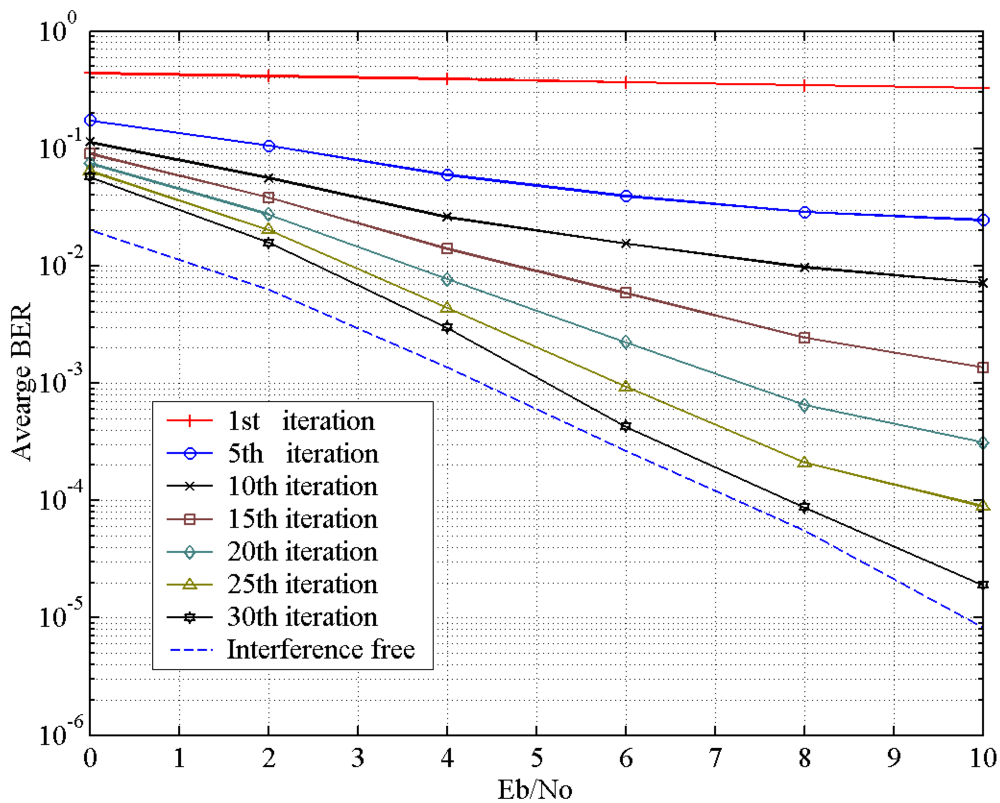

Figure. 5.9 BER performance of the adaptive iterative receiver with 20 users.

The maximum number of users for a system which the time domain adaptive iterative receiver can support for a target BER, at E_b/N_o 10 dB is shown in Figure. 5.10. For a BER of 10^{-4}, the number of users is 20 after 25 iterations. For a BER of 10^{-2}, the number of users is 35 after 25 iterations. It also shows that when the number of users increases, a higher number of iterations is required to achieve the same BER. For example, for five users, the receiver requires 10 iterations to achieve a BER of 2.5×10^{-3} while for 18 users, it requires 20 iterations to achieve the same BER.

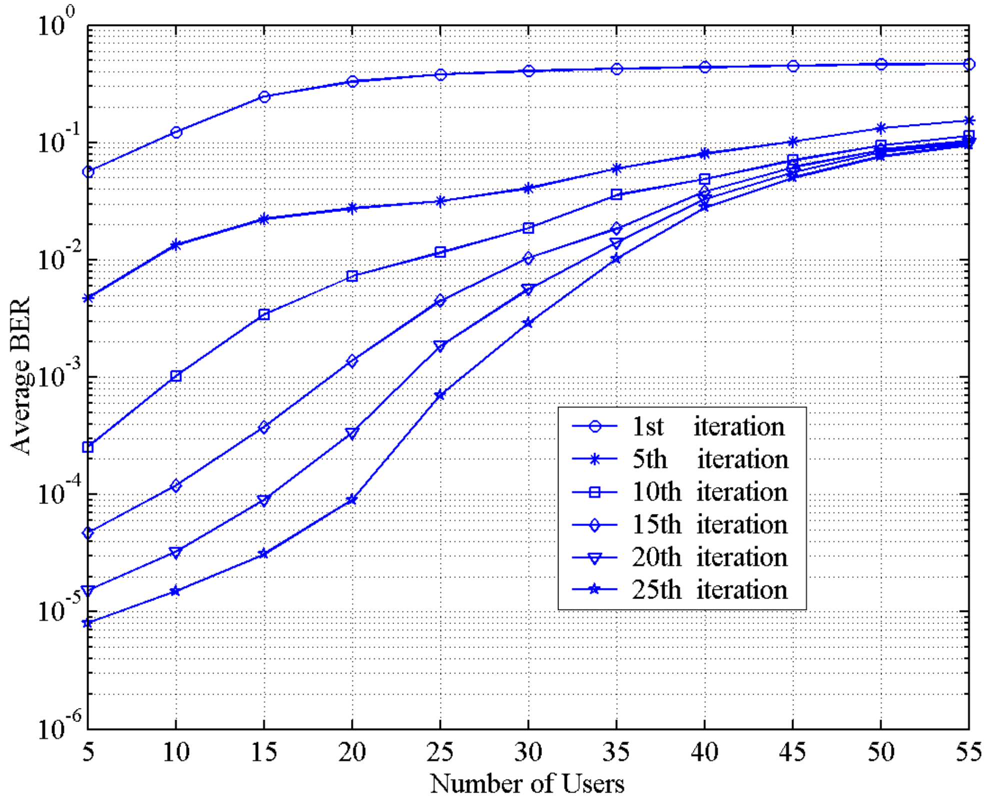

Figure. 5.10 BER of the frequency domain adaptive iterative receiver at E_b/N_o 10dB, for a variable number of users

5.6 Conclusion

In this Chapter, we present an adaptive iterative receiver based on normalized LMS (NLMS) algorithm for a layered space-time coded CDMA (LSTC-CDMA) system. The simulation results show that the adaptive iterative receiver effectively suppresses and removes the CCI and MAI using the interference suppression and cancellation techniques. The use of a decoding stage at each iteration allows for a greater performance improvement over multistage detectors, due to the higher reliability of the co-channel interference (CCI) and multiple access interference (MAI) estimation. Moreover, the system performance is also evaluated by using a semi-analytical approach and simulations, and there is an excellent agreement between two sets of results. Therefore, using a semi-analysis approach, which significantly reduces system simulation time, we can predict the system performance without actually simulating data transmission. The performance results of the system also show that the adaptive receiver can achieve the interference-free single user performance for a high signal to noise ratio (SNR).

However the computational complexity of the proposed adaptive receiver is still high, due to the iteration process. Therefore, to reduce the computational complexity, the frequency domain adaptive iterative receiver will be discussed in the next chapter.

Chapter 6

Frequency-domain Adaptive Iterative Receiver for Layered Space-time Coded CDMA Systems

In this chapter, a new low complexity frequency domain adaptive iterative receiver for a layered space-time coded CDMA (LSTC-CDMA) system is presented. The proposed frequency domain adaptive receiver is a modified structure of time domain adaptive iterative receiver for the downlink LSCT-CDMA system presented in Chapter 5. There is no a priori knowledge of channel state information (CSI), spreading sequences and fading coefficients available at the receiver. Training sequences for each user are transmitted at the start of the transmission. The proposed receiver consists of a normalized least mean square (NLMS) feed-forward filter and a feedback iterative parallel interference canceller operating in the frequency domain. It has the same performance as a time domain receiver with reduced complexity. Simulation results show that the proposed receiver approaches the interference-free single user performance for a high signal-to-noise ratio (SNR).

6.1 Introduction

Recently, a frequency domain equalizer (FDE) structure was proposed for SISO in [25-27, 77]. In [26, 79, 81-83] authors have shown that the FDE has been applied to the MIMO systems. Such a technique offers a significant reduction in the computation complexity in comparison to the time domain approach.

In this chapter, we propose a new frequency domain (FD) adaptive iterative receiver for a downlink LSTC-CDMA system under a quasi-static fading channel with no a priori knowledge of CSI, spreading sequences and fading coefficients. Assuming that all the users have the same number of antennas and each user can detect all other user's information and suppress them in its receiver, just like a conventional multi-user detection. Training sequences for each user are transmitted at the start of the transmission for each user. The proposed receiver applies the SISO adaptive structure proposed by Miller, S. L. [91] to the MIMO adaptive system and replaces a time domain adaptive equalizer with a frequency domain equalizer. Such a receiver can effectively mitigate CCI and MAI and thus improve the multiuser system performance. Moreover, the proposed frequency domain adaptive receiver based on the frequency domain equalizer shows a significant reduction in computation complexity and has the same or better adaptation performance compared to the time domain receiver. The simulation results show that the adaptive iterative receiver can also achieve the interference-free single user performance for a high value of a signal-to-noise ratio (SNR).

The rest of this chapter is organized as follows. Section 6.2 describes the system model of a downlink LSTC-CDMA system. In Section 6.3 we present the proposed frequency domain adaptive iterative receiver structure. The system complexity analysis of the proposed receiver structure is discussed in Section 6.4. In Section 6.5 the simulation results and discussions are presented. Finally in Section 6.6, conclusions are drawn

6.2 System Model

In this Chapter, we investigate the downlink LSTC-CDMA system, which was discussed in Chapter 5 for further computational complexity reduction purposes for the receiver structure. Therefore, the adaptive iterative receiver in Figure. 5.3 is modified for computational reduction purposes. Therefore, the new frequency domain adaptive receiver, which is proposed in this chapter, uses the frequency domain equalizer to replace the time domain equalizer in the adaptive iterative receiver. However, since we only consider the complexity at the receiver end, we still employ the same transmitter, as shown in Figure. 5.1 throughout this chapter.

Let $\mathbf{r}_{t,j}^{p}$ be the received signal vector at the receive antenna *j*, $j = 1, \mathbf{K}, M$, for symbol *t* of the *p*-th user, then $\mathbf{r}_{t,j}^{p}$ is given by

$$\mathbf{r}_{t,j}^{p} = \mathbf{S}\mathbf{H}_{t,j}^{p}\mathbf{b} + \mathbf{n}_{t,j}^{p} \tag{6.1}$$

where $\mathbf{r}_{t,j}^{p} = [r_{t,j}^{p,1}, \mathbf{K}\, r_{t,j}^{p,q}, \mathbf{K}, r_{t,j}^{p,L}]^T$ and $r_{t,j}^{p,q}$ is the received signal at the *q*-th chip of the *t*-th symbol for *j*-th antenna of the *p*-th user. $\mathbf{b}$ are the coded signal vectors transmitted by *K* users through *N* transmit antennas, given by

$$\mathbf{b} = [\mathbf{b}_1, \mathbf{b}_2, \mathbf{K}, \mathbf{b}_p, \mathbf{K}, \mathbf{b}_K]^T \tag{6.2}$$

where

$$\mathbf{b}_p = [b_p^1, \mathbf{K}, b_p^n, \mathbf{K}, b_p^N] \tag{6.3}$$

and $b_p^n, n = 1, \mathbf{K}, N$ and $p = 1, \mathbf{K}, K$, is the coded information bit of the *p*-th user for the *n*-th transmit antenna, and $[\mathbf{x}]^T$ is the transpose of a vector $\mathbf{x}$.

$\mathbf{S}$ represents the $L \times KN$ spread transmitted sequence of *K* users for *N* transmit antennas, denoted by

$$\mathbf{S} = [\mathbf{s}_1^1, \mathbf{K}, \mathbf{s}_1^N, \mathbf{K}, \mathbf{s}_p^n, \mathbf{K}, \mathbf{s}_K^1, \mathbf{K}, \mathbf{s}_K^N] \tag{6.4}$$

where $\mathbf{s}_p^n$ is the spread sequence corresponding to the *p*-th user and the *n*-th antenna, represented as

$$\mathbf{s}_p^n = [s_p^{n,1}, \mathbf{K}, s_p^{n,q}, \mathbf{K}, s_p^{n,L}]^T \tag{6.5}$$

and $s_p^{n,q}$, $n = 1, \mathbf{K}, N$, $p = 1, \mathbf{K}, K$, $q = 1, \mathbf{K}, L$, is the *q*-th chip of the spreading sequence and the *n*-th transmit antenna of the *p*-th user. For each user the spreading sequences are the same for all sub-streams.

$\mathbf{H}_{t,j}^p$ is the $KN \times KN$ complex channel matrix for the *p*-th user at symbol interval *t*, given by $\mathbf{H}_{t,j}^p = diag[\mathbf{h}_{t,j}^p, \mathbf{K}, \mathbf{h}_{t,j}^p]_{KN \times KN}$ where $\mathbf{h}_{t,j}^p$ is the $N \times N$ complex channel matrix of the *p*-th user at symbol interval *t*, represented by $\mathbf{h}_{t,j}^p = diag[h_{j,1}^p(t), \mathbf{K}\, h_{j,n}^p(t), \mathbf{K}, h_{j,N}^p(t)]_{N \times N}$ and $h_{j,n}^p(t)$ is the fading coefficient the *p*-th user from the *n*-th transmit antenna, $n = 1, \mathbf{K}, N$, to the *j*-th receive antenna, $j = 1, \mathbf{K}, M$.

The coded signal vectors, denoted by $\mathbf{b}$, transmitted by K users through N transmit antennas, is given by

$$\mathbf{b} = [\mathbf{b}_1, \mathbf{b}_2, \mathbf{K}, \mathbf{b}_p, \mathbf{K}, \mathbf{b}_K]^T \tag{6.6}$$

where

$$\mathbf{b}_p = [b_p^1, \mathbf{K}, b_p^n, \mathbf{K}, b_p^N] \tag{6.7}$$

and $b_p^n, n = 1, \mathbf{K}, N$ and $p = 1, \mathbf{K}, K$, is the coded information bit of the *p*-th user for the *n*-th transmit antenna, and $[\mathbf{x}]^T$ is the transpose of a vector $\mathbf{x}$. $\mathbf{n}_{t,j}^p$ is an $L\times 1$ noise vector at the receive antenna j of the p-th user, given by $\mathbf{n}_{t,j}^{p} = [n_{j,1}^{p}(t), \mathbf{K}, n_{j}^{p}(t), \mathbf{K} n_{j,L}^{p}(t)]^{T}$, where $n_{j,q}^{p}(t)$ is a Gaussian random variable with a zero mean and two sided power spectral density $N_o/2$ per dimension. The received signals for all receive antennas are arranged in a vector $\mathbf{R}_t^p$

$$\mathbf{R}_t^p = [\mathbf{r}_{t,1}^p, \mathbf{K}, \mathbf{r}_{t,j}^p, \mathbf{K}, \mathbf{r}_{t,M}^p]^T \qquad (6.8)$$

6.3 Receiver Structure

A block diagram of the proposed frequency domain adaptive iterative LSTC-CDMA receiver is shown in Figure. 6.1. It consists of K adaptive iterative LSTC-CDMA single user receivers, each with an adaptive detector followed by N parallel soft-input soft-output channel decoders. For the downlink system, assuming that all the users have the same number of antennas and each user can detect all other user's information and suppress them in its receiver, just like a conventional multi-user detection.

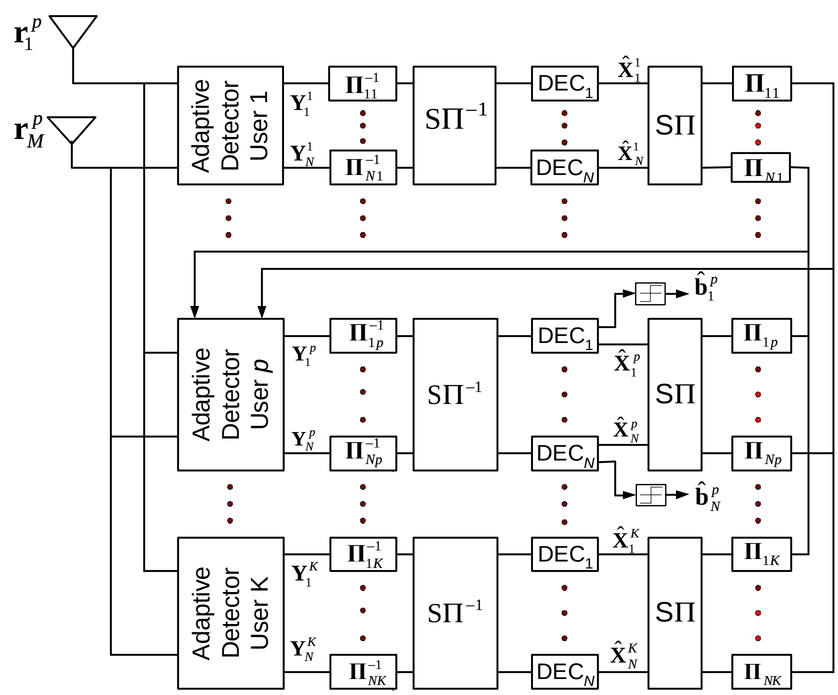

Figure. 6.1 Block diagram of iterative TLSTC - CDMA Receiver for p-th user

The received signals are first processed by the adaptive detector. The detector outputs, corresponding to the N transmitted antennas for each user, are then fed to the time and spatial deinterleavers, denoted by $\mathbf{\Pi}^{-1}$ and $\mathrm{S}\mathbf{\Pi}^{-1}$, respectively. The outputs of the deinterleavers are decoded by parallel MAP decoders. CCI and MAI interferences are cancelled by an iterative technique. The soft output of the MAP decoders from all users are sent to the spatial and time interleavers, and then fed back to the adaptive MMSE detector. A soft estimate of a particular user's signals transmitted from a given antenna is obtained by cancelling the interference from other antennas and other users.

6.3.1 Frequency Domain LSTC-CDMA Receiver

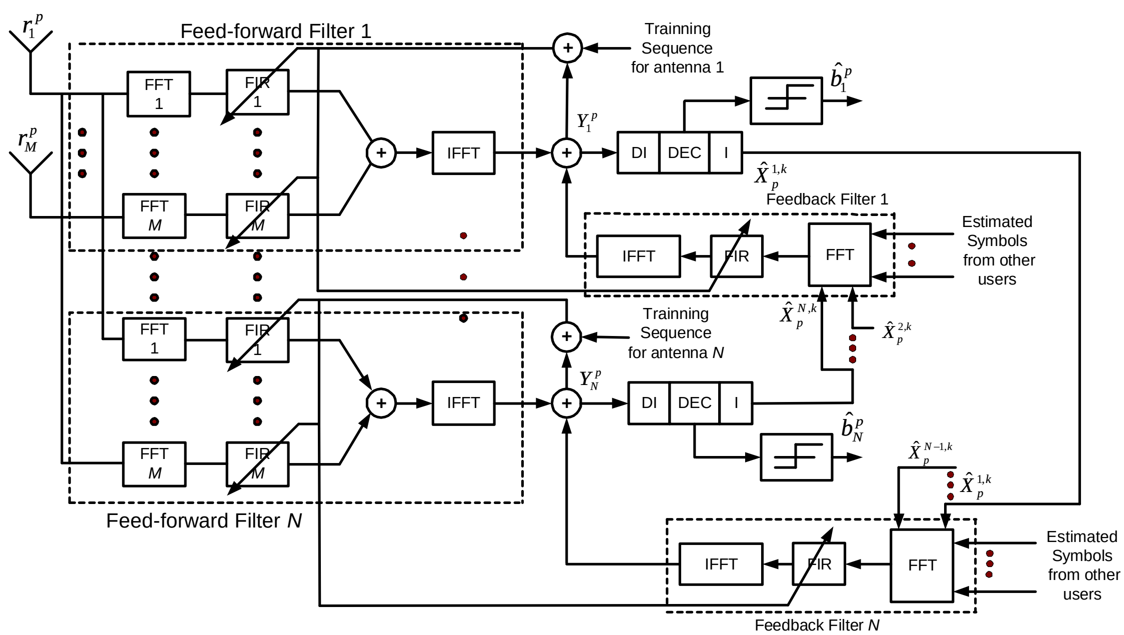

Figure.6.2 Block diagram of Frequency domain adaptive iterative TLSTC-CDMA receiver for the p-th user

It is well known that a linear convolution process can be carried out either in the time domain or the frequency domain. However, the frequency domain approach has been shown to have a much lower computation complexity [22]. In the proposed system, an adaptive frequency domain equalizer is employed in the adaptive detector. Each adaptive detector consists of feed-forward and feedback filters, as shown in Figure. 6.2. The frequency domain equalizer uses a frequency domain normalized Least Mean Square (NLMS) algorithm for an adaptation process. After the adaptive detection process, the detector outputs are passed to the time deinterleaver followed by the spatial-deinterleaver. The spatial-deinterleaver outputs are encoded by parallel MAP decoders. If the system performance achieves a satisfactory level, the decoder soft outputs are then passed to a decision device to make a decision for the desired outputs otherwise the iteration process is needed for further improvement in the interference suppression and cancellation.

In fact, because the inaccurate channel estimation in the adaptive scheme is in a high interference environment, an iterative process to remove the interferences from the received signal is needed to improve the system performance. . The detector soft outputs of the current stage are interleaved by a time and spatial interleaver, and then fed back into a feedback filter to be subtract from the feed-forward filter output for the next iteration process. In the iterative process the feed-forward filter suppress the interference while the feedback filter cancels the interference from adjacent antennas and other users.

Adaptive iterative frequency domain detector

In the feed-forward filter module, the adaptive feed-forward filter of each user is a frequency domain equalizer, used to estimate the channel coefficients and signature sequences of each user, as well as to suppress the interference in the system. The received signal at each receive antenna is transformed into the frequency domain using the fast Fourier transform (FFT) and the convolution is performed in the frequency domain. The equalizer outputs from all receive antennas are added to obtain a feed-forward filter output signal for each transmit antenna as shown in Figure. 6.2. The inverse fast Fourier transform (IFFT) transforms the feed-forward filter output signal from the frequency domain into the time domain.

The L-chips receive signals ($\mathbf{r}_{t,j}^{p}$) of the p-th user, as defined in Equation (6.3), at the symbol interval t are transformed into the frequency domain using the FFT. The output of each FFT module, denoted by $\mathbf{\Theta}_{t,j}^{p}$, is given by

$$\mathbf{\Theta}_{t,j}^{p} = fft\left(\mathbf{r}_{t,j}^{p}\right) \tag{6.9}$$

where $\mathbf{\Theta}_{t,j}^{p}$, $j = 1, \mathbf{K}, M$, is the received signal vector of the *j*-th receive antenna for the *p*-th user at symbol interval *t* in the frequency domain,

$$\mathbf{\Theta}_{t,j}^{p} = \left[\Theta_{t,j}^{p,1}, \mathbf{K}, \Theta_{t,j}^{p,q}, \mathbf{K}, \Theta_{t,j}^{p,L}\right] \tag{6.10}$$

and

$$\Theta_{t,j}^{p,q} = \sum_{l=0}^{L-1} r_{t,j}^{p,l} e^{\frac{-j2pql}{L}} \tag{6.11}$$

$fft(\cdot)$ represents the fast Fourier transform function, and $\Theta_{t,j}^{p,q}$, $q = 1, \mathbf{K}, L$, is the FFT transformation of the received signal for the *j*-th receive antenna of the *p*-th user at the *q*-th chip of the *t*-th symbol.

Let $\mathbf{w}_{j}^{p,k}(t)$ be an $L \times 1$ feed-forward tap coefficient vector for the *j*-th receive antenna of the *p*-th user during the *k*-th iteration at symbol interval *t*, given by

$$\mathbf{w}_{j}^{p,k}(t) = \left[w_{j,0}^{p,k}(t), \mathbf{K}, w_{j,q}^{p,k}(t), \ldots, w_{j,L-1}^{p,k}(t)\right]^{T} \tag{6.12}$$

where $w_{j,q}^{p,k}(t)$ is the feed-forward tap coefficient corresponding to the *q*-th chip of the spreading sequence.

Let $\mathbf{\Psi}_{t,j}^{p,k}$ represent the FFT transformed signals of $\mathbf{w}_{t,j}^{p,k}$ defined by

$$\mathbf{\Psi}_{t,j}^{p,k} = fft\left(\mathbf{w}_{j}^{p,k}(t)\right) \tag{6.13}$$

where

$$\mathbf{\Psi}_{t,j}^{p,k} = \left[\Psi_{t,j}^{p,k}(0), \mathbf{K}, \Psi_{t,j}^{p,k}(q), \mathbf{K}\, \Psi_{t,j}^{p,k}(L-1)\right] \tag{6.14}$$

and

$$\Psi_{t,j}^{p,k}(q) = \sum_{l=0}^{L-1} w_{j,l}^{p,k}(t) e^{\frac{-j2plq}{L}} \tag{6.15}$$

where $\Psi_{t,j}^{p,k}(q)$, $q=1,\mathbf{K},L$, is the FFT of the feed-forward tap coefficient for the *j*-th receive antenna at the *q*-th chip of the *p*-th user during the *k*-th iteration at symbol interval t. $\mathbf{\Theta}_{t,j}^{p}$ is then sent to the feed forward filter of the *j*-th antenna to perform the element-wise multiplication with the feed forward tap coefficient $\mathbf{\Psi}_{t,j}^{p,k}$ in the frequency domain.

The outputs of each feed forward filter are then added to obtain the detector output for each transmit antenna. The output of the adder for the *k*-th iteration at symbol interval t, for *i*-th antenna of the *p*-th user, denoted by $\overline{\mathbf{F}}_{t,p}^{i,k}$, is given by

$$\overline{\mathbf{F}}_{t,p}^{i,k}=\left(\sum_{j=1}^{M} diag\left(\mathbf{\Theta}_{t,j}^{p}\right)^{H}\cdot\mathbf{\Psi}_{t,j}^{p,k}\right) \tag{6.16}$$

where $diag(\cdot)$ and $(\cdot)^{H}$ denote the diagonal matrix and the conjugate transpose function. $\overline{\mathbf{F}}_{t,p}^{i,k}$ is then transformed back into the time domain by the inverse fast Fourier transform (IFFT). The feed-forward filter output for the *i*-th antenna of the *p*-th user during the *k*-th iteration at symbol interval *t*, is given by

$$\mathbf{F}_{t,p}^{i,k}=ifft(\overline{\mathbf{F}}_{t,p}^{i,k}) \tag{6.17}$$

where

$$\mathbf{F}_{t,p}^{i,k}=\left[F_{t,p}^{i,k}(0),\mathbf{K},F_{t,p}^{i,k}(q),\mathbf{K}\,F_{t,p}^{i,k}(L-1)\right] \tag{6.18}$$

and

$$F_{t,p}^{i,k}(q)=\frac{1}{L}\sum_{l=0}^{L-1}\overline{F}_{t,p}^{i,k}e^{\frac{-j2plq}{L}} \tag{6.19}$$

Let $\hat{F}_{t,p}^{i,k}$ represent the time domain feed-forward filter output for the *i*-th antenna of the *p*-th user during the *k*-th iteration at symbol interval *t*, defined by

$$\hat{F}_{t,p}^{i,k}=\mathbf{I}_{\mathbf{F}}\cdot\mathbf{F}_{t,p}^{i,k} \tag{6.20}$$

where $\mathbf{I}_F$ is defined by $\mathbf{I}_F = [1\ \mathbf{0}_{L-1}]$ and $\mathbf{0}_{L-1}$ is a row vector of length L-1 containing all zeros.

For the feedback filter module, the feedback filter output can be obtained in the same manner as the feed-forward filter process but the input of the feedback filter is the decoder soft output from the previous iteration. The estimated symbols from the decoder outputs are fed back to the feedback filter to cancel the interference from adjacent antennas of the user of interest and from the antennas of other users.

The symbol estimates from the output of the decoders are transformed into the frequency domain using the FFT and then passed to the feedback filter. The output of the FFT, denoted by $\mathbf{\Lambda}_{t,p}^{i,k}$, of the p-th user at symbol interval t, is given by

$$\mathbf{\Lambda}_{t,p}^{i,k} = fft\left(\underline{\hat{\mathbf{x}}}_{t,p}^{i,k}\right) \tag{6.21}$$

where

$$\mathbf{\Lambda}_{t,p}^{i,k} = \left[\Lambda_{t,p}^{i,k}(1), \mathbf{K}\, \Lambda_{t,p}^{i,k}(a), \mathbf{K}, \Lambda_{t,p}^{i,k}(KN-1)\right] \tag{6.22}$$

and

$$\Lambda_{t,p}^{i,k}(a) = \sum_{m=0}^{KN-2} \hat{x}_{t,p}^{m,k} e^{\frac{-j2pam}{KN-1}}; \quad \begin{cases} a \in (1\mathbf{K}\, KN-1) \\ p \in (1\mathbf{K}\, K) \end{cases} \tag{6.23}$$

where $\underline{\hat{\mathbf{x}}}_{t,p}^{i,k}$ is an (KN – 1)×1 vector of the estimated soft symbols, at the k-th iteration, from MAP decoders of all antennas of all users, except the i-th antenna of the p-th user, at symbol interval t, given by

$$\underline{\hat{\mathbf{x}}}_{t,p}^{i,k} = \left(\hat{\mathbf{x}}_{t,1}^{1,k}, \mathbf{K}, \hat{\mathbf{x}}_{t,1}^{N,k}, \mathbf{K}, \hat{\mathbf{x}}_{t,p}^{i,k}, \mathbf{K}, \hat{\mathbf{x}}_{t,K}^{1,k}, \ldots, \hat{\mathbf{x}}_{t,K}^{N,k}\right)^{\mathrm{T}} \tag{6.24}$$

where

$$\hat{\mathbf{x}}_{t,p}^{i,k} = \left(\hat{x}_{t,p}^{1,k}, \hat{x}_{t,p}^{2,k}, \ldots, \hat{x}_{t,p}^{i-1,k}, \hat{x}_{t,p}^{i+1,k}, \ldots, \hat{x}_{t,p}^{N,k}\right) \tag{6.25}$$

Let $\underline{\hat{\mathbf{w}}}_{b,p}^{i,k}(t)$ be the feedback filter coefficients of all users, except the ***i***-th antenna of the ***p***-th user, at symbol interval ***t*** in time domain, given by

$$\underline{\hat{\mathbf{w}}}_{b,p}^{i,k}(t) = \left[\mathbf{w}_{b,1,}^{1,k}(t), \mathbf{K}, \mathbf{w}_{b,1}^{N,k}(t), \mathbf{K}, \mathbf{w}_{b,p}^{i,k}(t), \mathbf{K}\mathbf{w}_{b,K}^{1,k}(t)\,\mathbf{K}, \mathbf{w}_{b,K}^{N,K}(t)\right]^{T} \tag{6.26}$$

where

$$\mathbf{w}_{b,p}^{i,k}(t) = \left[w_{b,p}^{1,k}(t), \ldots, w_{b,p}^{i-1,k}(t), w_{b,p}^{i+1,k}(t), \mathbf{K}w_{b,p}^{N,k}(t)\right] \tag{6.27}$$

Let $\mathbf{\Psi}_{t,b,p}^{i,k}$ represent the FFT of $\underline{\hat{\mathbf{w}}}_{t,b}^{i,k}(t)$, defined by

$$\mathbf{\Psi}_{t,b,p}^{i,k} = fft\left(\underline{\hat{\mathbf{w}}}_{b,p}^{i,k}(t)\right) \tag{6.28}$$

where

$$\mathbf{\Psi}_{t,b,p}^{i,k} = \left[\Psi_{b,p}^{k}(1), \mathbf{K}, \Psi_{t,b,p}^{k}(a), \mathbf{K}, \Psi_{t,b,p}^{k}(KN-1)\right] \tag{6.29}$$

and

$$\Psi_{t,b,p}^{k}(a) = \sum_{m=0}^{KN-2} w_{b,p}^{m,k}(t) e^{\frac{-j2pam}{KN-1}} \tag{6.30}$$

The output of the FFT, as denoted in Equation (6.21), is then applied to the feedback filter with the frequency domain feedback tap coefficients as defined in Equation (6.28) to perform the element-wise multiplication in frequency domain. The feedback filter output signals, defined by $\overline{\mathbf{F}}_{t,b}^{i,k}$, at symbol interval t, is given by

$$\overline{\mathbf{F}}_{t,b,p}^{i,k} = \left(diag\left(\mathbf{\Lambda}_{t,p}^{i,k}\right)^H \cdot \mathbf{\Psi}_{t,b,p}^{i,k} \right) \tag{6.31}$$

$\overline{\mathbf{F}}_{t,b,p}^{i,k}$ is then transformed back into time domain by the IFFT. The feedback filter output for the *i*-th antenna of the *p*-th user, during the *k*-th iteration, at symbol interval *t*, is given by

$$\mathbf{F}_{t,b,p}^{i,k} = ifft(\overline{\mathbf{F}}_{t,b,p}^{i,k}) \tag{6.32}$$

where

$$\mathbf{F}_{t,b,p}^{i,k} = \left[F_{t,b,p}^{k}(1), \mathbf{K}, F_{t,b,p}^{k}(a), \mathbf{K}\, F_{t,b,p}^{k}(KN-1)\right] \tag{6.33}$$

$$F_{t,b,p}^{k}(a) = \frac{1}{KN-1} \sum_{m=0}^{KN-2} \overline{F}_{t,b,p}^{m,k} e^{\frac{-j2pm}{KN-1}} \tag{6.33}$$

Let $F_{t,b,p}^{p,k}$ represent the time domain feedback filter output for the *i*-th antenna of the *p*-th user during the *k*-th iteration at symbol interval *t*, defined by

$$F_{t,b,p}^{p,k} = \mathbf{I}_{\mathrm{B}} \cdot \mathbf{F}_{t,b,p}^{i,k} \tag{6.34}$$

where $\mathbf{I}_B = [1 \;\; \mathbf{0}_{KN-1}]$, and $\mathbf{0}_{KN-1}$ is a row vector with the length of *KN*-1 containing all zeros.

The detected symbol of the *p*-th user obtained at the output of the adaptive detector for the *i*-th antenna during the *k*-th iteration at symbol interval *t*, denoted by $y_{t,p}^{i,k}$, given by

$$y_{t,p}^{i,k} = F_{t,p}^{i,k} + F_{t,b,p}^{p,k} \tag{6.35}$$

where $F_{t,p}^{i,k}$ and $F_{t,b,p}^{p,k}$ represent the feed-forward and the feedback filter outputs in the time domain, as given in Equation (6.20) and Equation (6.33), respectively.

The detector soft output $y_{t,p}^{i,k}$ in the time domain is then compared to the training sequence, and the difference between them, referred to as the detection error, is calculated. The detection error in the *k*-th iteration at symbol interval *t*, for the *i*-th antenna for the *p*-th user, denoted by $e_{t,p}^{i,k}$, is given by

$$e_{t,p}^{i,k} = y_{t,p}^{i,k} - x_{t,p}^{i,k} \tag{6.36}$$

where $x_{t,p}^{i,k}$ is the training sequence for the *i*-th antenna of the *p*-th user in the *k*-th iteration at symbol interval *t*.

The detection error is then used to adapt the feed-forward filter and feedback filter tap coefficients. After the mean square error (MSE) approaches a specified value, the training mode is switched to the decision directed mode, in which the training sequence is replaced by the hard decision output of each user detector. In the decision directed mode, the detection error is given by the difference between the detector output and the hard decision of the detector output.

The values of feed-forward filter tap coefficients, $\mathbf{w}_{t,j}^{p,k}(t)$, in Equation (6.12) and feedback filter tap coefficients, $\underline{\hat{\mathbf{w}}}_{t,b}^{i,k}(t)$, in Equation (6.26) are calculated by minimizing the mean square error, defined as z , between the training sequence and the detector soft output, given by

$$z = \min\left(E\left[\left| y_{t,p}^{i,k} - x_{t,p}^{i,k} \right|^2 \right] \right) \tag{6.37}$$

They can be determined recursively by an adaptive normalized Least Mean Square (NLMS) algorithm in the time domain [18] as follows

$$\mathbf{w}_j^{p,k}(t+1) = \mathbf{w}_j^{p,k}(t) + \frac{m_f}{a_f + \mathbf{r}_{t,j}^{p\,H}\mathbf{r}_{t,j}^{p}} e_{t,p}^{i,k}\mathbf{r}_{t,j}^{p} \tag{6.38}$$

$$\underline{\hat{\mathbf{w}}}_{b,p}^{i,k}(t+1) = \underline{\hat{\mathbf{w}}}_{b,p}^{i,k}(t) + \frac{m_b}{a_b + \underline{\hat{\mathbf{x}}}_{t,p}^{i,k\,H}\underline{\hat{\mathbf{x}}}_{t,p}^{i,k}} e_{t,p}^{i,k}\underline{\hat{\mathbf{x}}}_{t,p}^{i,k} \tag{6.39}$$

where $\mathbf{r}_{t,j}^{p}$ and $\underline{\hat{\mathbf{x}}}_{t,p}^{i,k}$ are defined in Equation (6.3) and Equation (6.24), respectively. m_f and m_b are the step sizes for the feed-forward and feedback adaptations, respectively and a_f and a_b are positive constants to prevent division by zero.

Let $\mathbf{E}_{f,j}^{p}(t)$ and $\mathbf{E}_{b,p}^{i,k}(t)$ represent a column vector of the error $e_{t,p}^{i,k}$ and the step size for the feed-forward (m_f) and feedback (m_b) filters of the *p*-th user, as defined by

$$\mathbf{E}_{f,j}^{p}(t) = \left[U_{f,j}^{p}(t)e_{t,p}^{i,k},\ 0_1, 0_2, \mathbf{K}\, 0_{L-1}\right]^T \tag{6.40}$$

$$\mathbf{E}_{b,p}^{i,k}(t) = \left[U_{b,p}^{i,k}(t)e_{t,p}^{i,k},\ 0_1, 0_2, \mathbf{K}\, 0_{KN-2}\right]^T \tag{6.41}$$

where $U_{f,j}^{p}(t)$ and $U_{b,p}^{i,k}(t)$ are, respectively, the normalized step size of the feed-forward and feedback filters, given by

$$U_{f,j}^{p}(t) = \frac{m_f}{a_f + R_{t,j}^{p}} \tag{6.42}$$

$$U_{b,p}^{i,k}(t) = \frac{m_b}{a_b + R_{t,b,p}^{i,k}} \tag{6.43}$$

where $R_{t,j}^{p}$ and $R_{t,b,p}^{i,k}$ are the signal symbol's energies of $\mathbf{r}_{t,j}^{p}$ and $\underline{\hat{\mathbf{x}}}_{t,p}^{i,k}$, respectively, in the time domain. The signal's energy calculation is first performed in the frequency domain approach and then transformed back into the time domain signal. The $R_{t,j}^{p}$ and $R_{t,b,p}^{i,k}$ are given by

$$R_{t,j}^{p} = \mathbf{I}_F \left\{ ifft\left(diag\left(\mathbf{\Theta}_{t,j}^{p}\right)^{H} \cdot \mathbf{\Theta}_{t,j}^{p} \right) \right\} \tag{6.44}$$

$$R_{t,b,p}^{i,k} = \mathbf{I}_{\mathbf{B}} i\left\{ fft\left(diag\left(\mathbf{\Lambda}_{t,p}^{i,k}\right)^{H} \cdot \mathbf{\Lambda}_{t,p}^{i,k} \right) \right\} \tag{6.45}$$

where $\mathbf{I}_F = [1 \ \mathbf{0}_{L-1}]$ and $\mathbf{I}_B = [1 \ \mathbf{0}_{KN-1}]$, where $\mathbf{0}_A$ is a row vector of length A containing all zeros. $\mathbf{\Theta}_{t,j}^{p}$ is an $L \times 1$ vector of the received signal in frequency domain defined in Equation (6.9) and $\mathbf{\Lambda}_{t,p}^{i,k}$ is an $(KN-1)$ vector of the symbol estimates in frequency domain defined in Equation (6.21). The updated feed-forward filter coefficients, $\mathbf{w}_{j}^{p,k}(t+1)$, and the feedback filter coefficients, $\underline{\hat{\mathbf{w}}}_{b,p}^{i,k}(t+1)$, can be written as

$$\mathbf{w}_{j}^{p,k}(t+1) = \mathbf{w}_{j}^{p,k}(t) + \mathbf{\Delta}_{f,j}^{p}(t) \tag{6.46}$$

$$\underline{\hat{\mathbf{w}}}_{b,p}^{i,k}(t+1) = \underline{\hat{\mathbf{w}}}_{b,p}^{i,k}(t) + \mathbf{\Delta}_{b,p}^{i,k}(t) \tag{6.47}$$

where $\mathbf{\Delta}_{f,j}^{p}(t)$ is the time domain update parameter of the feed-forward filter coefficients, given by

$$\mathbf{\Delta}_{f,j}^{p}(t) = \mathbf{I}_{\mathbf{F}} \cdot \left(ifft\left[\left(diag\left(\mathbf{\Phi}_{f,j}^{p}(t)\right)^{H} \cdot \mathbf{\Theta}_{t,j}^{p} \right] \right) \tag{6.48}$$

where $\mathbf{\Theta}_{t,j}^{p}$ is defined in Equation (6.9) and $\mathbf{\Phi}_{f,j}^{p}(t)$ is defined by

$$\mathbf{\Phi}_{f,j}^{p}(t) = fft\left(\mathbf{E}_{f,j}^{p}(t)\right) \tag{6.49}$$

Similarly, $\mathbf{\Delta}_{b,p}^{i,k}(t)$ is the time domain update parameter of the feedback filter coefficients, given by

$$\mathbf{\Delta}_{b,p}^{i,k}(t) = \mathbf{I}_{\mathbf{F}} \cdot \left(ifft \left[\left(diag\left(\mathbf{\Phi}_{b,p}^{i,k}(t) \right) \right)^{H} \cdot \mathbf{\Lambda}_{t,p}^{i,k} \right] \right) \tag{6.50}$$

where $\mathbf{\Lambda}_{t,p}^{i,k}$ is defined in Equation (6.21) and $\mathbf{\Phi}_{b,p}^{i,k}(t)$ is defined by

$$\mathbf{\Phi}_{b,p}^{i,k}(t) = fft\left(\mathbf{E}_{b,p}^{i,k}(t) \right) \tag{6.51}$$

Therefore, the values of feed-forward filter tap coefficients, $\mathbf{w}_{t,j}^{p,k}(t)$, in Equation (6.12) and feedback filter tap coefficients, $\underline{\hat{\mathbf{w}}}_{t,b}^{i,k}(t)$, in Equation (6.26) can be calculated recursively by using Equation (6.46) and Equation (6.47), respectively.

After the detection process, the detector outputs for user *p*, $y_{t,p}^{i,k}$, are fed to the time deinteleaver and followed by the spatial deinterleaver. The spatial deinterleaver outputs are then applied to the parallel MAP decoders to decode the outputs in time domain. The soft-output from the decoder is used to cancel interference in the feedback filter in the next iteration. The calculation of the soft-output symbol estimate in the *i*-th layer and *k*-th iteration for the *p*-th user with the BPSK modulation scheme was discussed in Chapter 5. This adaptive iterative detection/decoding process is repeated until the system performance achieves a satisfactory level and then the soft-outputs from the decoder in the last iteration are fed into a decision device.

6.4 Complexity Analysis

In this paper, we define the receiver computational complexity as the required number of signal processing operations per coded symbol and per user. As we want to compare the receiver complexity between the time and frequency domain implementations of adaptive iterative receivers, we will consider only the complexity of the detector since the decoder is the same for both implementations.

In the time domain adaptive detector [28], for each coded symbol per user and per iteration in the equalization process, each feed forward filter requires L multiplications while the feedback filter requires $KN-1$ multiplications. The coefficient-updating process requires $2L+1$ multiplications for the feed-forward tap coefficients, and $2KN-1$ multiplications for the feedback tap coefficients. Therefore the total number of operations is $KNI(3ML+M+3KN-2)$ multiplications for each coded symbol for K users, N transmit and M receive antennas at I iterations with the spreading sequence length L.

The computational requirement [28] for the frequency domain adaptive detector requires $\log_2(L)$ multiplications for each feed-forward filter, and $\log_2(KN-1)$ multiplications for each feedback filter, for each coded symbol per user per iteration. To update the tap coefficients, each feed-forward filter requires $M\log_2(2L+1)$ multiplications, while the feedback filter requires $\log_2(2KN-1)$ multiplications. Therefore the total number of operations is $KNI(M\log_2(L)+M(2L+1)+\log_2(KN-1)+\log_2(2KN-1))$ multiplications for each coded symbol. The comparison of the complexity between the two type detectors is shown in table 1.

Table 1. Complexity comparison between the time and frequency domain adaptive detectors

Algorithm	Number of multiplications
Time-domain detector	$KNI(3ML+M+3KN-2)$
Freq-domain detector	$KNI(M\log_2(L)+M\log_2(2L+1)+\log_2(KN-1)+\log_2(2KN-1))$

K = number of users, L = processing gain, N = number of transmit antennas,
M = number of receive antennas, and I = number of iteration

It can be observed from Table 1 that the computational complexity in the frequency domain is significantly lower than that of the time domain approach. For instance, assuming that K = 5, L = 7, N = M = 4, and I = 8, the computational complexity for the time and frequency domain detectors is 23360 and 5822, respectively. The complexity of the frequency domain detector can save about 75% in computational complexity compared to the time domain detector. If the processing gain is increased to 32, the computational complexity for the time and frequency domain detectors is 71360 and 8580. The reduction of the computational complexity in the frequency domain detector is about 88% compared to the time domain detector. Therefore, the computational complexity of the frequency domain detector is significantly lower than the time domain receiver in this example.

6.5 Performance Results

This section presents simulation results for the adaptive iterative LSTC-CDMA receiver operating in the frequency domain. We consider BPSK modulation and a quasi-static fading channel, for which the fading coefficients are constant within a frame, but change independently from one frame to another. The system operates in the training mode until the MSE reaches the minimum, at which point it switches to the decision directed mode. The constituent codes are non-systematic convolutional codes with the code rate of 1/2, memory order of 3 and the generating polynomials $g_1 = 15_8$ and $g_2 = 17_8$. The spreading sequences used are Gold sequences with the processing gain of 7. The proposed system is simulated with four transmit and four receive antennas, i.e., a 4×4 LSTC-CDMA system, with 130 information symbols in each frame per layer for each user. Therefore, each layer of the LSTC-CDMA system consists of 266 encoded symbols per frame.

The frame error rates (FER) of the time and frequency domain adaptive iterative MMSE single user receivers for various numbers of iterations are shown in Figure. 6.3. It can be observed that the system performance is significantly improved in the second iteration compared to the first iteration, and approaches the interference free bound in the 5^{th} iteration. The results also show that the frequency domain structures have the same performance as the time domain structures with a lower computational complexity.

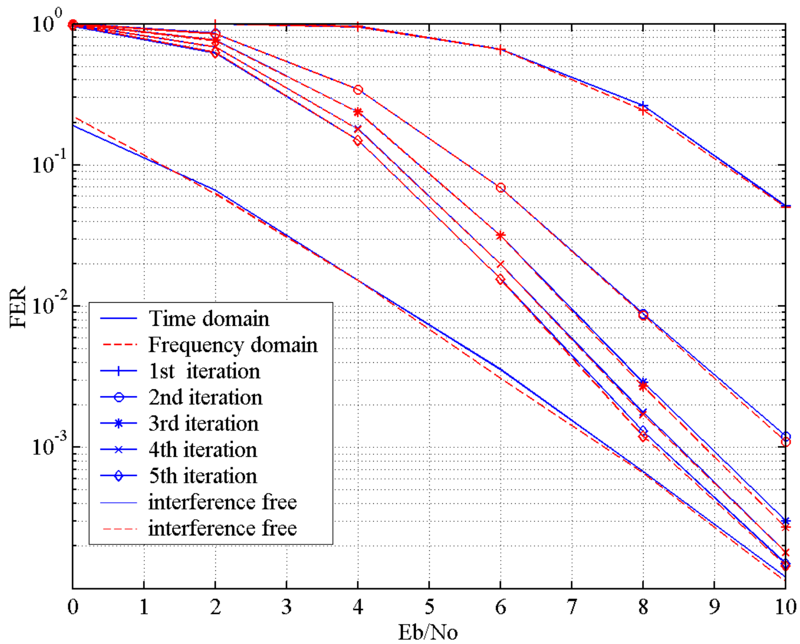

Figure. 6.3 Comparison of the time domain and frequency domain adaptive iterative MMSE receivers in a quasi-static Rayleigh fading channel.

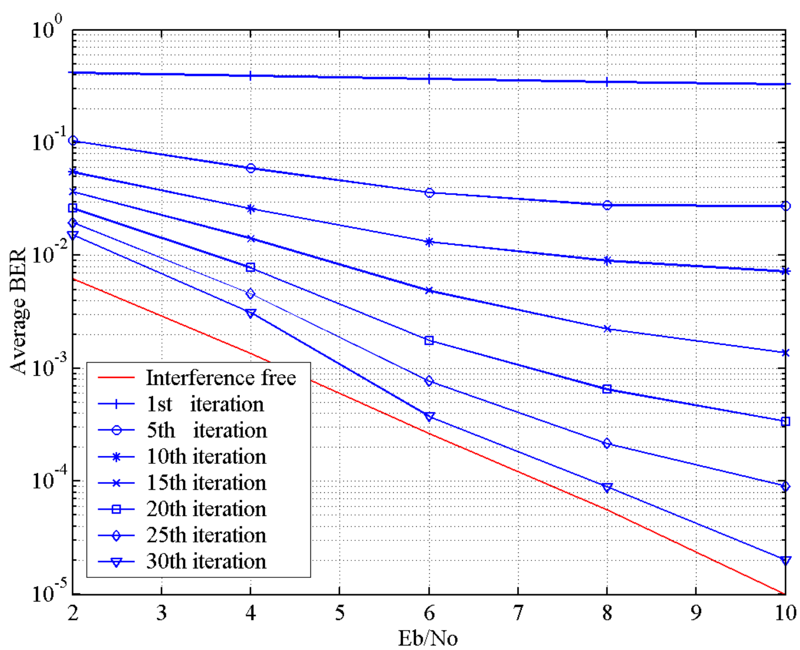

Figure. 6.4 BER performance of the frequency domain adaptive iterative receiver with 20 users.

Figure. 6.4 presents the system performance with 20 users for the frequency domain receiver. It is obvious that the proposed receiver effectively suppresses the interference and cancels the co-channel interference (CCI) and the multiple access interference (MAI) with a number of iterations. The performance of the system approaches the single user performance at the 30^{th} iteration.

The maximum number of users for a system with a frequency domain adaptive iterative receiver can support a target BER, at E_b/N_o 10 dB as shown in Figure. 6.5. For a BER of 10^{-4}, the number of users is 20 after 25 iterations. For a BER of 10^{-2}, the number of users is 35 after 25 iterations. It also shows that to increase the number of active users in the system, a higher number of iteration processes is needed to achieve a satisfactory system performance. For example, for 10 users, the receiver requires 10 iterations to achieve a BER of 10^{-3} while for 27 users, it requires 25 iterations to achieve the same BER.

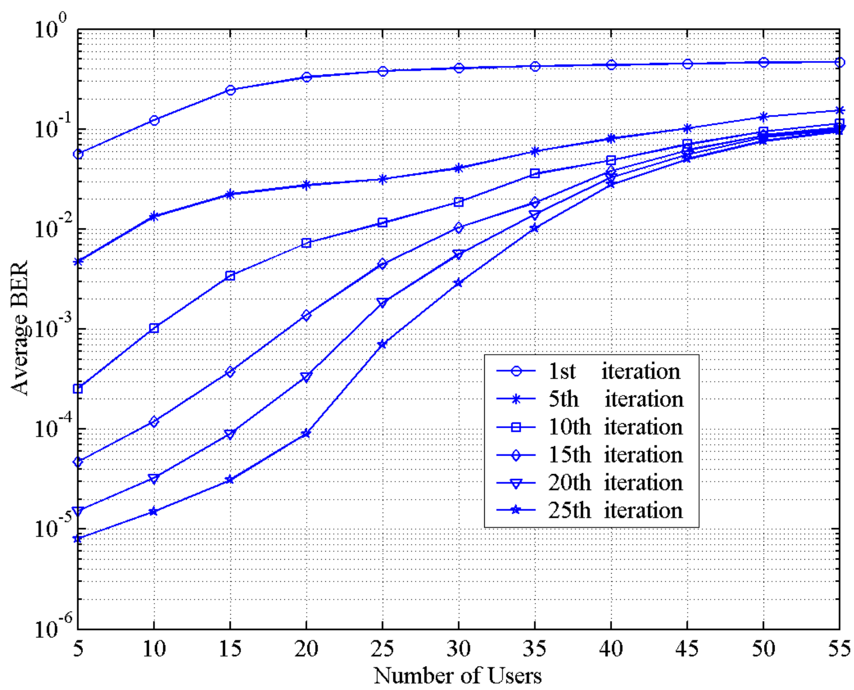

Figure. 6.5 BER of the frequency domain adaptive iterative receiver at E_b/N_o 10dB, for variable number of users

All performance results were obtained for a quasi-static fading channel. However, since the adaptive detector performance is sensitive to the channel estimation accuracy [75], the system performance is investigated for fading rates. Figure. 6.6 shows the performance of the frequency domain receiver for various values of normalized fading rates. The results show that the average BER of the adaptive iterative receiver is increased due to inaccurate channel estimation in fast fading channels. Therefore, the average BER of the adaptive receiver increases when the fade rate is increased, as shown in Figure 6.7. The detector is unable to track channel coefficients for normalized fade rates above 0.006.

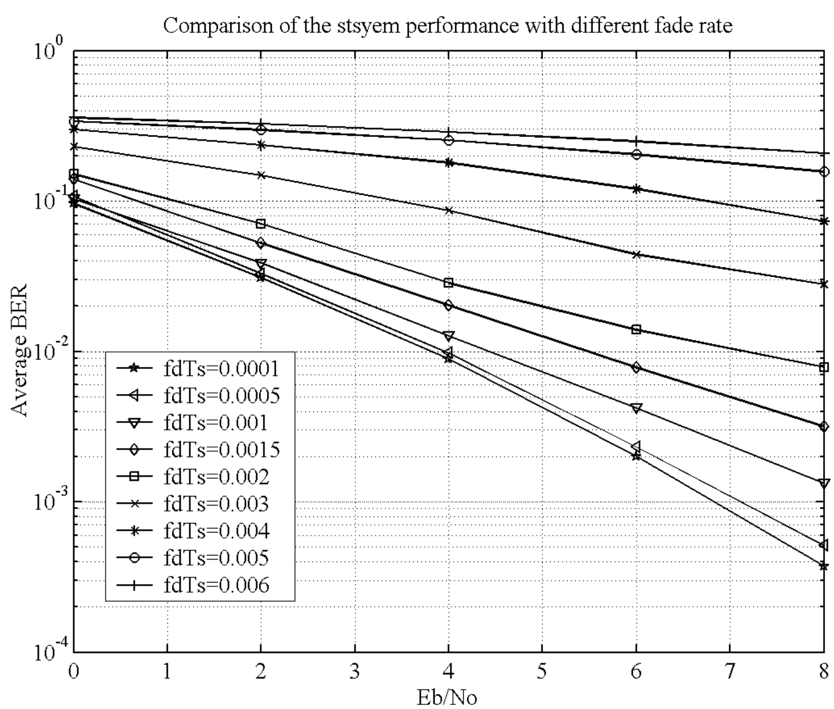

Figure. 6.6 BER performance of the frequency domain adaptive iterative receiver for various fade rates and five users

6.6 Conclusion

In this chapter, we present a low complexity frequency domain adaptive iterative receiver for a layered space-time coded CDMA (LSTC-CDMA) system. In comparison to the time domain receiver, the proposed frequency domain receiver has a lower computational complexity and achieves the same performance. For example, for a receiver with five users, four transmit and receive antennas, eight iterations and the processing gains L of 7 and 32, the computational complexity is 75 % and 88% lower than that of a time domain receiver, respectively. The simulation results show that the performance of the frequency domain adaptive receiver is identical to the performance of the time domain adaptive receiver. Also, the proposed receiver can suppress the interference and cancel the CCI and MAI interferences from the received signal with a number of iterations. The system performance is also investigated for various fading rates. The results show that the average BER of the adaptive iterative receiver is increased due to inaccurate channel estimation in fast fading channels. Therefore, the average BER of the adaptive receiver increases when the fade rate is increased. The detector is unable to track channel coefficients for normalized fade rates above 0.006. The simulation results show that the adaptive iterative receiver can achieve interference-free single user performance for a high signal to noise ratio (SNR).

Chapter 7

Conclusions

It was shown that in MIMO transmission schemes, the received signal is intrinsically affected by the co-channel interference (CCI) and multiple access interference (MAI). Several receiver structures, such as a minimum mean square error (MMSE) receiver and a parallel interference cancellation (PIC) receiver, have been developed but they require perfect a priori knowledge of channel state information (CSI) at the receiver end. In addition, they are based on non-adaptive receiver structures, which have a high computational complexity due to matrix inversion of the channel matrix.

Therefore, this thesis focuses on the design of a low computational complexity adaptive iterative receiver with an acceptable system performance for wireless MIMO communication systems. The thesis develops adaptive iterative receivers operating in time and frequency domains for a layered space-time codes and layered space-time coded DS-CDMA systems. The proposed receivers can effectively suppress and remove the CCI and MAI from the system with a low computational complexity compared to the non-adaptive MMSE receiver. In this thesis, we want to compare the receiver complexity among different implementations of the adaptive detectors in the adaptive iterative receiver, but we will consider only the complexity of the adaptive detectors since the decoder is the same in all detector implementations,

We first propose a time domain adaptive iterative receiver, based on a joint adaptive iterative detection and decoding algorithm, to adaptively suppress and cancel co-channel interference in a layered space-time coding system as discussed in Chapter 2. The receiver structure, utilizing an adaptive least mean square (LMS) algorithm, is proposed in the system. The performance and computational complexity of the proposed system is compared to that of the non-adaptive iterative MMSE receiver.

In the proposed receiver, the receiver can effectively suppress and cancel the CCI by performing interference suppression and cancellation techniques. The system performance of the proposed receiver approaches the performance of the non-adaptive iterative receiver with the number of iterations. The computational complexity of the proposed receiver is also investigated and it is shown that the computational complexity of the proposed adaptive iterative receiver is significantly reduced in comparison with the non-adaptive iterative MMSE receiver. The complexity is reduced from the order of M^3 in a non-adaptive receiver to the order of M in an adaptive receiver.

To increase the convergence speed of the LMS algorithm, we apply a partially filtered gradient LMS (PFGLMS) algorithm into the adaptive iterative receiver based on the LMS algorithm. The new proposed structure removes the LMS algorithm and replaces it with the PFGLMS algorithm. The comparison of the convergence speed shows that the PFGLMS has a faster convergence speed. The performance also shows that the PFGLMS based adaptive iterative receiver has a tracking ability in the rich scattering environment and in the fast fading channel and also approaches the performance of the non-adaptive MMSE receiver. Therefore the PFGLMS based receiver needs a shorter training period than that of the LMS receiver. However, the computational complexity of the PFGLMS-based receiver is slightly higher than that of the LMS-based receiver.

To further reduce the computational complexity, an adaptive iterative receiver based on the frequency domain approach is introduced in Chapter 4. A new frequency domain adaptive iterative receiver for MIMO systems based on a joint adaptive iterative detection and decoding structure is proposed. The proposed adaptive iterative receiver effectively reduces co-channel interference by interference suppression and cancellation techniques, has a significantly lower computational complexity and achieves the same performance compared to the time domain receiver. For example, for a receiver with four transmit and four receive antennas, 10 iterations, the computational complexity of the frequency domain receiver based on the LMS and PFGLMS algorithm is 63 % and 75% lower than that of a time domain receiver, respectively. Moreover, the detector based on the PFGLMS algorithm has a faster convergence speed and a better tracking ability compared to the LMS receiver in a dense interference environment with a slight increase in the complexity in terms of the number of multiplication. Therefore the PFGLMS detector needs a shorter training period than that of the LMS receiver.

In Chapter 5, we further extend the MIMO system to the MIMO-CDMA systems, where the interference level at the receiver is increased due to the additional co-channel interference (CCI) from adjacent layers and multi-access interference MAI from other users. In Chapter 5, we present an adaptive iterative receiver based on the normalized LMS (NLMS) algorithm for a layered space-time coded CDMA (LSTC-CDMA) system. The simulation results show that the proposed adaptive iterative receiver effectively suppresses and removes the CCI and MAI by using the interference cancellation technique. The performance shows that the system performance approaches the single user interference-free bound with a number of iterations at a high signal to noise ratio (SNR).

The simulation results show that an increase in the number of users requires a higher number of iterations to achieve the same BER performance. For example, for 10 users, the receiver requires 10 iterations to achieve a BER of 10^{-3} while for 27 users, it requires 25 iterations to achieve the same BER. Moreover, the system performance is evaluated by a semi-analytical approach and by simulations, and there is an excellent agreement between the two sets of results. Consequently, the use of the semi-analysis approach, which significantly reduces system simulation time, can predict the system's performance without actually simulating data transmission.

In Chapter 6, we introduce a low complexity frequency domain adaptive iterative receiver for a layered space-time coded CDMA (LSTC-CDMA) system in order to further reduce the receiver computational complexity. The proposed receiver structure is employed from the time domain adaptive iterative receiver structure from Chapter 5. The difference is, the adaptive detector in Chapter 5 performs adaptation in the time domain and the adaptive detector in Chapter 6 performs adaptation in the frequency domain. In comparison to the time domain receiver, the proposed frequency domain receiver is significantly lower in computational complexity and achieves the same performance. For example, for a receiver with five users, four transmit and receive antennas, eight iterations and processing gains L of 7 and 32, the computational complexity is 75 % and 88% lower than that of a time domain receiver, respectively. The system performance is also investigated for various fading rates. The results show that the average BER of the adaptive iterative receiver is increased due to inaccurate channel estimation in fast fading channels. Therefore, the average BER of the adaptive receiver increases as the fade rate is increased. The detector is unable to track channel coefficients for normalized fade rates above 0.006. The simulation results show that the adaptive iterative receiver can also achieve the interference-free single user performance for a high signal to noise ratio (SNR).

BIBLIOGRAPHY

[1] Z. Chen, J. Yuan, and B. Vucetic, "Improved space-time trellis coded modulation scheme on slow Rayleigh fading channels," *Electronics Letters*, vol. 37, pp. 440-441, 2001.

[2] V. Tarokh, N. Seshadri, and A. R. Calderbank, "Space-time codes for high data rate wireless communication: performance criterion and code construction," *Information Theory, IEEE Transactions on*, vol. 44, pp. 744-765, 1998.

[3] R. Lupas and S. Verdu, "Near-far resistance of multiuser detectors in asynchronous channels," *Communications, IEEE Transactions on*, vol. 38, pp. 496-508, 1990.

[4] S. Verdu, "Minimum probability of error for asynchronous Gaussian multiple-access channels," *Information Theory, IEEE Transactions on*, vol. 32, pp. 85-96, 1986.

[5] R. Lupas and S. Verdu, "Linear multiuser detectors for synchronous code-division multiple-access channels," *Information Theory, IEEE Transactions on*, vol. 35, pp. 123-136, 1989.

[6] U. Madhow and M. L. Honig, "MMSE interference suppression for direct-sequence spread-spectrum CDMA," *Communications, IEEE Transactions on*, vol. 42, pp. 3178-3188, 1994.

[7] S. Marinkovic, B. Vucetic, and A. Ushirokawa, "Space-time iterative and multistage receiver structures for CDMA mobile communication systems," *Selected Areas in Communications, IEEE Journal on*, vol. 19, pp. 1594-1604, 2001.

[8] X. Wang and H. V. Poor, "Iterative (turbo) soft interference cancellation and decoding for coded CDMA," *Communications, IEEE Transactions on*, vol. 47, pp. 1046-1061, 1999.

[9] H. El Gamal and E. Geraniotis, "Iterative multiuser detection for coded CDMA signals in AWGN and fading channels," *Selected Areas in Communications, IEEE Journal on*, vol. 18, pp. 30-41, 2000.

[10] P. Patel and J. Holtzman, "Analysis of a simple successive interference cancellation scheme in a DS/CDMA system," *Selected Areas in Communications, IEEE Journal on*, vol. 12, pp. 796-807, 1994.

[11] P. Patel and J. Holtzman, "Performance comparison of a DS/CDMA system using a successive interference cancellation (IC) scheme and a parallel IC scheme under fading," presented at Communications, 1994. ICC 94, SUPERCOMM/ICC '94, Conference Record, Serving Humanity Through Communications. IEEE International Conference on, 1994.

[12] H. Yang, F. Yuan, and B. Vucetic, "Performance of space-time trellis codes in frequency selective WCDMA systems," presented at Vehicular Technology Conference, 2002. Proceedings. VTC 2002-Fall. 2002 IEEE 56th, 2002.

[13] M. L. Honig, G. K. Woodward, and Y. Sun, "Adaptive iterative multiuser decision feedback detection," *Wireless Communications, IEEE Transactions on*, vol. 3, pp. 477-485, 2004.

[14] M. Honig, V. Tripathi, and Y. Sun, "Adaptive decision feedback turbo equalization," presented at Information Theory, 2002. Proceedings. 2002 IEEE International Symposium on, 2002.

[15] J. Li, K. B. Letaief, and Z. Cao, "Adaptive cochannel interference cancellation in space-time coded communication systems," *Communications, IEEE Transactions on*, vol. 50, pp. 1580-1583, 2002.

[16] J. Choi, H. Yu, and Y. H. Lee, "Adaptive MIMO decision feedback equalization for receivers with time-varying channels," *Signal Processing, IEEE Transactions on [see also Acoustics, Speech, and Signal Processing, IEEE Transactions on]*, vol. 53, pp. 4295-4303, 2005.

[17] J. Jiang, Y. Zhu, C. Shen, and S. Mei, "Adaptive V-BLAST with partial channel state information feedback," presented at Communications, 2004 and the 5th International Symposium on Multi-Dimensional Mobile Communications

Proceedings. The 2004 Joint Conference of the 10th Asia-Pacific Conference on, 2004.

[18] S. S. Haykin, *Adaptive filter theory*, 4th ed. Upper Saddle River, N.J.: Prentice Hall, 2002.

[19] B. Vucetic and J. Yuan, *Turbo codes : principles and applications*. Boston: Kluwer Academic Publishers, 2000.

[20] B. Vucetic and J. Yuan, *Space-time coding*. Hoboken, NJ: Wiley, 2003.

[21] J. S. Lim, "Fast adaptive filtering algorithm based on exponentially weighted least-square errors," *Electronics Letters*, vol. 35,no. 22, pp. 1913-1915, 1999.

[22] N. Bershad and P. Feintuch, "A normalized frequency domain LMS adaptive algorithm," *Acoustics, Speech, and Signal Processing [see also IEEE Transactions on Signal Processing], IEEE Transactions on*, vol. 34, pp. 452-461, 1986.

[23] A. Burg, M. Rupp, N. Felber, and W. Fichtner, "Practical low complexity linear equalization for MIMO-CDMA systems," presented at Signals, Systems & Computers, 2003 The Thrity-Seventh Asilomar Conference on, 2003.

[24] A. Burg, M. Rupp, S. Haene, D. Perels, N. Felber, and W. Fichtner, "Low complexity frequency domain equalization of MIMO channels with applications to MIMO-CDMA systems," presented at Vehicular Technology Conference, 2003. VTC 2003-Fall. 2003 IEEE 58th, 2003.

[25] M. V. Clark, "Adaptive frequency-domain equalization and diversity combining for broadband wireless communications," *Selected Areas in Communications, IEEE Journal on*, vol. 16, pp. 1385-1395, 1998.

[26] J. Coon, S. Armour, M. Beach, and J. McGeehan, "Adaptive frequency-domain equalization for single-carrier MIMO systems," presented at Communications, 2004 IEEE International Conference on, 2004.

[27] D. Falconer, S. L. Ariyavisitakul, A. Benyamin-Seeyar, and B. Eidson, "Frequency domain equalization for single-carrier broadband wireless systems," *Communications Magazine, IEEE*, vol. 40, pp. 58-66, 2002.

[28] J. J. Shynk, "Frequency-domain and multirate adaptive filtering," *Signal Processing Magazine, IEEE*, vol. 9, pp. 14-37, 1992.

[29] G. J. Foschini, "Layered space-time architecture for wireless communication in a fading environment when using multi-element antennas," *Bell Labs Technical Journal*, vol. 1, pp. 41-59, 1996.

[30] C. Teekapakvisit, V. D. Pham, and B. Vucetic, "An Adaptive Iterative Receiver for Space-time coding MIMO Systems," *3rd Workshop on the Internet, Telecommunications and Signal Processing*, 2004.

[31] C. Teekapakvisit, V. D. Pham, and B. Vucetic, "An Adaptive Iterative Receiver for Space-time coding MIMO Systems," *Journal of Telecommunications and Information Technology (JTIT)*, vol. 1/2006, 2006.

[32] C. Teekapakvisit, Y. Li, V. D. Pham, and B. Vucetic, "Frequency domain adaptive iterative receiver for layered space-time coding CDMA systems," presented at Signal Processing and Its Applications, 2005. Proceedings of the Eighth International Symposium on, 2005.

[33] G. J. Foschini and M. J. Gans, "On limits of wireless communications in a fading environment when using multiple antennas," *Wireless Personal Communications*, vol. 6, pp. 311-355, Mar. 1998.

[34] C. E. Shannon, "A mathematical theory of communication," *Bell Labs Technical Journal*, vol. 27, pp. 379-423, 1948.

[35] E. Telatar, "Capacity of multiantenna Gaussian channels," *AT&T-Bell Labs., Internal Tech. Memo.*, 1995.

[36] E. Biglieri, J. Proakis, and S. Shamai, "Fading channels: information-theoretic and communications aspects," *Information Theory, IEEE Transactions on*, vol. 44, pp. 2619-2692, 1998.

[37] V. Tarokh, H. Jafarkhani, and A. R. Calderbank, "Space-time block codes from orthogonal designs," *Information Theory, IEEE Transactions on*, vol. 45, pp. 1456-1467, 1999.

[38] A. Wittneben, "A new bandwidth efficient transmit antenna modulation diversity scheme for linear digital modulation," presented at Communications, 1993. ICC

93. Geneva. Technical Program, Conference Record, IEEE International Conference on, 1993.

[39] N. Seshadri and J. H. Winters, "Two signaling schemes for improving the error performance of frequency-division-duplex (FDD) transmission systems using transmitter antenna diversity," presented at Vehicular Technology Conference, 1993 IEEE 43rd, 1993.

[40] S. M. Alamouti, "A simple transmit diversity technique for wireless communications," *Selected Areas in Communications, IEEE Journal on*, vol. 16, pp. 1451-1458, 1998.

[41] H. Jafarkhani, *Space-time coding : theory and practice*. Cambridge: Cambridge University Press, 2005.

[42] G. J. Foschini. and M. J. Gans., "Layered space-time architecture for wireless communication in a fading environment when using multi-element antennas," *Bell Labs Technical Journal*, vol. 1, pp. 41-59, 1996.

[43] G. J. Foschini, D. Chizhik, M. J. Gans, C. Papadias, and R. A. Valenzuela, "Analysis and performance of some basic space-time architectures," *Selected Areas in Communications, IEEE Journal on*, vol. 21, pp. 303-320, 2003.

[44] H. E. Gamal and A. R. Hammons, Jr., "A new approach to layered space-time coding and signal processing," *Information Theory, IEEE Transactions on*, vol. 47, pp. 2321-2334, 2001.

[45] C. Berrou, A. Glavieux, and P. Thitimajshima, "Near Shannon limit error-correcting coding and decoding: Turbo-codes. 1," presented at Communications, 1993. ICC 93. Geneva. Technical Program, Conference Record, IEEE International Conference on, 1993.

[46] X. Wang and H. V. Poor, "Iterative (turbo) soft interference cancellation and decoding for coded CDMA," *Communications, IEEE Transactions on*, vol. 47, 1999.

[47] A. J. Viterbi, *CDMA : Principle of Spread Spectrum Communication*: Addison Wesly, 1995.

[48] E. H. Dinan and B. Jabbari, "Spreading codes for direct sequence CDMA and wideband cellular networks," *IEEE Communications Magazine*, pp. 48-54, sept 1998.

[49] R. Gold, "Optimal binary sequences for spread spectrum multiplexing (Corresp.)," *Information Theory, IEEE Transactions on*, vol. 13, pp. 619-621, 1967.

[50] R. Gold, "Maximal recursive sequences with 3-valued recursive cross-correlation functions (Corresp.)," *Information Theory, IEEE Transactions on*, vol. 14, pp. 154-156, 1968.

[51] M. P. Lotter and L. P. Linde, "A comparison of three families of spreading sequences for CDMA applications," presented at Communications and Signal Processing, 1994. COMSIG-94., Proceedings of the 1994 IEEE South African Symposium on, 1994.

[52] H. Murata and S. Yoshida, "Trellis-coded co-channel interference canceller for cellular radio," presented at Universal Personal Communications. 1995. Record., 1995 Fourth IEEE International Conference on, 1995.

[53] H. Yoshino, K. Fukawa, and H. Sukuki, "Interference cancelling equalizer (ICE) for mobile radio communication," *Vehicular Technology, IEEE Transactions on*, vol. 46, pp. 849-861, 1997.

[54] J. Li, K. B. Letaief, R. S. Cheng, and Z. Cao, "Adaptive antenna arrays for cochannel interference cancellation in space-time coded systems," presented at Vehicular Technology Conference, 2001. VTC 2001 Spring. IEEE VTS 53rd, 2001.

[55] B. Widrow, P. E. Mantey, L. J. Griffiths, and B. B. Goode, "Adaptive antenna systems," *Proceedings of the IEEE*, vol. 55, pp. 2143-2159, 1967.

[56] S. Verdu, *Multiuser detection*. Cambridge ; New York: Cambridge University Press, 1998.

[57] H. Jafarkhani, *Space-Time Coding*: Cambridge University Press, 2005.

[58] M. K. Varanasi and B. Aazhang, "Multistage detection in asynchronous code-division multiple-access communications," *Communications, IEEE Transactions on*, vol. 38, pp. 509-519, 1990.

[59] P. W. Wolniansky, G. J. Foschini, G. D. Golden, and R. A. Valenzuela, "V-BLAST: an architecture for realizing very high data rates over the rich-scattering wireless channel," presented at Signals, Systems, and Electronics, 1998. ISSSE 98. 1998 URSI International Symposium on, 1998.

[60] G. D. Golden, C. J. Foschini, R. A. Valenzuela, and P. W. Wolniansky, "Detection algorithm and initial laboratory results using V-BLAST space-time communication architecture," *Electronics Letters*, vol. 35, pp. 14-16, 1999.

[61] L. Yang, S. Cheng, and H. Wang, "Partial decision ordered successive interference cancellation detection algorithm for VBLAST," presented at Personal, Indoor and Mobile Radio Communications, 2004. PIMRC 2004. 15th IEEE International Symposium on, 2004.

[62] H. Kim and H. Park, "An improved V-BLAST receiver based on reliability normalization," presented at Vehicular Technology Conference, 2004. VTC2004-Fall. 2004 IEEE 60th, 2004.

[63] R. M. Buehrer, N. S. Correal-Mendoza, and B. D. Woerner, "A simulation comparison of multiuser receivers for cellular CDMA," *Vehicular Technology, IEEE Transactions on*, vol. 49, pp. 1065-1085, 2000.

[64] D. Guo, L. K. Rasmussen, and T. J. Lim, "Linear parallel interference cancellation in long-code CDMA multiuser detection," *Selected Areas in Communications, IEEE Journal on*, vol. 17, pp. 2074-2081, 1999.

[65] A. Nahler, R. Irmer, and G. Fettweis, "Reduced and differential parallel interference cancellation for CDMA systems," *Selected Areas in Communications, IEEE Journal on*, vol. 20, pp. 237-247, 2002.

[66] D. Divsalar, M. K. Simon, and D. Raphaeli, "Improved parallel interference cancellation for CDMA," *Communications, IEEE Transactions on*, vol. 46, pp. 258-268, 1998.

[67] G. Xue, J. Weng, T. Le-Ngoc, and S. Tahar, "Adaptive multistage parallel interference cancellation for CDMA over multipath fading channels," presented at Vehicular Technology Conference, 1999 IEEE 49th, 1999.

[68] R. M. Buehrer and S. P. Nicoloso, "Comments on “Partial parallel interference cancellation for CDMA”," *Communications, IEEE Transactions on*, vol. 47, pp. 658-661, 1999.

[69] B. Farhang-Boroujeny, *Adaptive Filters, Theory and Applications*. Baffines Lane, Chichester, West sussex, PO 19 1UD, England: John Wiley & Sons Ltd,, 1998.

[70] H. El Gamal and A. R. Hammons, Jr., "A new approach to layered space-time coding and signal processing," *Information Theory, IEEE Transactions on*, vol. 47, pp. 2321-2334, 2001.

[71] G. Jian and Y. Dacheng, "Comprehesion of adaptive iterative decoding algorithms of turbo codes," presented at Personal, Indoor and Mobile Radio Communications, 2001 12th IEEE International Symposium on, 2001.

[72] S. Marinkovic, B. S. Vucetic, and J. Evans, "Improved iterative parallel interference cancellation for coded CDMA systems," presented at Information Theory, 2001. Proceedings. 2001 IEEE International Symposium on, 2001.

[73] L. Bahl, J. Cocke, F. Jelinek, and J. Raviv, "Optimal decoding of linear codes for minimizing symbol error rate (Corresp.)," *Information Theory, IEEE Transactions on*, vol. 20, pp. 284-287, 1974.

[74] G. H. Golub and C. F. Van Loan, *Matrix computations*, 3rd ed. Baltimore: Johns Hopkins University Press, 1996.

[75] M. Stojanovic, J. G. Proakis, and J. A. Catipovic, "Analysis of the impact of channel estimation errors on the performance of a decision-feedback equalizer in fading multipath channels," *Communications, IEEE Transactions on*, vol. 43, pp. 877-886, 1995.

[76] S. Im, "A normalized block LMS algorithm for frequency-domain Volterra filters," presented at Higher-Order Statistics, 1997. Proceedings of the IEEE Signal Processing Workshop on, 1997.

[77] D. D. Falconer and S. L. Ariyavisitakul, "Broadband wireless using single carrier and frequency domain equalization," presented at Wireless Personal Multimedia Communications, 2002. The 5th International Symposium on, 2002.

[78] A. A. Gray, S. D. Hoy, and P. Ghuman, "Adaptive LMS processing architectures employing frequency domain sub-convolution," presented at Circuits and Systems, 2004. ISCAS '04. Proceedings of the 2004 International Symposium on, 2004.

[79] H. H. Dam, S. Nordholm, and H. J. Zepernick, "Frequency domain adaptive equalization for MIMO systems," presented at Vehicular Technology Conference, 2003. VTC 2003-Fall. 2003 IEEE 58th, 2003.

[80] R. Kalbasi, R. Dinis, D. D. Falconer, and A. H. Banihashemi, "Layered space-time receivers for single-carrier transmission with iterative frequency-domain equalization," presented at Vehicular Technology Conference, 2004. VTC 2004-Spring. 2004 IEEE 59th, 2004.

[81] R. Kalbasi, R. Dinis, D. Falconer, and A. Banihashemi, "An iterative frequency-domain layered space-time receiver for SDMA systems with single-carrier transmission," presented at Acoustics, Speech, and Signal Processing, 2004. Proceedings. (ICASSP '04). IEEE International Conference on, 2004.

[82] L. Martoyo, T. Weiss, F. Capar, and F. K. Jondral, "Low complexity CDMA downlink receiver based on frequency domain equalization," presented at Vehicular Technology Conference, 2003. VTC 2003-Fall. 2003 IEEE 58th, 2003.

[83] X. Zhu and R. D. Murch, "Layered space-frequency equalization in a single-carrier MIMO system for frequency-selective channels," *Wireless Communications, IEEE Transactions on*, vol. 3, pp. 701-708, 2004.

[84] P. S. R. Diniz, E. A. B. Silva, and S. L. Netto, *Digital Signal Processing, System Analysis and Design*, 2002.

[85] H. Huang, H. Viswanathan, and G. J. Foschini, "Multiple antennas in random code CDMA systems: transmission, detection and spectral efficiency," presented at Wireless Communications and Networking Conference, 1999. WCNC. 1999 IEEE, 1999.

[86] R. L.-U. Choi, K. B. Letaief, and R. D. Murch, "MIMO CDMA antenna systems," presented at Communications, 2000. ICC 2000. 2000 IEEE International Conference on, 2000.

[87] L. Mailaender, "Linear MIMO chip equalization for the CDMA downlink," presented at Signal Processing Advances in Wireless Communications, 2003. SPAWC 2003. 4th IEEE Workshop on, 2003.

[88] S. Marinkovic, "Interference mitigation in CDMA and space-time coded MIMO systems," Thesis (Ph. D.) Telecommunications Laboratory, Dept. of Electrical and Information Engineering, University of Sydney, 2002., 2002, pp. 182 p.

[89] F. Petre, G. Leus, L. Deneire, and M. Moonen, "Space-time coding for single-carrier block-spread CDMA cellular downlink," presented at Global Telecommunications Conference, 2003. GLOBECOM '03. IEEE, 2003.

[90] F. R. P. Cavalcanti, A. L. F. de Almeida, C. E. R. Fernandes, and W. C. Freitas, Jr., "BLAST/MIMO performance with space-time processing receivers," presented at Personal, Indoor and Mobile Radio Communications, 2002. The 13th IEEE International Symposium on, 2002.

[91] S. L. Miller, "An adaptive direct-sequence code-division multiple-access receiver for multiuser interference rejection," *Communications, IEEE Transactions on*, vol. 43, pp. 1746-1755, 1995.

[92] S. ten Brink, "Convergence behavior of iteratively decoded parallel concatenated codes," *Communications, IEEE Transactions on*, vol. 49, pp. 1727-1737, 2001.

[93] J. G. Proakis, *Digital communications*, 4th ed. Boston: McGraw-Hill, 2001.

[94] G. Xue and L. Chengshu, "An analysis of HD-parallel interference cancellation in asynchronous DS-CDMA system," presented at Communication Technology Proceedings, 2000. WCC - ICCT 2000. International Conference on, 2000.

[95] R. Damani, M. Nasiri-Kenari, and M. G. Shayesteh, "Multistage interference cancellation methods for multiuser DS/CDMA detection and performance analysis," presented at Vehicular Technology Conference, 2001. VTC 2001 Fall. IEEE VTS 54th, 2001.

[96] H. El Gamal and A. R. Hammons, Jr., "Analyzing the turbo decoder using the Gaussian approximation," *Information Theory, IEEE Transactions on*, vol. 47, pp. 671-686, 2001.

[97] P. Bell, “ Time-frequency duality,” IEEE Trans. Info. Theory,. Vol. 10, pp.18-33, Jan. 1964.